

**Further Development and Applications of Capillary
Electrophoresis with Capacitively Coupled Contactless
Conductivity Detection and
Sequential Injection Analysis in Analytical Chemistry**

Inauguraldissertation

zur

Erlangung der Würde eines Doktors der Philosophie

vorgelegt der

Philosophisch-Naturwissenschaftlichen Fakultät

der Universität Basel

von

Marko STOJKOVIC

aus

Serbien

Basel, 2013

Genehmigt von der Philosophisch-Naturwissenschaftlichen Fakultät auf Antrag von

Prof. Dr. Peter C. Hauser und

Prof. Dr. Edwin C. Constable

Basel, den 10.12.2013

Prof. Dr. Jörg Schibler

Dekan

Acknowledgements

Finishing the PhD was only possible with the help of many people over the last five years. To them I shall be always grateful.

Firstly, I would like to express my deepest gratitude to my supervisor Prof. Peter Hauser for giving me the opportunity to be a member of his research team. He has introduced me to different analytical techniques and attractive projects. His great ideas, suggestions and guidance, corrections, and above all patience were essential for the projects outcome. I am also thankful to him for sharing selflessly his passion in electronics with me.

My next acknowledgement goes to Prof. Edwin Constable for his support during my last months of my PhD. He allowed me to finalize and finish all my projects, and helped me in the process with his clever suggestions. In addition, my profound gratitude goes to Beatrice Erismann for her enthusiastic help and enormous administration work she did during my studies. I would also like to thank to the co-authors of my publications for their support Dr. Peter Brodmann, Dr. Thanh Duc Mai, Dr. Narasimha Rao Uda and Joel Koenka.

Secondly, my sincere thanks goes to all the past and present members in Prof. Hauser's group for their friendliness and for the warm atmosphere: Dr. Xiao Yang Gong, Dr. Aiping Schuchert-Shi, Dr. Hong Heng See, Dr. Worapan Pornsila, Dr. Jorge Saiz, Benjamin Bomastik, Igor Petrovic, Julius Thumbi, Ralf Dumler, Neha Shastry, Duy Anh Bui. I would like to extend my acknowledgment to Dr. Vladimir Cmiljanovic, Dr. Natasa Cmiljanovic, Dr. Biljana Bozic-Weber, and Srboljub Vujovic for their endless moral support throughout my study. Many thanks to Mr. Andres Koller from the Workshop for his advantages technical asset in many system constructions and to Mr. Markus Hauri for his always welcomed ordering chemicals and equipment.

Thirdly, I would like to acknowledge the Swiss National Science Foundation for giving me financial support for my PhD study.

And finally, my warmest gratitude is to my family for their encouragement that gave me strength to complete my hard and demanding PhD studies. Above all, I am grateful to my wife Ana and eternally indebted to her love and nobility, her companionship and belief in me.

Summary

This dissertation is based on the further development and applications of capillary electrophoresis (CE) with capacitively coupled contactless conductivity detection (C^4D), *i. e.* sequential injection analysis (SIA) applications when coupled with CE- C^4D , or determination and quantification of various ions that are not or barely UV absorbed.

A purpose made CE- C^4D system was used for determination of the DNA fragments of different length, using additives to modify the medium and to sieve charged anions according to their size. We determined DNA mass ladder and PCR products from various sources. Feasibility of the C^4D method and its practical application in the separation of DNA fragments was studied and as far as we are concerned has not been implemented for the routine analysis yet. CE- C^4D method demonstrated separation with much shorter analysis time than the standard gel-electrophoresis used in conventional approach. No derivatization or sample preparations were necessary.

Further on, we investigated employment of an automated system with a sequential injection analysis (SIA) manifold based on a syringe pump and multiport valve coupled with CE- C^4D . Hydrodynamic pumping was introduced for electrophoretic separation of most commonly used artificial sweeteners. Compounds were determined in their anionic form at a high pH. Without any surfactant or modifier to reverse the electroosmotic flow, higher separation efficiency was noticed. The conditions were optimized either for better detection limits or for shorter analysis time. In addition, band broadening was observed due to pressure caused by hydrodynamic pumping. Therefore, the requirement of the narrow capillary of 10 μm for sensitive detection was necessary. The best compromise for differences between analysis time and separation efficiency was found. This coupled system setup approved to complete all operation steps to perform complex measurements with possibility to change any of the parameters during the measurements, among which sampling, separation, detection, data acquisition and polarity of the high-voltage.

SIA-CE-C⁴D composition was afterwards engaged with an array of 16 contactless conductivity detectors aligned on the capillary for real time monitoring of the entire electrophoretic separation. For better control of pressurization, some modifications were implemented, demonstrating the developments of the peaks throughout the whole capillary.

Dual capacitively coupled contactless conductivity detector was implemented. Both channels were brought into line in a bridge mode where one acts as a reference with subtracted signal. As a result, the electronic zero setting of the baseline, caused by conductivity change of the background buffer, was not necessary as in previous versions of the cell. All the differences in buffer content are consequently considered.

At the end, study on the effect of buffer concentration on the sensitivity was taken into consideration. Narrow capillaries employed, resulted in high signal-to-noise ratio when higher buffer concentration are used. Several fundamental aspects of the axial capacitively contactless conductivity detection were investigated in order to explain this uncertain effect. The performance, behavior and the cell geometry of a new detector design are reported but some evidence of the solution for this problem is still missing.

TABLE OF CONTENTS

Summary	3
1. Introduction	7
1.1 Capillary Electrophoresis (CE)	7
1.1.1. Historical review of capillary electrophoresis.....	7
1.1.2. Principles of capillary electrophoresis	9
1.1.3. Modes of capillary electrophoresis	18
1.1.4. Detection in capillary electrophoresis	21
1.1.4.1. Optical detection	21
1.1.4.2. Mass spectrometry (MS).....	22
1.1.4.3. Electrochemical detection	23
1.2 Capacitively Coupled Contactless Conductivity Detection in Capillary Electrophoresis (CE-C⁴D)	26
1.2.1. Basic principles and configuration of CE- C ⁴ D	26
1.2.2. Applications of CE- C ⁴ D.....	28
1.3 Capillary electrophoresis coupled with sequential injection analysis	29
1.4 Research objectives	33
2. Results and Discussion	36
2.1 Determination of PCR products by capillary electrophoresis with contactless conductivity detection	36
2.2 Determination of artificial sweeteners by capillary electrophoresis with contactless conductivity detection optimized by hydrodynamic pumping	44
2.3 Referenced capacitively coupled conductivity detector for capillary electrophoresis	52

2.4 Real time monitoring in capillary electrophoresis (CE) using C⁴D array detector..	62
2.5 Study on the effect of the electrolyte concentration on the sensitivity of the axial capacitively coupled contactless conductivity detector when used with very narrow capillaries.....	71
2.5.1 Introduction	71
2.5.2. Experimental	74
2.5.3. Results and Discussion.....	75
2.5.3.1. Investigation of the Influence of Stray Capacitance on the Effect of Buffer Concentration on the Peak Sensitivity	75
2.5.3.2. Explanation From the Fundamental Aspect.....	79
2.5.3.3. Stacking Phenomena	82
2.5.4. Conclusion.....	85
2.5.5. References	86
Appendix.....	87
3. References.....	89
4. Curriculum Vitae.....	96
5. List of publications and posters.....	99

1. Introduction

1.1 Capillary Electrophoresis (CE)

1.1.1. Historical review of capillary electrophoresis

Electrophoresis is a separation technique that is based on the differential motion of charged molecules through a specific medium under the influence of an electric field induced by electrodes. The migration of the molecules depends on their size, charge, shape, and the physicochemical characteristics of the medium. Although Reuss first observed what he called electro-osmosis in 1809 [1], it was Kohlrausch who investigated and formed the theoretical aspects of the electrokinetic phenomenon in 1897 [2]. In the period from 1859 to 1864, August Töppler developed a method of optical detection of moving boundaries in liquids where he measured so-called “schlieren” (shadows) as changes in optical properties. These theoretical and experimental methods contributed to forming the basis of Arne Tiselius’s “moving boundary electrophoresis” method in 1930s [3]. During his research, he achieved separation according to the differences in electrophoretic mobilities of serum proteins in solution. This method will be hereinafter referred to as zone electrophoresis, as the separation mechanism is based on differences in the charge to mass ratio of the analytes. Later, during the 1940s and 1950s, two additional methods were developed and are known as isotachopheresis and isoelectric focusing. Isotachopheresis utilizes a discontinuous electric field to form sharp boundaries among analytes and depends on the differences of migration velocities of the sample constituents [4]. Isoelectric focusing as a separation technique is based on the different isoelectric points (pI) of the analyte components, where the (pI) is the point where an analyte has an overall net charge of zero [5]. In 1967, Hjerten *et al.*[6], employed for the first time open tube capillary electrophoresis with UV detection, where he rotated millimeter-bore quartz-glass capillaries around their longitudinal axis to reduce the effects of convection. Not long after, Mikkers’ research group achieved zone electrophoresis with conductivity and UV detection, in narrow-bore Teflon capillaries of 200 μm inner diameter [7]. In addition, during the early 1980s, instead of planar gel media, capillaries filled with buffer solution were rather used. For the first time, 75 μm inner diameter capillaries

were employed by Jorgenson and Lukacs [8-10] and coupled with an on-column fluorescence detector to separate amino acids. With this approach, in a view of using such narrow capillaries, it was observed that the heat generated by applying high voltages of 30 kV was efficiently dissipated. Thus, Jorgensen explained the comparison among operational parameters and separation efficiency. He predicted the possible achievements of high performance capillary electrophoresis (HPCE) as an analytical approach. Nowadays, modern CE is expanding more towards research for miniaturized and automated portable systems. Despite the narrower high-tech fused silica capillaries with internal diameters of 10-50 μm , the majority of development in this area has changed. It has been devoted to faster and better separation and detection on microchannels with Lab-on Chip mode or automated with Lab-on-Valve mode by conjunction with sequential injection analysis. The capabilities of CE are spreading and proving to be useful in applications over a wide range of disciplines, varying from analytical biotechnology, bioanalysis, over pharmaceutical, clinical to separations in environmental sciences. Up to now, CE has been shown to be a very convenient and effective method of analysis where small volumes of sample are available.

1.1.2. Principles of capillary electrophoresis

In the capillary electrophoresis method, electrically charged ions in a narrow-bored fused silica capillary are acted upon by an electric field to achieve separation. The principle of separation is based on the size-to-charge ratio of specific species of interest when an electrical field is applied. The analytes will move within a conductive electrolyte solution according to their charge orientation toward the electrode of opposite charge at a speed that corresponds to their mass. Capillaries allow fast analysis times at voltages up to 30 kV, consuming small samples in the μL range and buffer solutions in the mL range, which in return place CE as a method of choice for various analytical problems.

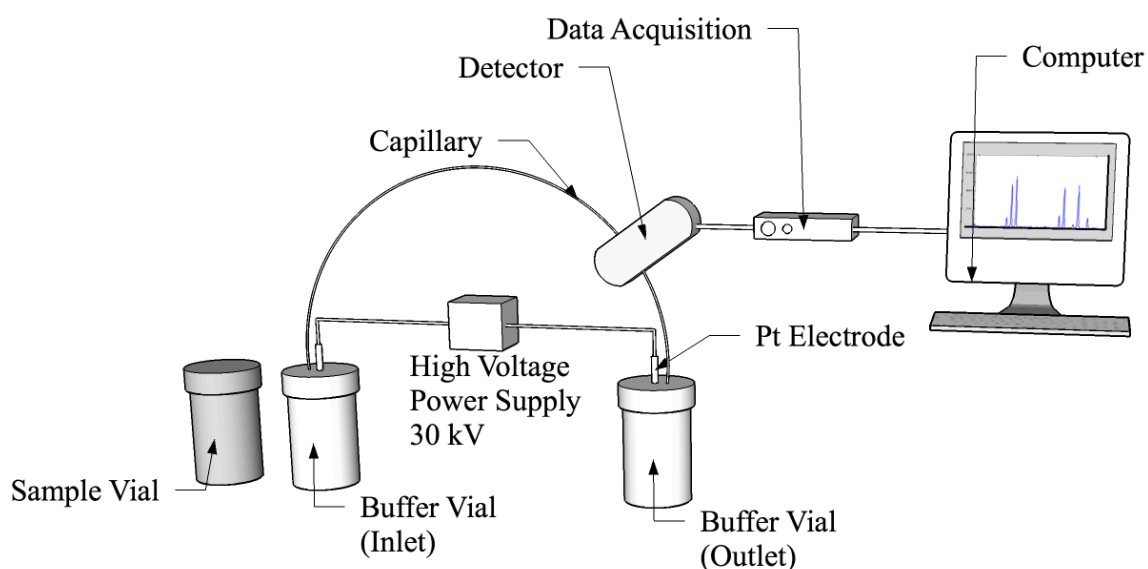


Figure 1. Conventional CE system diagram

Relatively simple instrumentation is necessary to carry out capillary electrophoresis. A general schematic drawing of a CE system is shown in figure 1. The most important components are sample and buffer vials, a fused silica capillary, high-voltage power supply with an upper limit of 30 kV, detector, and data acquisition system. The content of the buffer vials must be the same and match the content of the capillary. Each end of the capillary is dipped into the buffer vials together with the electrodes. Electrodes are usually made of platinum and are placed to provide electrical contact between the high-voltage power supply and the capillary. To load a sample onto the column, an inlet buffer vial has to be replaced with the sample vial that contains analyte dissolved in electrolyte buffer solution or in water. The injection time, usually

measured in seconds, varies depending on the mode of injection: electrokinetic by applying an electric field or hydrodynamic by applying the pressure. After swapping the sample vial with the inlet buffer vial again, high voltage is applied. An employed electric field initiates the migration of the analytes towards the detector where they are visualized. The detector is arranged on-column, near the capillary end, and the output signal of the detector is processed and recorded with the data acquisition system. On the computer, the data is presented as an electropherogram that indicates the detector response as a function of time. With the addition of features such as autosamplers, multiple injection devices, programmable power supplies, multiple detectors, fraction collection, and computer interfacing, this basic setup can be expanded.

1.1.2.1. Electrophoretic mobility

Electrophoretic separation in CE is based on the differential migration velocity of charged species or solutes in an applied electric field. Ion velocity can be defined as

$$v = \mu_e E \quad (\text{eq. 1})$$

where

- v = ion velocity in cm s^{-1}
- μ_e = electrophoretic mobility in $\text{cm}^2 \text{s}^{-1} \text{V}^{-1}$
- E = the electric field strength in V cm^{-1}

The applied electric field (E) is a function of the applied high voltage and the total capillary length. The electrophoretic mobility (μ_e) for a particular ion or medium is a constant that specifies how fast each can move through a buffer solution. A molecule with charge q can be determined by two forces, electric force (F_e) and frictional force (F_f), where the electric force (F_e) can be described as an ion velocity force through a medium and is given as a function of the electric field and ion charge by

$$F_e = q E \quad (\text{eq. 2})$$

and the frictional force (F_f) as the force of viscosity for an ion while migrating through (movement along) the buffer medium. For a spherical ion, Stokes' Law can express frictional force:

$$F_f = 6 \pi \eta r v \quad (\text{eq. 3})$$

where q = charge of ion
 η = viscosity of the solution
 r = ion radius
 v = ion velocity

Both of these forces are competing for the spherical ion with radius r during the electrophoresis. Therefore, at the steady state they balance each other as they are equal but with opposite directions

$$F_e = F_f \quad (\text{eq. 4})$$

or

$$q E = 6 \pi \eta r v \quad (\text{eq. 5})$$

Therefore, the electrophoretic mobility of an ion for a given set of conditions is constant and can be defined with the following equation:

$$\mu_e = \frac{q}{6 \pi \eta r v} \quad (\text{eq. 6})$$

As concluded from the equation 6, differences in the charge-to-size ratio of analyte ions show that higher charge and smaller size result in higher electrophoretic mobilities, and conversely, large minimally charged species have lower mobilities. Thus, the charge can be influenced by pH changes and some complexing reagents used can affect the ion radius.

Electrophoretic mobility of different ions or media dictates the migration velocities under the induced electric field and therefore makes it possible to determine and separate mixtures of different analytes and solutes. Nevertheless, it is also influenced by other factors such as electroosmotic flow (EOF) of the buffer solution and temperature.

1.1.2.2. Sample Injection in CE

One of the principle advantages of CE is the ability to inject quite small volumes of sample. Regular injection volumes range from picoliters to nanoliters. There are two methods to introduce the sample into the capillary. One is hydrodynamic injection by aspiration or siphoning and pressure, and the other is electrokinetic injection. Hydrodynamic injection, also referred to as hydrostatic injection, is accomplished by the application of a pressure difference between the two ends of a capillary. Injection by siphoning can be realized by positioning the injection end of the capillary into the sample vial. Injection will follow by elevating the sample vial and capillary injection end to a specific height for a certain period of time. Elevated sample vial is on the height that is higher than the opposite capillary end as shown in figure 2. This principle is used for all hydrodynamic injection modes and during pressurized injection; pressure is applied to the sample vial, whereas during vacuum injection, vacuum is positioned at the opposite capillary end while drawing the sample into the capillary. Automated hydrodynamic injection was developed and studied by Rose and Jorgenson *et al.*[11] to identify the operational error usually caused during the manual injection. Also considered was the time for the sample vial to travel up and down throughout the injection process, during which hydrodynamic pressure is created and causes the sample to be drawn into the capillary.

Electromigration or electrokinetic injection is achieved by simply turning on the voltage for a certain period of time. To perform the injection, the electrode and the injection end of the capillary are only shifted from the buffer vial and dipped into the sample vial. After applying the injection voltage for a brief time period, the sample is drawn into the capillary end by both electrophoretic migration of charged ions of the sample and electroosmotic flow (EOF) of the sample solution.

In electrokinetic injection, two possible types of bias may appear: one as a result of the fact that each analyte in the sample solution has a different mobility, and the other as a difference in conductivities between the sample solution and the running buffer. Only in the case when the injection is made from the sample prepared in buffer will differences of both electrophoretic mobilities and electroosmotic flow not be considered and thus no changes in the injected amount would occur.

These potential problems in sampling are usually caused due to strong dependence of sample loading on the EOF, mobility of individual solutes and matrix composition. With automated CE systems, reproducibility of the separation has been improved. The primary limitation of the hydrodynamic methods is that they are poorly applicable to the injection of high viscosity samples. However, they are easy to perform with a high rate of injection reproducibility, and possibility to be automated. They are currently the most commonly used sample injection methods in capillary electrophoresis. Despite the sample bias, the electrokinetic injection technique is mostly used when hydrodynamic injection is not effective or when the capillary is filled with gels or high viscosity media. The development of new modes would help to overcome this bias and place electrokinetic injection as the method of choice in capillary electrophoresis separations.

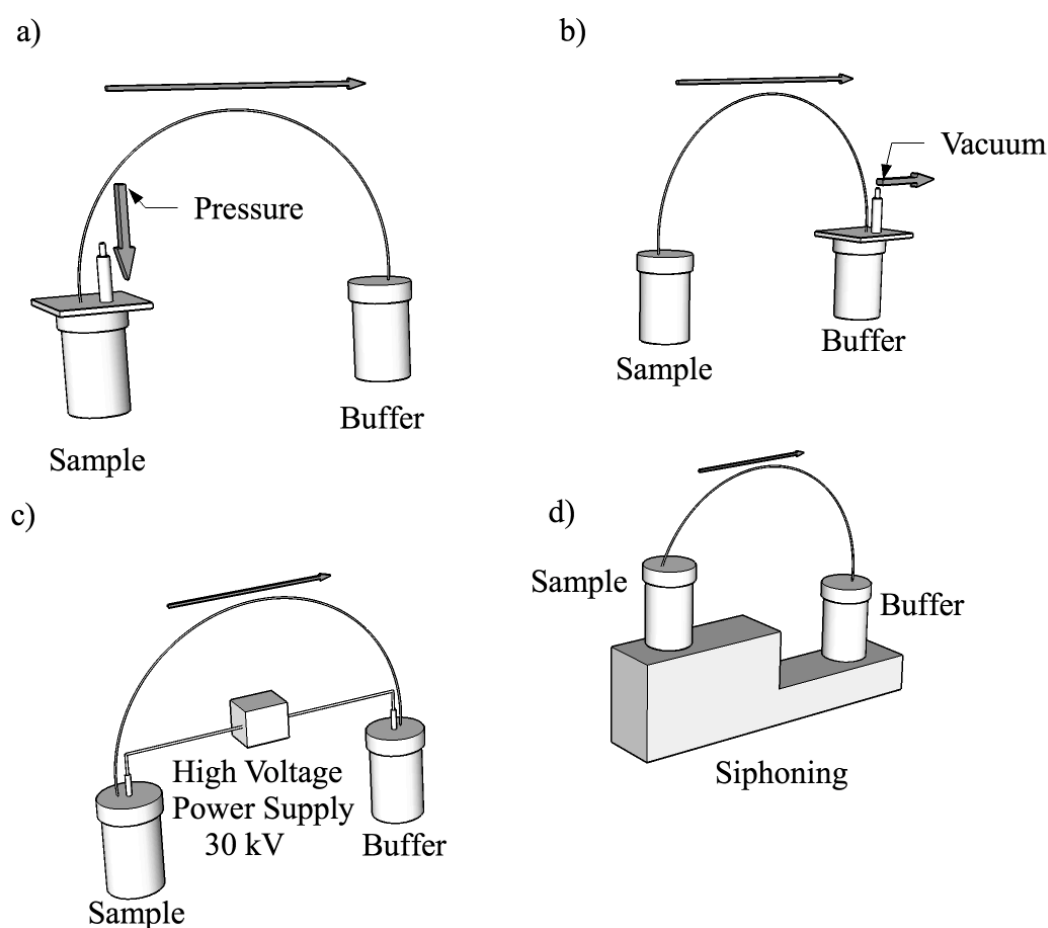


Figure 2. Custom injection methods in CE:

- a) pressure (compressed gas), b) vacuum, c) electrokinetic, d) siphoning

For most of the injection modes, one rule is present: the capillary has to be physically shifted from the buffer vial to the sample vial and vice versa. A lot of approaches for automated sample injection have been reported. As described by Deml *et al.* [12], a sampling method for capillary electrophoresis, which is an electric analogy of the splitter in chromatography, was developed. In 1987, Tsuda *et al.* [13] relied on rotary-type injection, used previously for liquid chromatography, that can be employed under high electrical field. A simple sampling device where the sample is introduced without mixing with the buffer solution by means of two feeders perpendicular to the capillary tube was reported by Verheggen *et al.* [14]. The use of microinjectors was presented for the first time by Ewing *et al.* [15], where the technique employing micropipettes of $< 1\mu\text{m}$ in outer tip diameter was utilized. One of the newest advances was presented by Liu and Dasgupta *et al.* [16], where they described a simple sampling device, whereby the sample is directly introduced into capillary by means of two feeders, placed perpendicular to the capillary tube. Two independent research groups by Kubáň *et al.* [17] and by Fang *et al.* [18], announced in 1997, the introduction of flow-based injection for CE with a specially tailored interface. Using this approach, where the capillary is positioned at the interface and the sample is delivered via interface to the injection end of the capillary, pressure is applied with an assisted motor-driven syringe pump. Regarding this technique, interface-based injection has been coupled in flow injection or sequential injection capillary electrophoresis and has helped to increase efficiency of separations in CE.

1.1.2.3. Electroosmotic flow (EOF)

Another contribution of the capillary to electrophoretic separation is a phenomenon also known as electroosmotic flow or electro (endo) osmosis or only EOF. It occurs under the influence of an applied electrical field resulting in the bulk movement of a liquid, moving all analytes in one direction regardless of their charge. Therefore, presence of EOF is important for simultaneous separation of both cations and anions in a single run, which would be impossible without EOF. Neutral ions in normal CE mode are undetectable due to their co-migration with the EOF. Another benefit of EOF is its feasibility for analyzing species with different charge-to-mass ratios within a reasonable analysis time.

Fused silica is the material generally adopted for capillaries. EOF is caused by the charge on the interior surface of the capillary wall. The interior surface in a fused silica capillary is covered with silanol groups (SiOH), which are typically ionized (hydrolyzed) to their negatively charged silanol form (SiO⁻) when aqueous buffer solution is introduced. The negatively charged wall attracts cations that are hydrated from the electrolyte solution, forming an electrical diffuse double layer as shown in figure 3. These cations, also known as counter ions, are essentially aligned in two regions. Closely attached to the capillary wall, a Stern layer, or so-called fixed layer, is formed but is in a sufficient density to neutralize all negative charges. Therefore a second outer layer of cations is formed, “the diffuse layer” (Gouy-Chapman layer) [19], that extends into the bulk of the solution. In an electrical field, the diffuse layer migrates toward the cathode. It pulls water along and creates the electroosmotic flow as a pumping action. Therefore, the direction of the electroosmotic flow will directly depend on the sign of the charge on the capillary wall. The EOF is always migrating toward the electrode with the same charge as the surface of the capillary wall. Thus if there is an uncharged wall, there should be no EOF.

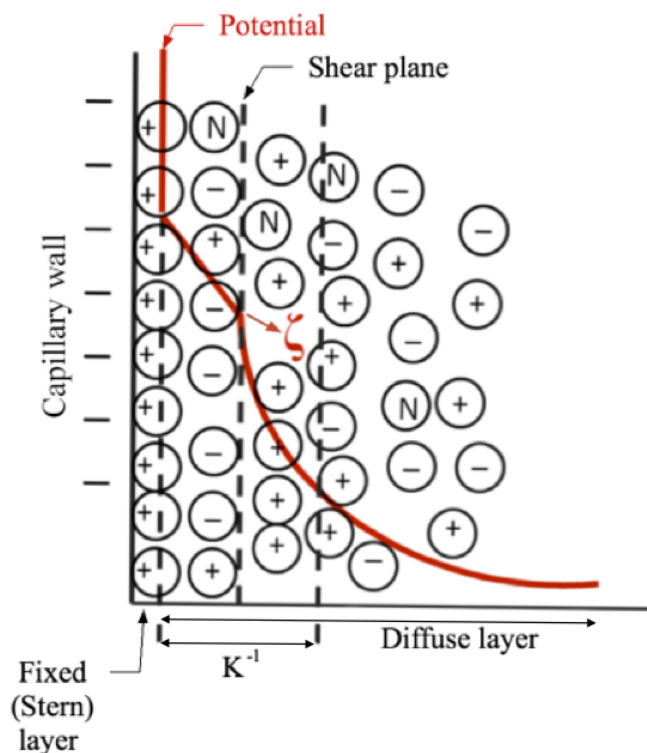


Figure 3. Course of the ζ -potential and interior surface of fused silica capillary

At the boundary plane (plane of shear) between the fixed and the diffuse layer, an electrical potential, also known as zeta potential, is developed. It depends on the electrical double layer thickness and the charge density of the diffuse layer. As shown in figure 3, in the diffuse layer this potential drops to zero. The EOF velocity and mobility are proportional to the zeta potential as given by the Smoluchowski equation,

$$v_{EOF} = \frac{\epsilon \zeta}{\eta} E \quad (\text{eq. 7})$$

or

$$\mu_{EOF} = \frac{\epsilon \zeta}{\eta} \quad (\text{eq. 8})$$

where v_{EOF} = velocity of the buffer

μ_{EOF} = EOF mobility

ζ = zeta potential of the wall, which is defined as the voltage drop
between the Stern layer and the shear layer

ϵ = dielectric constant of the buffer

Electroosmotic flow across the capillary is almost uniform resulting in a flat plug flow, which opposes the parabolic shape of laminar flow usually present in the systems where the plug is pumped by a pressure differential, such as HPLC. The comparison between EOF and laminar flow is shown in figure 4. The benefit of such a profile as a flat plug flow is that the initial velocity of all solutes that are acted upon by the EOF is the same, despite their cross-sectional position in the capillary. In this way band broadening is greatly reduced and, as a result, narrow peaks of high efficiency are achieved.

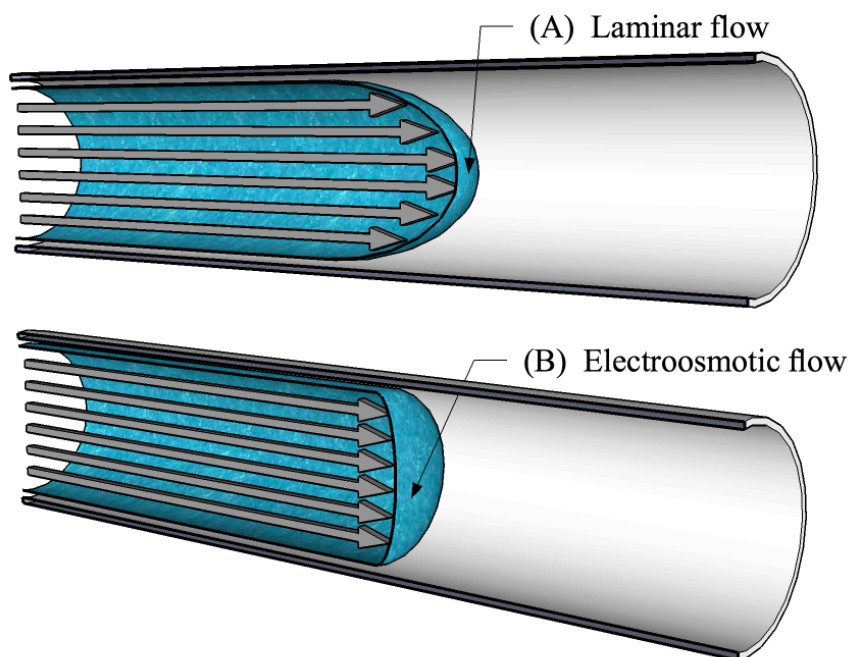


Figure 4. Comparison of flow profiles in (A) HPLC and (B) CE

Injecting and measuring migration time of some neutral compounds can be done experimentally to determine the electroosmotic flow. Specific characteristics of the neutral marker have to be considered. It should be neutral at the pH of the electrolyte solution, pure, identifiable by the detector, and there should be no interference with the capillary wall. It is described as a function of the effective length of the capillary, which is a distance from the injection end of the capillary to the detector, and the electric field applied.

$$\mu_{EOF} = \frac{l_{eff} L}{V t} \quad (\text{eq. 9})$$

where

l_{eff} = effective length of the capillary

L = total capillary length

V = voltage applied

t = migration time of EOF (neutral) marker

It is essential to keep the electroosmotic flow constant. Any variations can lead to incorrect results. If it changes, migration time of the analytes will change or errors in quantitative and qualitative analysis can occur. All variables that can affect the EOF should be considered, such as variation of the electric field where decreasing the voltage will directly influence the EOF, lowering pH will result in lower EOF, and temperature fluctuations. Higher temperatures will lower the buffer solution viscosity by 2-3 % per °C and therefore increase the EOF. Variations of the buffer concentration affect the compactness of the double layer and therefore the zeta potential. If the ionic strength of the buffer solution decreases, it results in double layer broadening, increased zeta potential and stronger EOF. Adding a buffer modifier can affect the double layer in the capillary wall and consequently decrease or completely reverse the EOF. For example, adding the polymer polyethylene glycol (PEG) or surfactant polysorbate 20 will reduce the EOF while addition of quaternary ammonium compounds (CTAB, TTAB), mostly known as cationic detergents, will completely reverse the EOF. Usually, their presence is required in the running buffer, which can cause interaction with some of the analytes.

1.1.3. Modes of capillary electrophoresis

Capillary electrophoresis is comprised of diverse modes of separation that have different separative and operative characteristics. In general, CE is defined as a combination of many electrophoretic and chromatographic techniques and can be further divided into capillary zone electrophoresis (CZE), capillary isoelectric focusing (CIF), capillary gel electrophoresis (CGE), capillary isotachopheresis (CITP), micellar electrokinetic capillary chromatography (MEKC), and capillary electro-chromatography (CEC).

Capillary Zone Electrophoresis (CZE) is distinguished by the employment of open capillaries and approximately lower viscosity buffer systems. Separation of analytes relies on different electrophoretic and electroosmotic velocities of the ionic species and the background electrolyte according to their migration in the electric field. It is the most extensive mode of CE and has been used for many analytes. Cations are

accelerated by the electroosmotic flow and migrate towards the cathode, whereas anions, although attracted by the anode, are swept towards the anode due to the bulk flow of electrophoretic medium. Neutral species are not separated electrophoretically as they co-migrate with the EOF, so in this respect, CZE is not the method of choice for neutral ions.

Capillary Isoelectric Focusing (CIEF) as a separation mode is based on the isoelectric pH or pI of the molecule and its migration in an electric field. At a specific pH (pI), certain molecules possess both a positive and negative charge, and behave as neutral since the charges cancel each other. Therefore, they should not move when the electric field is applied. In CIEF, a special mixture of buffers, also known as ampholytes, is employed to generate a pH gradient within the capillary. The ampholytes will arrange themselves under the applied electric field from a strong acid to the strong base throughout the capillary. Analytes will migrate through this pH gradient until they reach equal pH at their pI. Since they are uncharged at that point, they cease migrating. After focusing, it is necessary to mobilize them toward the detector, which is usually utilized with applied pressure flow. This mode is often used for the separation of proteins or closely related species.

Capillary Gel Electrophoresis (CGE) is analogous to gel electrophoresis where the separation is based on viscous drag. The capillary is filled mostly with gel or some other high viscosity medium. The EOF is usually repressed in which case the movement of the analytes is assigned only to electrophoresis. CGE relies on separation of molecules that are distinct in size yet not in significant charge-to-mass ratio. Application of this method is mainly beneficial for analysis of DNA fragments or weight analysis of proteins treated with detergent.

Capillary Isotachopheresis (CITP) is accomplished when the sample plug is restrained between two different electrolyte solutions in a constant electric field. First buffer or leading electrolyte, possess mobility higher than anything else in the separation and opposite, second buffer or trailing electrolyte, holds the lowest mobility of all. It is required that the charge of the analytes and the buffers has the same sign. After applied voltage, separation will not be observed with peaks but instead, the sample will form certain zones aligned one next to another according to

their mobilities. The length of the zone is proportional to the concentration of the analyte within that zone. This method is commonly used in pre-concentration or sample purification steps but nowadays is finding practical use in the determination of pharmaceuticals [20], proteins [21] and particles [22].

Micellar Electrokinetic Capillary Chromatography (MEKC) is a combination of principles from both capillary zone electrophoresis and chromatography that can separate neutral and charged species. As electrophoresis is impossible for uncharged analytes, it is necessary to employ some agent that will transport them along the capillary. The most commonly used modifier is charged detergent sodium dodecyl sulphate (SDS) in concentrations high enough to form micelles. As the specific disposition of the detergent, micelles have a lipophilic inner part and hydrophilic outer surface and have tendency to constantly form and disperse. The mechanism of the method is based on the difference in partitioning between micelles and the running buffer. Micelles in this method are behaving like stationary phases, whereas the running buffer acts like the mobile phase. Separation with the MEKC is utilized for large range of small-uncharged molecules, which are also adequately lipophilic to conjoin with the micelle such as drugs, peptides, proteins, pesticides etc.

Capillary Electro-chromatography (CEC) is a fusion of electrophoresis and liquid chromatography techniques. The principle is similar to the MECK mode and can be described as a partitioning technique where the molecules are distributed amongst stationary and moving phases. Different analytes will tend to bind in bigger or smaller magnitudes with the stationary phase, effecting the separation. CEC capillaries are most frequently packed with the same particles employed in HPLC columns. In CEC, electroosmotic flow is used to press the mobile phase down the column. Improved separation efficiency results with the plug flow over laminar flow in pressure-driven systems. CEC is often present in online pre-concentration prior to separation and detection [23] but is also found practical when related to mass spectroscopy.

1.1.4. Detection in capillary electrophoresis

To present some valuable data from the separation technique, it is elementary to detect and measure the analytes. Detection in CE is an important challenge; due to small detection volumes, samples should be generally concentrated for proper analytical detection. Detection can be qualitative and quantitative. Polyimide coated capillaries from 10 μm to 100 μm are in most cases employed in CE. Many CE detections techniques are comparable to those customized for liquid chromatography. Most of the detections are carried out on-capillary, and the most frequently used will be described herein.

1.1.4.1. Optical detection

Optical detection schemes are reasonably easy to setup and are very often used in CE. On-capillary detection is possible with UV-transparent fused silica capillaries, since the light source can be focused directly on the capillary. By far, absorbance and fluorescence detectors are the types encountered most in CE instrument systems [24].

1.1.4.1.1. UV/Vis Spectrophotometry

The most frequently used detector in CE is the UV/Vis absorbance detector. This popularity comes from its universal nature and its accessibility from HPLC work. Absorbance detectors rely on the absorbance of light energy from the light source, of UV wavelengths by the analytes. As the analytes pass from the light source to the light detector, this absorbance creates a shadow where the intensity is directly proportional to the quantity of material present. It is an on-column detection technique, with insensitivity to temperature changes and is classified as non-destructive for the analytes. For species like inorganic ions, aminoacids, sugars *etc.*, which are non-UV-absorbing, detection is carried out in the indirect mode where a chromophore is supplemented with the background electrolyte, thus the chromophore appears with lower sensitivity and insufficient linearity. The fused silica capillary as sample holder passes through the UV/Vis detector where wavelengths of 200 nm and above may be employed without complications. A small

section of the polyimide coating of the capillary is removed, considering that section as an optical window. As the capillary tube is thin compared to conventional path lengths, care has to be taken with the detector design. Notably narrow capillaries compromise detector sensitivity so capillaries with less than 50 μm ID are not favored. For precise results, the light beam has to be of a small diameter and focused on that capillary section directly. The disadvantage of the method is that the capillary is fragile and prone to break. On the other side, running buffer should not be optically active in the range of the analyte [25].

1.1.4.1.2. Fluorescence

Fluorescence spectrometry is adapted in CE in the same way as UV/Vis spectrometry. The system uses an external source of energy to excite the analyte to a higher energy state at one wavelength. When the excited analyte returns back to its ground state, it emits energy of a lower wavelength. In CE systems [8], fluorescent detectors generally employ lasers as the excitation source of energy. Their main advantage is that they project light of high intensity at a specific wavelength onto a very narrow channel of the capillary or in the microchip format [26], which as an outcome has good excitation efficiency. In their absorbance wavelengths and excitation, analytes can vary and therefore a fluorescent detector will not be able to detect all sample components. The sensitivity obtained from the detector can be from 10 to 1000 times better than an absorbance detector [27]. A drawback of this method is that analytes of interest in CE are not always fluorescent, so derivatizing agents are utilized to act as labels for the compound. Those markers are mostly organic aromatics and have excitations from 250 nm to 500 nm.

1.1.4.2. Mass spectrometry (MS)

Mass spectrometry is a specific strategy that can confirm and give very important structural information about analytes. It has been considered as a destructive, end-column and sensitive detection method. Thus it has been used more than UV/Vis, laser induced fluorescence or electrochemical detectors. MS is an instrument to determine most biological molecules, such as peptides and proteins [28-31]. The coupling of CE with mass spectrometry gives an additional dimension of analysis in addition to

detection. CE data responds with migration time and quantity while MS gives info on the species charge and also provides data of molecular weight along with structural information. One of the first form of MS paired with CE was electrospray MS [32]. In CE setup, the outlet end of the capillary is inserted into the electrospray interface. As the volume from the capillary is very small, make-up liquid, known as Sheath solvent, is pumped. The liquid is mixed with a flowing gas stream and dispensed into a spray. The ionized analyte particles pass through the MS detector as the spray vaporizes. The MS system scans through the range of mass values. If the widths of the peaks in CE are very small, the MS instrument has to scan fast or peaks can be missed.

The interfacing of commercial CE with commercial MS system has been inspected for a large number of applications in forensics, environmental analysis, bioanalysis, pharmaceutical analysis and the study of metabolites;. [33-39]. The model of these systems favors UV or alternative detectors prior to MS interface; however, the connection of two systems is expensive, complicated and unavailable for many laboratories.

1.1.4.3. Electrochemical detection

Electrochemical detection methods such as potentiometric, amperometric and conductometric modes have been shown to be very applicable in conjunction with CE. Interferences of high electric fields, electrode placement, and materials used for production and modification of the electrodes are the main concerned topics. The advantages for this coupled systems, regarding sensitivity and selectivity, are reported with a large number of applications [40-42].

1.1.4.3.1. Potentiometric detection

For potentiometric detection as a simple routine mode, application of the external voltage is not necessary. This system relies on reference and working electrodes where a potential is measured on the working electrode, a so-called ion-selective electrode (ISE), in contact with an analyte ion. Membranes can be crystalline-, glass- or liquid containing an active ionophore, but are specific and porous only for the favorable ions. Determination of organic and inorganic cations with ISE was

demonstrated by Nann and Simon *et al.* [43]. Ion-selective electrodes were initially used for investigations in this CE mode, but recently coated wire electrodes in which the wire is coated with thin layer film containing the ionophore of interest have been introduced. This approach of coated-wire ion selective electrodes was employed by Schnierle *et al.* [44] for the analysis of selected organic ions.

This can be considered as the most selective electrochemical method as the electrodes are limited to ions of particular sign and charge number. Complexity of the potentiometric detection involves also handling, sensor preparation, vulnerable micromanipulations and limited lifetime. Reviews on applications and principles of potentiometric detection in CE are available [45-50].

1.1.4.3.2. Amperometric detection

Amperometric mode of detection with CE is considered a powerful analytical technique with high sensitivity, good selectivity and low cost. In amperometric detection the current change between oxidation and/or reduction of electroactive analyte ions, is measured. A triple electrode setup is a prerequisite, namely use of a working, reference and an auxiliary electrode that controls the potential drop between working and reference electrode. The mechanism is based upon the sustained potential applied between working and reference electrode where the electron transfer is measured as the resulting current between working and auxiliary electrodes. Current flow through the working electrode is proportional to the electron transfer and as such, corresponds to the solute concentration. In CE, separation is usually performed at microampere levels and potentials at kilovolt levels, while the detector cell has to operate at picoampere currents and millivolt potentials. Amperometric detection is suitable for species that possess redox potential, like neurotransmitters [51], aromatic amines [52], carbohydrates [53], phenols *etc.* Amperometric detectors are also used for the detection of biogenic amines at levels low as 10^{-8} M [54]. Recent reviews on amperometric detection for CE are available [55-63].

1.1.4.3.3. Conductivity detection

Distinguished from potentiometric and amperometric detection, conductivity detection has been estimated as the most universal mode that accompanies all charged species. The measurement of the signal, as the analyte response, can be performed directly or indirectly. By definition, it can be considered as the change in conductivity of the bulk solution between two electrodes as analyte passes through the electrode gap. If any sort of molecule changes the conductivity between the electrodes, it can be detected and measured response will be proportional to the concentration of the ions. Analytes are determined only if they are ionized in the background electrolyte solution (BGE). A conductivity detector cell embodies two inert electrodes, mostly platinum, across which a high frequency AC signal is applied to produce a current. During the detection, alternating current is utilized instead of direct current (DC) to prevent electrolysis reactions on the electrode surfaces and polarization of the electrodes. Another reason not to use DC is to avoid possible interference from the detection electronics. This current yields the resistance and conductivity according to Ohm's law. Detector response as a current signal comes from the difference in conductivities between analyte ions and BGE co-ions of the same charge. Greater difference arises with higher detector response. Conductivity detection draws attention, as it requires no unnecessary chemical properties and therefore has been an attractive method for CE analysis. Two modes of conductivity detections, contact or contactless, are possible either with or without galvanic contact between electrolyte solution and the electrodes [48]. There are no principal dissimilarities between them and both have been developed and made commercially accessible. An operating frequency of 1 kHz is necessary when working with the contact mode, whereas for contactless mode several hundred kHz are often required. A high frequency contactless conductivity detector for isotachopheresis was introduced for the first time by Gas *et al.* [64] in the late 1970's. In the background electrolyte, ions are always in excess and therefore a baseline signal and noise are constantly present at the detector. For this mode of detection, it is preferred to choose a low conductivity background electrolyte with high ionic strength, as sensitivity of the detection is as a result of the background conductivity. Conductivity detection has been used for the determination of charged species with relatively high specific conductivity that are non-UV or poor UV absorbing such as inorganic ions [65, 66], metal ions [67, 68], aminoacids [69, 70, 61, 63] or in

pharmaceutical and clinical analysis [71, 72] *etc.* Details on further applications and principles of conductivity detection are available [73-75, 60, 76, 50, 77, 78]. Conductivity methods require very small amounts of the sample, mostly in the microliter range, while the low detection limits (LOD) allow analysis on sub-picogram amounts of analyte. They offer excellent selectivity in complexed samples due to lower electroactive interferences than the spectroscopic interferences.

The advantage of electrochemical detection schemes is that they are not limited by wavelengths as in optical detection. On the other side, when using electrochemical methods for quantification, there is an evident limitation in selectivity. To overcome this limitation, affiliation among electrochemical quantification methods with a separation step should be considered.

1.2 Capacitively Coupled Contactless Conductivity Detection in Capillary Electrophoresis (CE-C⁴D)

1.2.1. Basic principles and configuration of CE-C⁴D

The first no galvanic contact of electrodes with the solution was reported on a high-frequency conductance microcell for the determination of conductivity in streaming solutions or solvents in the early 1980's by Pungor *et al.* [79]. The conductance of potassium chloride and glucose solution within the range of different concentrations was measured by studying the applicability of the cell for flow injection. The usefulness of the cell coupled with ion chromatography was illustrated [80].

The fundamental setup of an axial C⁴D configuration was introduced into CE by two independent research groups in 1998, Zemmann and co-workers [75, 81] and Fracassi da Silva and Do Lago [82]. This setup as illustrated in figure 5 A, is yet currently in use. Two short electrodes of a few millimeter lengths, composed of either short metallic tubes or conductive silver varnish, are separated by a gap of 1 mm and positioned side by side around the capillary. Faradaic shielding (gap of 1 mm) is used to prevent direct capacitive coupling between the electrodes causing stray capacitance, which can result in an additional background signal. The shielding is normally made of thin copper foil with a drilled hole of 400 μm for the standard capillary of 365 μm outer

diameter size. Two external electrodes, namely actuator and pick-up electrodes, form two capacitors (C) and are connected with the resistor (R) via electrolyte solution in the capillary. The equivalent circuitry for a conventional contactless conductivity cell is shown in figure 5 B.

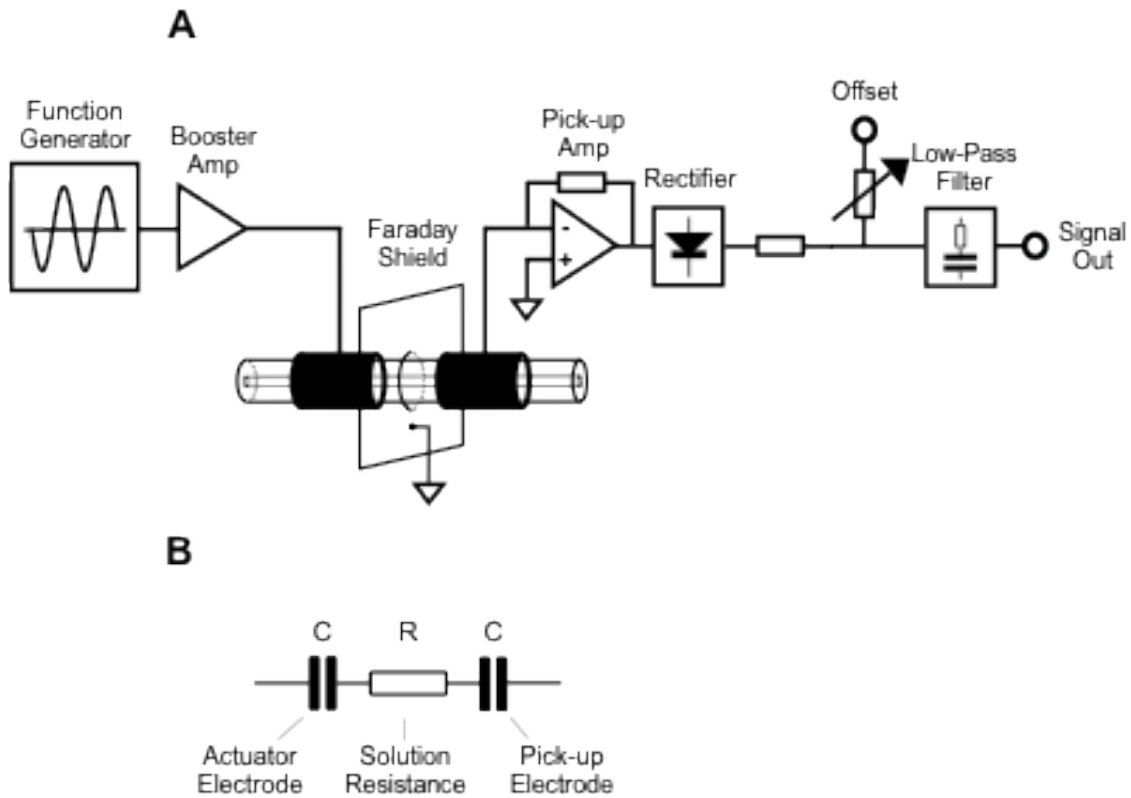


Figure 5: Schematic drawing of C⁴D in an axial arrangement:

A Schematic drawing of the electronic circuitry,

B Simplified circuitry

It is possible to pass an excitation ac-voltage at the actuator electrode of significantly higher frequency of several hundred kHz through the cell. While passing through such a circuitry, current (i) is dependent on the applied ac-voltage (V) and frequency (f) as described by the equation:

$$i = \frac{V}{R + \frac{1}{\pi f C}} \quad (\text{eq. 10})$$

The current is restricted by capacitances from both electrodes at lower frequencies. On the other side, for higher frequencies only the solution resistance determines the current and not the capacitance at the electrodes. Regarding the equation 10, current (I) results in a plateau value. This approach where no contact is established between electrodes and the solution, results in a greater distance between capacitors and therefore smaller capacitance. Thus, higher frequencies are required, usually higher than 100 kHz. Custom value of 300 kHz is estimated as optimal [83]. Gathered by the pick-up electrode, AC current signal is converted into voltage using a feedback resistor and amplified to acquire a recordable DC signal that shifts as conductivity varies. To obtain the best resolution of the analog-to-digital converter, before rectifying measured signal, background signals should be suppressed. As an outcome of this, conductivity changes of the solution within the capillary between two electrodes can be monitored. In the work of Kubáň and Hauser, more elemental overview of C^4D is described [84, 83, 85].

With an easy setup in C^4D , precise alignment of the electrodes along the capillary is matching with a wide range of capillary diameters. Many advantages can be obtained with axial alignment and contactless configuration, such as characteristic decoupling from the employed electric field for separation, the possibility to miniaturize the detector cell due to its construction simplicity and the prevention of fouling and corrosion of the electrodes. When UV detection is employed, removal of a section of the polyimide coating of the capillary is necessary to endorse radiation, whereas in C^4D is not. Nowadays, commercialized C^4D detectors are available (www.edaq.com, www.istech.at) and the possibility to couple them, not just with CE but also with other separation techniques such as FIA, IC or HPLC, is feasible.

1.2.2. Applications of CE- C^4D

Capillary electrophoresis has been utilized in many different fields. Advantages include: fast results with high resolution and separation efficiency due to applied high voltages or low reagent and sample consumption, high selectivity, along with low effects from matrices in samples and simple sample preparation over enzymatic or chromatographic methods. Typically, conductivity detection is a universal method

that is easy to fabricate at low cost. Uncomplicated cell geometry and simple electronic circuitry mean that C⁴D cell can be made in-house, which gives enough reasons for its acceptance in several research groups. Since its arrival in CE, analyses were applied for species that are not-UV absorbed such as inorganic ions. High separation efficiency was provided with direct detection carried out with C⁴D. Successful analysis of species in complex sample matrices have been reported [86, 65]. Determination of both cations and anions in a single sample of rain, where it was possible to determine 21 cations and anions in one run, was reported by Kuban *et al.* [87]. After protonation or deprotonation of organic acids and bases, determination with CE-C⁴D is possible. Fatty acids, alkylammonium cations, and alkylsulfonic anions were determined with indirect C⁴D [88-90]. Underivatized and free amino acids and related compounds were also identified [91, 92, 63]. Contactless conductivity detection has been successfully performed on a microchip platform [93-96, 62, 97-101]. Several review articles on applications of C⁴D in CE have been published emphasizing environmental, pharmaceutical and forensic fields among others [102, 23, 103, 85, 104-106, 77, 78]. C⁴D applications have spread to other separation techniques such as ion chromatography [107], HPLC [108, 109, 70] and flow-injection analysis [17, 110-112]. Although Haddad and co-workers [113] have used C⁴D in electrochromatography, applications of C⁴D in CEC in general have been very limited to date. Kubáň *et al.* explained the determination of inorganic cations by OT-CEC using an anionic polymer wall-coating as stationary phase [114].

1.3 Capillary electrophoresis coupled with sequential injection analysis

Until the 1990s, flow-injection analysis (FIA) was generally welcomed in academic analytical chemistry laboratories as an automated method whereby into a solution with continuous flow, sample is injected into the continuous flow of a carrier solution. The injected sample solution forms a zone that flows toward the detector. This aspect has been used to develop FIA systems for a wide range of analytical techniques. Sequential injection (SI) is a novel technique that evolved from FI [115], and is based on computer controlled programmable flow allowing rapid, precise, efficient injection of samples and reagents into one channel. J. Ružicka and G. D. Marshall introduced sequential injection analysis (SIA) for the first time in 1990 [116], where they

employed the “stopped” flow method for the analysis of thiocyanates. Soon afterwards, Ružicka also reported the first review on the principles of SI flow methodology [117]. From that time, the expansion of SIA was eminent and a diverse spectrum of applications was reported [118-122].

The basis of SIA is that the method relies on multi-tasks that can easily be performed in a single channel regarding controlled partial dispersion and repeatable sample manipulation. Multi-tasking is only possible by employing a multi-port selection valve to redirect solutions according to the controlled program. A schematic diagram of the conventional SIA configuration is given in figure 6.

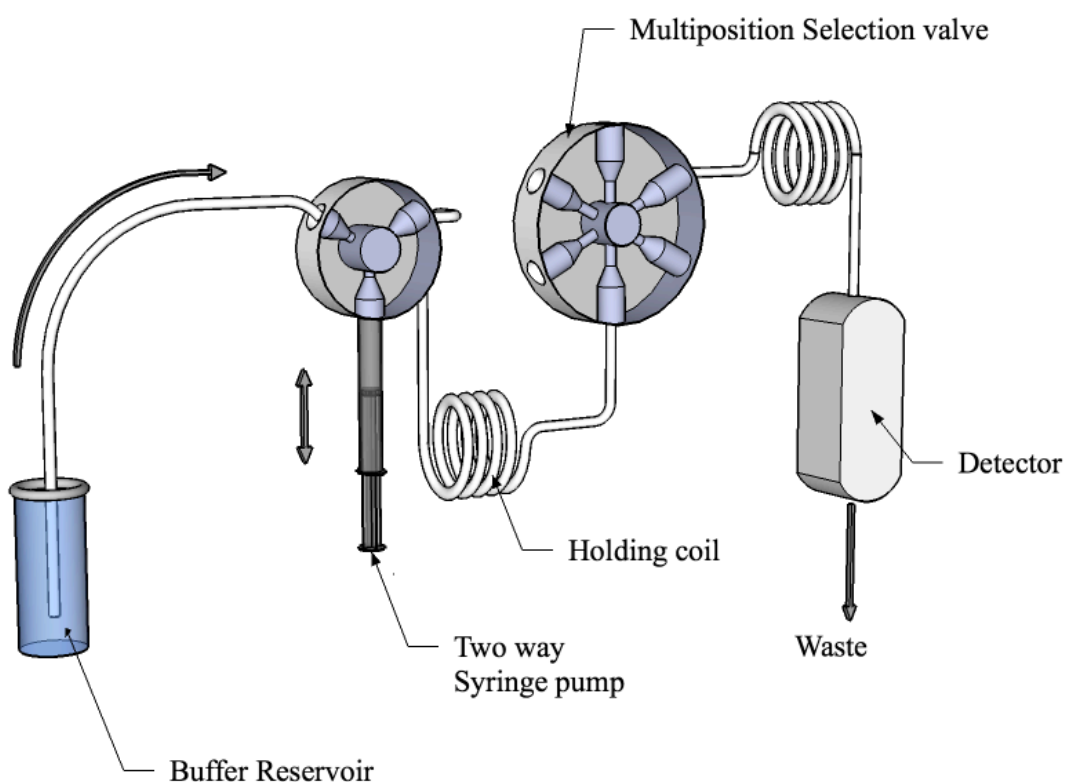


Figure 6. Schematic diagram of the basic SIA system setup

The performance of SIA depends on a multi-position selection valve and the driving force. The device that provides the force is usually either a peristaltic or a piston pump. A computer controls the whole system and, aspiration of the liquids is mostly carried out by the selection valve and propulsion with a two-way motor driven pump.

Recent introduction of the micro SI lab-on-valve (LOV) is considered to be the third generation of FIA [123], where even lower consumption of reagents and samples is required. These developments where every part of the equipment can be unified and modeled in one box, and where small volumes are needed for measurements, can be considered as a great opportunity for clinical and environmental analysis [124-127]. Enhanced functionality of the flow cell for detection as well as descended integrated instrumentation for fast, automated analysis were becoming beyond the abilities of many research groups due to challenges in equipment support and construction disputes. This was overcome with the arrival of the Lab-at-Valve (LAV) modified configuration of SIA, where the flow cell is integrated onto the selection valve meaning that all the components are remaining attached to the purchased valve. Hence, this recent development exhibits all the ease-of-use of LOV and since then, the growth in applications has been noted [128-130].

In SIA, if determination of more than one compound is necessary, derivatization of the analytes with chemicals is usually required. This makes the flow analysis scheme very complicated. On the other side, coupling of the SIA is more desirable with LC or CE because these present no complicated technical confrontations. As an automated system, SIA also uses pressure to initiate the flow as in LC. Some drawbacks such as the high costs of instrumentation or equipment maintenance along with the high backpressure during the analytical procedure have had a negative impact on its prevalence. Coupling SIA with CE, which is based on a syringe pump and multi-position selection valve, makes SIA capable of simultaneous detection. Moreover, this combination of powerful separation mechanisms of electrophoresis with automated SI technique manifests with advanced aspects of both, CE and SIA, *i.e.* high separation efficiency, absence of experimental complications, small solution consumption together with the accurate manipulation of small liquid volumes, and is program controlled. Although, it can be a technical challenge when the pressure-induced flow from SIA confronts the plug flow in CE, the employment of a syringe pump concedes reproducible pressurization of the capillary for injection. In addition, the use of a syringe pump allows capillary rinsing and conditioning without the need to modify the instrument. However, the required use of the high voltages can cause some deficiency and malfunctions (defect) of the electronic controls. Employment of capillaries in CE necessitates low injection volumes in the nL range and therefore

flow splitting is needed. This has been accomplished with specially designed interfaces that are compatible with flow mode as well as with capillary electrophoresis mode [131, 132, 18, 17, 133-136]. Schematic drawing of a conventional SIA-CE combination and commonly used interfaces are shown in figure 7.

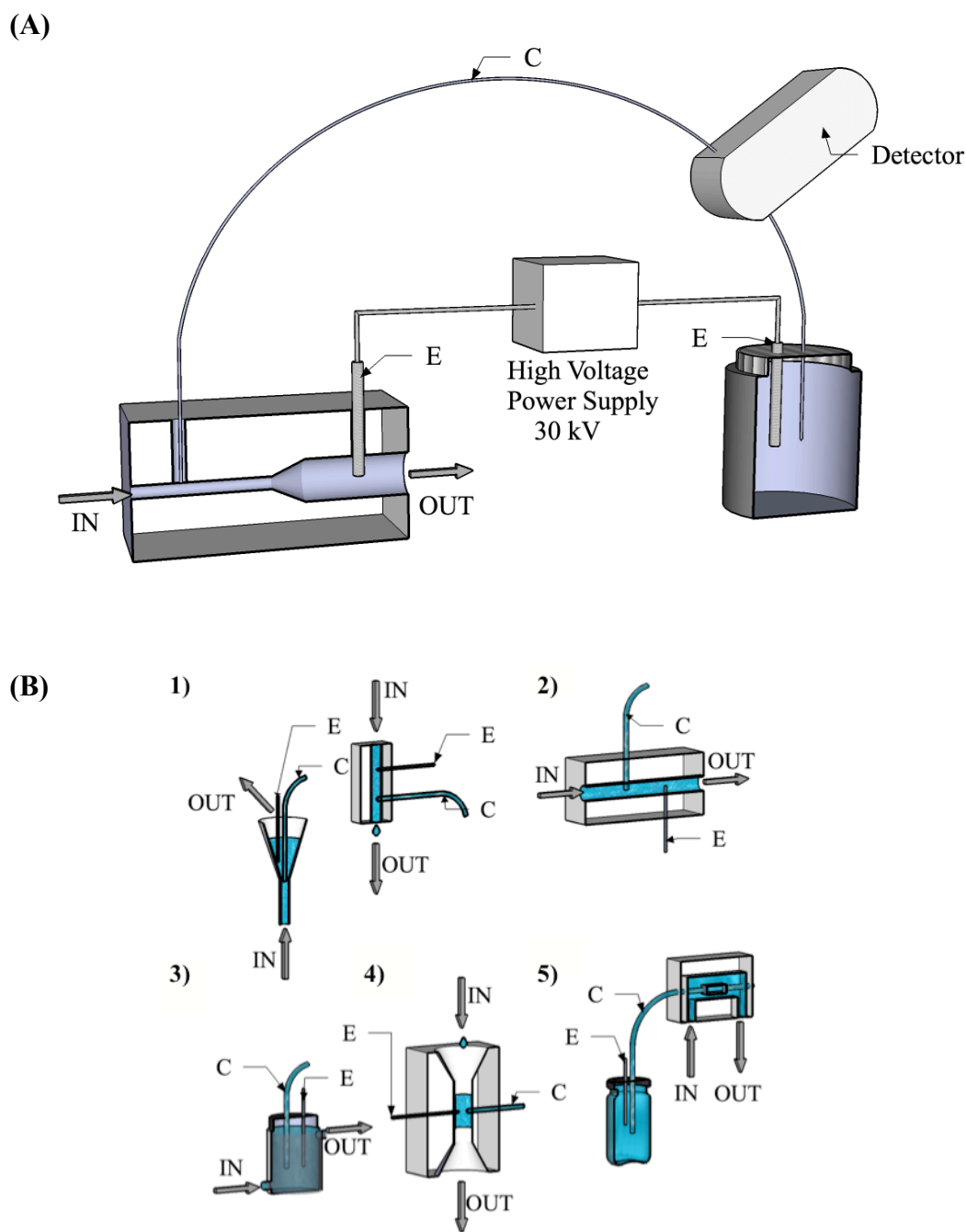


Figure 7. (A) Schematic drawing of conventional SIA-CE setup and (B) Some of split-flow interfaces: 1) conical and H-chip design, 2) lockable split-flow interface, 3) flushed vial interface, 4) falling-drop interface, 5) membrane

based on-capillary interface; Electrode (E), capillary (C), flow entrance (IN), outlet (OUT).

In 1997, flow-based techniques coupled with CE were first reported by Kubán *et al.* [17] and Fang *et al.* [18] and in 2003 in the work of Ružicka and co-workers, insulin derivatization and anion separation were demonstrated [137, 135]. In the work of Hauser and co-workers, C^4D was employed for the rapid separation and detection of inorganic cations and anions in a short capillary [138]. Using the same detection method, in the work of Mai *et al.* [139] reported the on-site monitoring of the concentrations of inorganic anions and cations. They also showed an optimized system for automated on-line preconcentration before separation in order to improve CE detection limits by determining drug residues in water [140]. From the same group separation of carboxylates and 16 fast inorganic anions and slow organic anions was reported [141]. Zacharis *et al.* [136] demonstrated the combination of a SIA-CE system with laser-induced fluorescence as a detection method. More reports of the extension of CE with SIA systems can be found in [142-145, 133, 146].

1.4 Research objectives

Five correlative research objectives were pursued in this dissertation mainly to further develop and investigate CE- C^4D techniques in order to extend the applications of capacitively coupled conductivity detection in capillary electrophoresis and to examine modifications to such a system, including coupling with sequential injection analysis. In detail description of the projects is in the chapter of Results and Discussion. Different cell designs and system settings were tested to determine the performance, cell geometry and feasibility of the method. Some of the fundamental aspects were investigated and reported hereinafter. According to interrelated similarities among projects, suitable approach was undertaken.

- I. *Application of capillary electrophoresis with C^4D for determination of DNA fragments.*** DNA was chosen as the desired target for this dissertation due to the possibility that this application can be useful for the identification of specific microorganisms in cell culture. Moreover, genetically modified organisms derived from food must be specially labeled or banned and for this

reason, simple ways to detect them are required. Over the past few decades, hundreds of applications have been reported for CE-C⁴D but to the best of our knowledge none have involved the determination of DNA fragments. The composition of the buffer was examined in order to reach effective determination of DNA fragments. The developed method was compared with the most commonly used technique for this application, slab gel electrophoresis. Two CE instruments with C⁴D detectors were used for the measurements: a commercial instrument and a homemade system. Commercial bench-top CE system is directed towards laboratory usage and is not meant to be portable diagnostic platform, although it provides the basis for many medical diagnostics. On the other side, the homemade system is portable and well suited for various diagnostics in the clinic or in the field and can be used for practical realization of point-of-care applications such as public health surveillance and clinical medicine. This combination of portability, performance and cost-effectiveness of the system will enable more accessible healthcare.

II. *Application of sequential injection analysis coupled with CE-C⁴D for pressure-assisted separation of artificial sweeteners.* The employment of pressure assistance for electrophoretic separation was suggested for the determination and separation of the most commonly used artificial sweeteners. CE-C⁴D was coupled with a sequential injection analysis (SIA) manifold that is based on a bidirectional syringe pump and a multiposition selection valve. Namely, aspartame, cyclamate, saccharin and acesulfame K were quantified by hydrodynamic pumping optimized for two sets of conditions, either for low detection limits or for fast analysis time. Employment of the commercial CE instrument was not suitable for carrying out measurements, as it was not possible to use narrow internal diameter capillaries. Reason for employment of the narrow capillaries was the band broadening generated by hydrodynamic pumping. It has been shown that narrow capillaries can be applied to SIA-CE-C⁴D for measurements done in food samples without degradation of the detection limits and with improvement of the separation efficiency. All the operation steps and measurements were controlled with the computer with possibility to modify electrophoretic parameters during the experiment run.

- III. ***Exploration of a referenced C^4D detector cell and its features in CE.*** A dual C^4D detector for CE was developed with such an approach that the changes in the buffer composition are instantly accounted for. In previous versions of the cell, electronic zero setting of the baseline was adjusted manually but that is no longer needed with this version. The new C^4D cell design is demonstrated for the detection and determination of inorganic cations in capillary electrophoresis.
- IV. ***Real time monitoring in CE using an array of C^4D detectors.*** The SIA-CE- C^4D system was optimized for operation where pressure was incorporated for sample injection and positioning along the fixed capillary when an array of 16 C^4D detectors is employed. The use of a computer controlled motor driven syringe pump allows for different variations of the flow and consequently can be used to obtain separation profiles. Determination of inorganic anions and cations was examined. Constant progress of the peaks movement from the injected sample plug and passing throughout an array of 16 detectors was demonstrated. Until now, only simulated monitoring using special software has been possible for studying the electrophoretic processes throughout the capillary. With such a system setup, it is possible to do in-situ investigation of the fundamental and background processes of the separation *i.e.* peak shapes, separation dynamics, conductivity changes *etc.*
- V. ***Study on the effect of the electrolyte concentration.*** The detectors in C^4D are in most cases used with low conductivity buffer solutions. When the higher conductivity buffers were employed with very narrow capillaries, high signal-to-noise ratio was noticed. That was not in agreement with the fundamental aspects of the axial contactless conductivity detection. In order to clarify the unexpected effect of the buffer concentration on sensitivity and to reach a better understanding of the performance of C^4D in capillary electrophoresis, particular investigations were carried out. Studies on some of the fundamental processes of the cell such as behavior, response and properties together with the geometry of the new cell design are reported. It opens the possibility that the present effect is a result of the synergistic effect of several factors, although some of the aspects are explained, the solution for the problem still remains to be investigated.

2. Results and Discussion

Most of the sections from this thesis have been published or are in press to journals in analytical chemistry. Accordingly, topics in this section will be presented with a resume of five projects gathered with reprints of two published articles, two manuscripts in press and an on-going project. At the start, Chapter 2.1 describes the application of contactless conductivity detection in capillary electrophoresis with determination of PCR products. The work, where hydrodynamic pumping coupled with an SIA system has been used for separation and determination of the most commonly used artificial sweeteners, is presented in Chapter 2.2. Chapter 2.3 is devoted to a brief study that has been undertaken on the further development of the C⁴D detector, and a report of the cell behavior is detailed. As described in Chapter 2.4, further exploration and monitoring of the separation dynamics within the capillary, using array of 16 C⁴D detectors combined with the SIA-CE-C⁴D system, was investigated. In Chapter 2.5, characteristics and specific fundamental behaviors of the cell are explained in order to investigate the effect of the conductivity of the electrolyte solution on the sensitivity of the cell. At the end, one article previously described in Chapter 2.1, will be presented in appendix.

2.1 Determination of PCR products by capillary electrophoresis with contactless conductivity detection

The routine method for DNA analysis is electrophoresis on a slab gel, but with CE, faster separation can be managed without derivatization and labeling of the samples. As the CE process also offers the possibility to be automated, C⁴D was found as a good alternative method. Separations of DNA fragments and PCR products were studied. Electrophoretic separation was carried out initially for DNA mass ladder accommodating fragments of 100, 200, 400, 800, 1200, and 2000 bp to cover a wide range of interest. This has been successfully achieved with contactless conductivity detection after encompassing optimized separation conditions such as type and concentration of the sieving matrix, type and pH of background electrolyte solution, applied high-voltage *etc.* Low viscosity not cross-linked polyacrylamide, namely Polyvinylpyrrolidone, at a concentration of 5% was adopted as a sieving polymer after careful study on the effect of the concentration. As predicted, increased

concentration prompted an enhanced baseline resolution in a separation buffer comprised of 20 mM Tris and 20 mM 2-(cyclohexylamino)ethansulphonic acid at pH 8.5. A bacterial plasmid DNA template isolated from *Escherichia Coli* was used for PCR reaction to synthesize two desired fragments of specific size. Sizes were selected to fit into the range of the DNA mass ladder for easier comparison. Hydrodynamic injection was carried out as it allows analysis without additional purification of the sample. Determination was successful but the results from that experiment, observed from the electropherograms, showed considerably low sensitivity due to inappropriate setup for PCR reaction where not enough cycles were performed resulting with low concentrations of the PCR sample. To anticipate this factor, another PCR reaction for two designed fragments was carried out by increasing the number of PCR cycles. Satisfactory detection and improvement of sensitivity was observed. Following adequate detection of bacterial plasmid PCR product, further analysis of a food sample regarding genetically modified organisms (GMO) deriving from genomic DNA soybeans were accomplished. All optimized conditions for determination of PCR products were considered and employed. When compared with the conventional slab gel electrophoresis that takes usually 2 h for convenient separation, with CE-C⁴D determination was completed in less than 30 min. Moreover, the potential for development of miniaturized and portable instruments appears, as some of the measurements were carried out on the in-house built portable instrument, see figure 8.

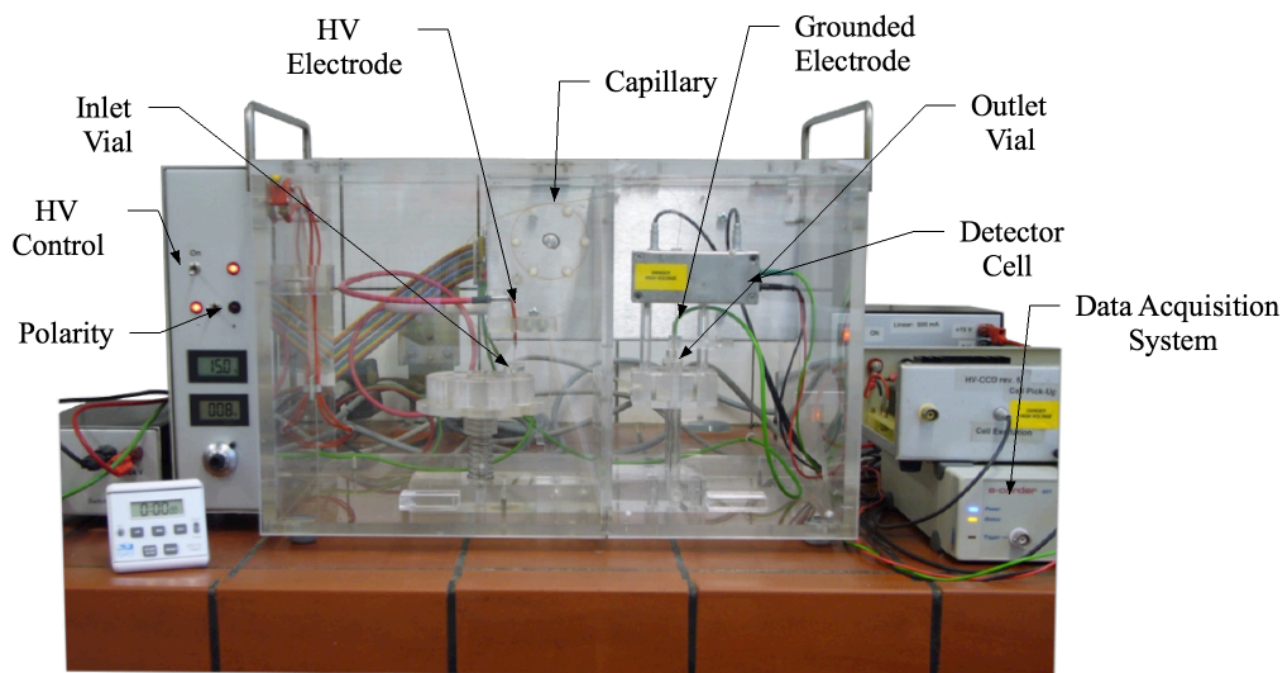


Figure 8. Portable purpose made CE-C⁴D system

1st project:

**Determination of PCR products by capillary electrophoresis with contactless
conductivity detection**

Journal of Separation Science (2012), 35, 3509-3513

Marko Stojkovic¹
Narasimha R. Uda¹
Peter Brodmann²
Milica Popovic¹
Peter C. Hauser¹

¹Department of Chemistry,
University of Basel, Basel,
Switzerland

²Biosafety Laboratory, State
Laboratory Basel City, Basel,
Switzerland

Received August 21, 2012

Revised September 5, 2012

Accepted September 5, 2012

Research Article

Determination of PCR products by CE with contactless conductivity detection

The use of CE with contactless conductivity detection for the determination of PCR products is demonstrated for the first time. The separation of specific length PCR products according to their size could be achieved using 5% PVP as a sieving medium in a separation buffer consisting of 20 mM Tris and 20 mM 2-(cyclohexylamino)ethansulphonic acid (pH 8.5). A fused silica capillary of 60 cm length and 50 μm id and an applied separation voltage of -15 kV were employed and separations could be completed within 20–50 min. PCR amplified DNA fragments of different sizes obtained from different bacterial plasmid templates as well as a fragment from genomic DNA of genetically modified soybeans could be successfully identified.

Keywords: Capillary electrophoresis / Contactless conductivity / Detection / Genetically modified organisms / PCR fragments
DOI 10.1002/jssc.201200800

1 Introduction

CE has a number of advantages compared to planar gel electrophoresis. In case of CE, higher voltages can be applied and therefore faster separation times are obtained; staining with toxic chemicals such as ethidium bromide is not required for detection and the CE process can easily be automated. For these reasons, CE is now used routinely for DNA sequencing. On the other hand, other forms of DNA analysis, such as the determination of restriction fragment length polymorphism and the simple analysis of PCR-amplified DNA fragments, are often still carried out by planar electrophoresis and have only partly been replaced by capillary methods.

In both formats, planar electrophoresis and CE, DNA fragments are separated by their size in a sieving matrix. Conventionally, cross-linked polyacrylamide gels have been used very frequently in planar electrophoresis. In contrast, in CE, entangled not cross-linked polymer solutions are now commonly used as the sieving material [1]. The polymer solutions should have low viscosity for easy handling, and should have the ability to coat the capillary wall in order to suppress the EOF and prevent adsorption of analytes. Many different polymers have been studied for the separation of DNA fragments such as linear polyacrylamide, PVP, poly-N,N-dimethylacrylamid, polyvinylalcohol, polyethyleneoxide, and various cellulose derivatives such as hydroxyethyl cellulose, hydroxypropyl cellulose. For details see these review articles [2, 3].

Correspondence: Dr. Peter C. Hauser, Department of Chemistry, University of Basel, Spitalstrasse 51, 4056 Basel, Switzerland
E-mail: peter.hauser@unibas.ch
Fax: + 41-61-267-1013

Abbreviation: C⁴D, capacitively coupled contactless conductivity detection

Detection for DNA in CE is usually carried out via UV-absorption as described previously [4–7] or for sequencing and when low detection limits are required by fluorescence as described previously [8–11]. However, labeling is generally required for the latter method.

Capacitively coupled contactless conductivity detection (C⁴D) is an attractive alternative detection method. It is inherently much simpler than optical detection and suitable for any ionic species without requiring derivatization. The technique also enables the design of inexpensive and compact, portable, battery-operated CE instruments [12–16]. The standard UV detection, on the other hand, is not readily implemented for such instruments due to the high power consumption of conventional UV lamps. For details on C⁴D, recent review articles are available [17–20].

A few instances of the detection of DNA in CE by conductivity measurements have been reported. Galloway et al. [21] used conventional contact conductivity measurements in 2002 for the detection of PCR products in electrochromatography. In 2005, Abad Villar et al. [22] demonstrated the suitability of C⁴D for the detection of a DNA fragment on a lab-on-chip device. Xu et al. [23] used a potential gradient detector (a form of indirect conductometric detection) for determining DNA ladder segments and this was followed by a paper using carbon nanotubes in the sieving medium and C⁴D [24]. Mühlberger et al. [25] reported the separation and detection of a ladder on a microfluidic chip using contactless conductivity measurement. Although these studies indicated the possibilities, practical uses of CE-C⁴D for DNA analysis have not yet been shown. In this paper, the application of the determination of PCR products from plasmid DNA and also from genomic DNA is demonstrated. Different fragments obtained from bacterial plasmid templates were first determined. This application may be useful, for example, for the identification of particular microorganisms in

Table 1. List of primers used for PCR amplification of the DNA fragments

	Primer name	Primer sequence (5'–3')
1	B1 ⁸ HisDELYodASKA (Forward primer)	CGATTCGCTTTACAAACTGGCTGTTGCTTAGGTGTC
2	B2 ⁸ HisDEL-BlcASKA (Forward primer)	CGCCTGCTGCCGCTGGTGGCGGC
3	R ⁸ ASKAseq, cloning (Reverse primer)	CAGGTCGACCCTTAGCGGCCGATAGGCC
4	F-pCM655 (Forward primer)	GAGCGGATAACAATTTACACAGGAAACAG
5	F-SEQ pCM655 (Forward primer)	CGGTACGTCGGACCGCGACATGT
6	R-SEQ pCM655 (Reverse primer)	CACCGCGTACTGCCGCCAGGCA
7	Soy-F (Forward primer)	GAAGCAACCAAACATGATCTC
8	Soy-R (Reverse primer)	ATGGATCTGATAGAATTGACGTTA

cell cultures. The second application concerned the identification of genetically modified soybeans. In many jurisdictions, food derived from genetically modified organisms must be specially labeled or is even banned completely, and therefore simple means for their detection are desired. The developed method for the analysis of PCR products is suitable for implementation on portable CE-C⁴D instruments, and has the potential for field measurements.

2 Materials and methods

2.1 Chemicals

PVP (MW 1 300 000) was obtained from Sigma-Aldrich (Buchs, Switzerland), Tris and CHES were obtained from Fluka (Buchs, Switzerland). The DNA mass ladder was purchased from Invitrogen (Carlsbad, CA, USA) that is composed of an equimolar mixture of six low-mass ladder DNA fragments of 100, 200, 400, 800, 1200, and 2000 bp (base pairs). DNA Taq polymerase with 10× Thermopol reaction buffer and deoxynucleoside triphosphates (dNTP's) were obtained from New England Biolabs (Maine, USA) and oligonucleotide primers from Mycosynth (Balgach, Switzerland). The DNA template for genetically modified organism soybean flour was obtained from the Cantonal Laboratory of Basel-City and the genomic DNA was extracted by using the genomic extraction REExtract-N-AmpTM Seed PCR Kit obtained from Sigma (St. Louis, Missouri, USA).

2.2 PCR

Plasmid DNAs (pCA24N-Yoda, pCA24N-Blc, and pCM655Empty) were transformed and isolated from the XL1-Blue strain by using a Wizard plus Miniprep Kit from Promega (Madison, WI, USA) and genomic DNA of genetically modified soybeans (soybean template Roundup Ready GM-Soybean-EX961053A) by using the REExtract-N-AmpTM Seed PCR Kit. These DNA sources were used as templates for the production of PCR fragments of the specific sizes of 180, 400, 489, 555, and 674 bp by using corresponding primers (Table 1). All PCRs were performed

on an Eppendorf PCR Thermal Cycler (Hamburg, Germany). The PCR reactions were carried out in a total volume of 50 µL, containing 300 nM of each primer (forward and reverse), 4% DMSO, 1.6 mM dNTP's (0.4 mM each), 5 U Taq polymerase, 10× Thermopol reaction buffer, 100 ng of template for genomic DNA, and 50 ng of plasmid DNA. The PCR reaction consisted of an initial denaturation step at 95°C for 3 min followed by 40 PCR cycles, each cycle consisting of denaturation at 95°C for 3 min, annealing at 59.5°C for 1 min, and extension at 72°C for 3 min. The final elongation was for 10 min at 72°C to ensure full extension of all amplified fragments. The PCR products were purified on Wizard SV PCR-Gel cleanup minicolumns (Promega) and eluted with 10 mM Tris-HCl (pH 7.5) containing 1 mM EDTA. This buffer was selected as it corresponds to the buffer in which the DNA mass ladder was supplied.

2.3 Instrumentation

Two CE instruments with contactless conductivity detectors were used for the measurements: a commercial as well as an in-house constructed system. The commercial instrument was a PrinCE 500 (Prince Technologies, Emmen, the Netherlands) and used for the work presented in Figs. 1–3. The unit built by us was based on the design of a portable, battery-powered instrument described earlier [16], but utilized a high-voltage supply from Spellman (CZE 2000R, Spellman, Pulborough, UK) capable of delivering up to 30 kV and was mains powered. It was used for the measurements presented in Figs. 4 and 5. The detectors employed with both instruments were also constructed in-house according to a design reported earlier [26]. The signals were monitored and recorded with an e-corder data acquisition system (eDAQ, Denistone East, NSW, Australia).

2.4 CE

Fused silica capillaries of 60 cm length, 50 µm id, and 365 µm od (Polymicro Technologies, Phoenix, AZ, USA) were used for the CE measurements. New capillaries were conditioned by rinsing with 0.1 M NaOH for 20 min and

then with deionized water for 20 min, followed by 0.1 M HCl, and again with deionized water for 20 min. Before each run, a capillary was rinsed with the background buffer for 3 min. The system was then equilibrated by applying the separation voltage until a stable baseline was obtained. For the analysis of DNA ladder and PCR samples, hydrodynamic injection was used. On the instrument constructed internally this was carried out by siphoning, through lifting the injection part of capillary up to 30 cm height, and on the commercial instrument, a pressure of 13.8 kPa was applied. In both cases, the injection time was 45 s. The background buffer consisted of 20 mM Tris, 20 mM CHES (pH 8.5), and 5% PVP (except where stated otherwise).

3 Results and discussion

3.1 Selection of sieving polymer and choice of the buffer

As sieving matrix a PVP-based medium reported by Xu et al. [23] and used in their work using potential gradient detection was adopted. The polymer was employed by Xu et al. [23] for its relative low viscosity and its ability to coat the inner capillary surface and thereby minimize the EOF. Important for application in CE-C⁴D is also its electrical neutrality. As background electrolyte, a buffer composed of 20 mM Tris/CHES (pH 8.5) was used. This was also adopted from Xu et al., but used at a lower concentration to improve baseline stability.

Initially, the experiments were carried out with a DNA mass ladder containing fragments of 100, 200, 400, 800, 1200, and 2000 bp that covers the broad range of interest for the PCR products to be detected. The effect of the concentration of PVP for the range from 1 to 6% w/v on the separation is shown in Fig. 1. Note that due to the responsiveness of C⁴D to all ionic species, several peaks caused by constituents of the buffer solution in which the ladder is contained are also observed. As expected, an increase in the concentration of the polymer led to increased delay times for the fragments and increasingly improved separation between the peaks. For concentrations of PVP from 1 to 3%, the separation was not adequate due to strong interference of the buffer matrix. For the higher concentrations of the polymer, the ladder components were well separated and removed from peaks due to the matrix alone. However, in contrast to the normal tasks of CE it is not just necessary to achieve baseline separation of the fragments, but normally the spacing of the peaks should be adequate to allow distinction of the PCR products of interest for a task at hand. The concentration of 5% was adopted for the subsequent work. Solutions of higher concentrations (6% and more) were not suitable, as flushing of the capillary was found exceedingly difficult due to the higher viscosity. Note that, this concentration is higher than that used by Xu et al., who reported 2%. Also tested was the influence of the applied separation voltage between 12 and 21 kV using the buffer containing 5% PVP and the results are shown

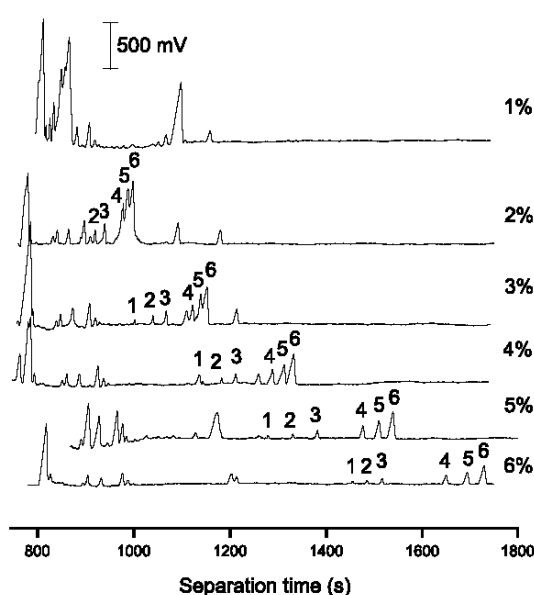


Figure 1. Electropherograms of low-mass DNA ladder fragments of (1) 100 bp, (2) 200 bp, (3) 400 bp, (4) 800 bp, (5) 1200 bp, and (6) 2000 bp in different concentrations of PVP w/v. Experimental conditions: fused silica capillary of 60 cm total and 55 cm effective length with 50 μ m id. Buffer: 20 mM Tris, 20 mM CHES (pH 8.5). Separation voltage: -16 kV.

in Fig. 2. Clearly, variation of the high voltage is a convenient method to achieve the desired compromise between the required separation (spacing of the peaks) and the analysis time.

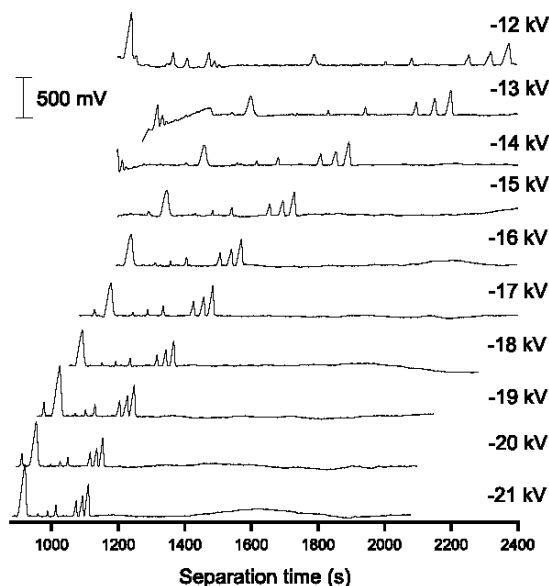


Figure 2. Electropherograms of low-mass ladder DNA fragments in a buffer consisting of 20 mM Tris, 20 mM CHES, and 5% PVP at different separation voltages. Other conditions as for Fig. 1.

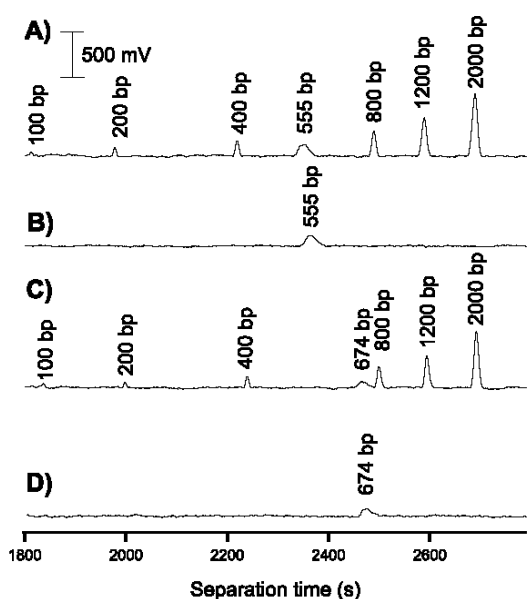


Figure 3. Electropherograms of PCR products from bacterial plasmids pCA24N-Blc, pCA24N-YodA with and without low-mass DNA ladder. (A) PCR fragment of pCA24N-Blc bacterial plasmid of 555 bp length with the low-mass DNA ladder, (B) PCR fragment of 555 bp, (C) PCR fragment of pCA24N-YodA bacterial plasmid of 674 bp length with the low-mass DNA ladder, (D) PCR fragment of 674 bp. Separation voltage: -10 kV. Other conditions as for Fig. 2.

3.2 Analysis of PCR samples

3.2.1 Bacterial plasmid DNA

The first experiments were carried out using the plasmid DNA isolated from *Escherichia coli* bacteria. Two PCR reactions were carried out; one PCR reaction using primers 1 and 3 and plasmid DNA, pCA24N-YodA, as template and another PCR reaction using primers 2 and 3 and plasmid DNA, pCA24N-Blc, as template yielding fragments of 674 bp and 555 bp, respectively. The PCR products were injected hydrodynamically, because they contain a high salt concentration that prevents electrokinetic injection without prior to desalting of the sample. Hydrodynamic injection allows direct analysis of PCR products without further purification of the PCR product. The resulting electropherograms are shown in Fig. 3. The products of 674 and 555 bp could be clearly detected and are positioned between the peaks for the fragments of 400 and 800 bp of the low-mass DNA ladder. However, the peaks for the PCR products showed a relatively low sensitivity. Note that a relatively low separation voltage of -10 kV was employed in order to achieve baseline separation, resulting in relatively long electropherograms.

In the second experiment, another plasmid DNA template pCM655-Empty was used as a PCR template with two pairs of primers: primers 4 and 6 and primers 5 and 6 (Table 1), to yield two fragments of 489 bp and 180 bp, respec-

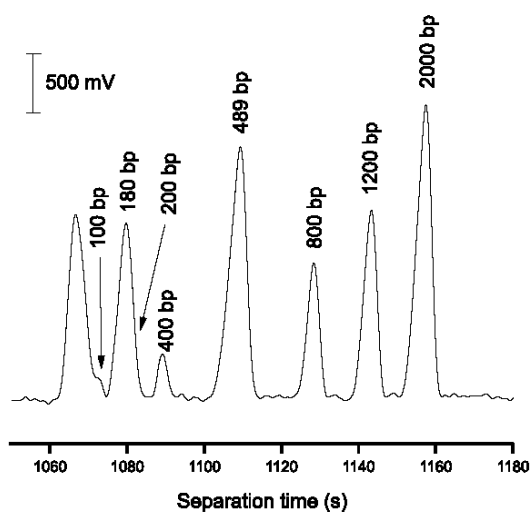


Figure 4. Electropherogram of PCR products from bacterial plasmid pCM655-Empty of 180 bp and 489 bp length with the low-mass DNA ladder. Capillary: 56 cm total length and 51 cm effective length. Separation voltage: -20 kV. Other conditions as for Fig. 2.

tively. In order to obtain a higher concentrations of the PCR products and thus to improve detection sensitivity, the number of PCR cycles was increased to 40. The product was mixed with the ladder consisting of the six entities of 100, 200, 400, 800, 1200, and 2000 bp fragments, and then separated by the CE-C⁴D procedure. The resulting electropherogram is shown in Fig. 4. As expected, the new tall peak corresponding to the 489 bp fragment is located nicely between the 400 and 800 bp ladder peaks. This was possible with the relatively high separation voltage of -20 kV leading to a considerably faster separation time, about 20 min duration, than for the previous separation. Under these conditions, the second PCR product of 180 bp, with its comparatively high concentration, overlaps with the smaller peak of the 200 bp fragment of the ladder. The even smaller peak of the ladder fragment of 100 bp is also found to overlap with an unidentified peak (left most peak in the electropherogram) due to a background ion in the sample matrix. An improved separation of these early peaks, if necessary, would be possible by a reduction of the separation voltage.

3.2.2 Genetically modified soybeans

After successful detection of PCR product of the plasmid DNA, the detection of PCR product from genomic DNA of genetically modified soybeans was investigated as a prominent representative of an application of PCR for the identification of food samples. Roundup Ready GM-Soybean-EX961053A was used as a genomic DNA template. The forward Soy-F and reverse Soy-R primers from Table 1 were designed in order to obtain a PCR product of 400 bp length. The annealing temperature of the primers was optimized to $T_a = 55.5^\circ\text{C}$ and the number of PCR cycles was 30. The resulting capillary

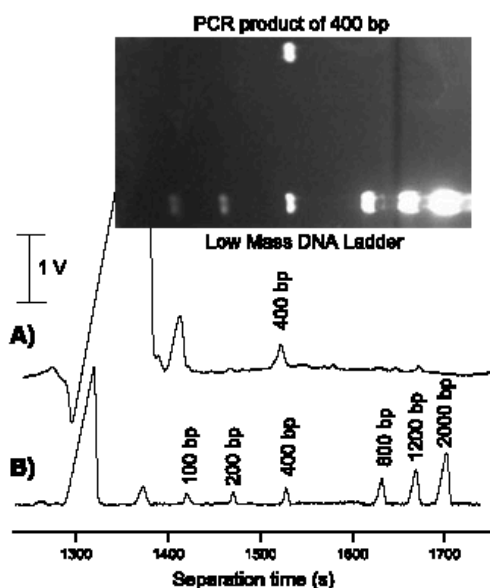


Figure 5. Electropherograms of the PCR product from Roundup Ready GM-Soybean-EX961053A of 400 bp length (A) and low-mass ladder (B). Separation voltage: -15 kV. Other conditions as for Fig. 2. The inset is a picture of the ethidium bromide stained agarose gel also showing both separations.

electropherograms of PCR product and ladder are shown in Fig. 5 along with a picture of a conventional 1% agarose slab gel electrophoresis. Note that this conventional agarose gel electrophoresis separation required approximately 2 h, whereas the separation by CE could be completed in less than 30 min using optimized conditions. The left most peaks in the capillary electropherogram are again due to unidentified matrix elements from the sample.

4 Concluding remarks

It has been demonstrated that CE-C⁴D is suitable for the determination of PCR products and may be employed in the detection of DNA fragments amplified from varied sources. The method is more easily automated than the currently still widely used slab gel separations. The separation could be achieved in a much shorter period of time, and further optimization in this regard is possible. CE-C⁴D does not require sample preprocessing and there is no need for labeling. A further advantage is the simplicity of the method and the potential for implementation of the method in portable instruments. This is demonstrated by the results presented in the last two figures, which were obtained on the quasifield portable instrument built in house, and are undistinguishable from the measurements carried out on the conventional commercial instrument.

The authors would like to thank Zhang Ling, and Gong Xiao Yang for some preliminary tests and Marc Creus for assistance

with the PCR experiments. This work has been supported through grant nos. 200020–126384/1 and 200020–137676/1 from the Swiss National Science Foundation.

The authors have declared no conflict of interest.

5 References

- [1] Karger, B. L., Chu, Y. H., Foret, F., *Annu. Rev. Biophys. Biomol. Struct.* 1995, **24**, 579–610.
- [2] Barbier, V., Viovy, J.-L., *Curr. Opin. Biotechnol.* 2003, **14**, 51–57.
- [3] Xu, F., Baba, Y., *Electrophoresis* 2004, **25**, 2332–2345.
- [4] Beckmann, A., Gebhardt, F., Brandt, B. H., *J. Chromatogr. B* 1998, **710**, 75–80.
- [5] Giovannoli, C., Anfossi, L., Tozzi, C., Giraudi, G., Vanni, A., *J. Sep. Sci.* 2004, **27**, 1551–1556.
- [6] Stellwagen, N. C., Gelfi, C., Righetti, P. G., *Biopolymers* 1997, **42**, 687–703.
- [7] Wang, Q., Xu, X., *Chin. Chem. Lett.* 2003, **14**, 1278–1280.
- [8] Akbari, A., Marthinsen, G., Lifjeld, J. T., Albrechtsen, F., Wennerberg, L., Stenseth, N. C., Jakobsen, K. S., *Electrophoresis* 2008, **29**, 1273–1285.
- [9] García-Cañas, V., González, R., Cifuentes, A., *J. Agric. Food Chem.* 2002, **50**, 4497–4502.
- [10] Mátyás, G., Giunta, C., Steinmann, B., Hossle, J. P., Hellwig, R., *Hum. Mutat.* 2002, **19**, 58–68.
- [11] Skeidsvoll, J., Magne, U. P., *Anal. Biochem.* 1995, **231**, 359–365.
- [12] Blanco, G. A., Nai, Y. H., Hilder, E. F., Shellie, R. A., Dincoski, G. W., Haddad, P. R., Breadmore, M. C., *Anal. Chem.* 2011, **83**, 9068–9075.
- [13] Kubáň, P., Seiman, A., Makarotseva, N., Vaher, M., Kaljurand, M., *J. Chromatogr. A* 2011, **1218**, 2618–2625.
- [14] Kumar, A., Burns, J., Hoffmann, W., Demattio, H., Malik, A. K., Matysik, F. M., *Electrophoresis* 2011, **32**, 920–925.
- [15] Ryvolova, M., Preisler, J., Brabazon, D., Macka, M., *TrAC, Trends Anal. Chem.* 2010, **29**, 938–938.
- [16] Kubáň, P., Nguyen, H. T. A., Macka, M., Haddad, P. R., Hauser, P. C., *Electroanalysis* 2007, **19**, 2059–2065.
- [17] Kubáň, P., Hauser, P. C., *Electrophoresis* 2011, **32**, 30–42.
- [18] Kubáň, P., Hauser, P. C., *Electrophoresis* 2009, **30**, 176–188.
- [19] Trojanowicz, M., *Anal. Chim. Acta* 2009, **653**, 36–58.
- [20] Matysik, F. M., *Microchim. Acta* 2008, **160**, 1–14.
- [21] Galloway, M., Soper, S. A., *Electrophoresis* 2002, **23**, 3760–3768.
- [22] Abad-Villar, E. M., Kubáň, P., Hauser, P. C., *Electrophoresis* 2005, **26**, 3609–3614.
- [23] Xu, Y., Qin, W., Li, S. F. Y., *Electrophoresis* 2005, **26**, 517–523.
- [24] Xu, Y., Li, S. F. Y., *Electrophoresis* 2006, **27**, 4025–4028.
- [25] Mühlberger, H., Hwang, W., Guber, A. E., Saile, V., Hoffmann, W., *IEEE Sens. J.* 2008, **8**, 572–579.
- [26] Zhang, L., Khaloo, S. S., Kubáň, P., Hauser, P. C., *Meas. Sci. Technol.* 2006, **17**, 3317–3322.

2.2 Determination of artificial sweeteners by capillary electrophoresis with contactless conductivity detection optimized by hydrodynamic pumping

To control separation in capillary electrophoresis, it is necessary to optimize the system for accurate injection, separation, and detection as well as to record data in an independent way. For these purposes, a new system has been established on the basis of CE-C⁴D, combined with a sequential injection manifold. This setup utilizes a stepper-motor driven syringe pump connected to a holding coil for a multiport selection valve. A splitting needle valve was used for adjustment of the flow into two streams toward two solenoid isolation valves used for flushing of the capillary and accurate hydrodynamic injection. The high-voltage end was embedded in a safety box to prevent electrical arcing that can in turn lead to failure of the electric instrumentation in the system set-up. The entire modus operandi, along with flushing the interface and capillary, injection, separation, data recording, automatic switching of the high-voltage polarity and trigger respectively, was controlled with command sequences written in the software PumpLink. Modifications were possible even during a separation run. Notwithstanding, for optimizing resolution and analysis time, superimposition of a hydrodynamic flow has to be considered as one of the most useful parameters, although it tends to lead to band broadening. Employment of the narrow diameter capillaries can significantly decrease this conflicting effect and improve separation efficiency. Rapid separation of the most commonly used artificial sweeteners, namely aspartame, cyclamate, saccharin and acesulfame-K, was carried out with the application of pressure induced by the micro movement of the motor driven pump. Injection of the sample was performed with precise control and amount of the applied pressure for hydrodynamic pumping. Pressurization was determined using the flow rate with pressure drop and diameter and the length of the tubing. In comparison with conventional CE separation, analysis times for two differently optimized sets of measurements were reduced from 7 min to 3 min in the first case when a large sample plug was injected, and around 70 sec for a very small injection plug. The repeatabilities are similar in both cases whereas the limits of detection for the large plug were around 10 times lower than the values from the small injection plug.

2nd project:

Determination of artificial sweeteners by capillary electrophoresis with contactless conductivity detection optimized by hydrodynamic pumping

Analytica Chimica Acta (2013), 787, 254-259



Determination of artificial sweeteners by capillary electrophoresis with contactless conductivity detection optimized by hydrodynamic pumping



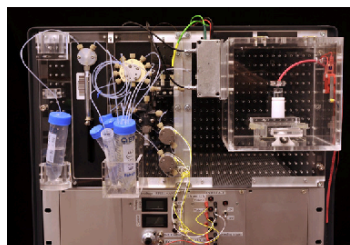
Marko Stojkovic, Thanh Duc Mai, Peter C. Hauser^{*}

Department of Chemistry, University of Basel, Spitalstrasse 51, 4056 Basel, Switzerland

HIGHLIGHTS

- Capillaries of 10 μm ID were employed.
- Superimposed hydrodynamic pumping is possible without penalty in band broadening with such narrow capillaries.
- Analysis times of less than 3 min were possible.
- The use of a computer controlled sequential analysis system allows flexible optimization of injection volumes and pumping rates.
- Detection limits in the low μM range were achieved.

GRAPHICAL ABSTRACT



ARTICLE INFO

Article history:

Received 10 April 2013
Received in revised form 16 May 2013
Accepted 23 May 2013
Available online 3 June 2013

Keywords:

Artificial sweeteners
Capillary electrophoresis
Contactless conductivity detection
Hydrodynamic flow
Sequential injection analysis

ABSTRACT

The common sweeteners aspartame, cyclamate, saccharin and acesulfame K were determined by capillary electrophoresis with contactless conductivity detection. In order to obtain the best compromise between separation efficiency and analysis time hydrodynamic pumping was imposed during the electrophoresis run employing a sequential injection manifold based on a syringe pump. Band broadening was avoided by using capillaries of a narrow 10 μm internal diameter. The analyses were carried out in an aqueous running buffer consisting of 150 mM 2-(cyclohexylamino)ethanesulfonic acid and 400 mM tris(hydroxymethyl)aminomethane at pH 9.1 in order to render all analytes in the fully deprotonated anionic form. The use of surface modification to eliminate or reverse the electroosmotic flow was not necessary due to the superimposed bulk flow. The use of hydrodynamic pumping allowed easy optimization, either for fast separations (80 s) or low detection limits (6.5 $\mu\text{mol L}^{-1}$, 5.0 $\mu\text{mol L}^{-1}$, 4.0 $\mu\text{mol L}^{-1}$ and 3.8 $\mu\text{mol L}^{-1}$ for aspartame, cyclamate, saccharin and acesulfame K respectively, at a separation time of 190 s). The conditions for fast separations not only led to higher limits of detection but also to a narrower dynamic range. However, the settings can be changed readily between separations if needed. The four compounds were determined successfully in food samples.

© 2013 Elsevier B.V. All rights reserved.

1. Introduction

Artificial sweeteners are widely used as additives in food, beverages and pharmaceutical products as a low calorie alternative to natural sugar. Diabetes patients, who have to control blood sugar, make use of them, as well as persons who wish to control their body weight or are concerned about dental caries. Since these

^{*} Corresponding author. Tel.: +41 61 267 1003; fax: +41 61 267 1013.
E-mail address: peter.hauser@unibas.ch (P.C. Hauser).

sweeteners are prepared by chemical synthesis, their presence in food is however the cause of extensive consumer mistrust [1]. Frequently used are aspartame, cyclamate, saccharin and acesulfame K. These compounds are often employed in combination as this leads to the masking of undesired aftertastes, such as bitterness [2]. The exact composition used in these mixtures is important in order to correctly balance the tastes.

The most common method for the determination of the artificial sweeteners is HPLC [2]. However, cyclamate requires chemical derivatization to make it detectable by the most commonly employed UV-absorbance method due to a lack of a chromophore. For this and other reasons few HPLC methods for the concurrent determination of the sweeteners exist and usually have been based on detection by mass-spectrometry [2]. An attractive alternative is capillary electrophoresis (CE) due to its simplicity, high separation power, relatively short analysis times and low consumption of consumables. Pesek and Matuska [3], Walker et al. [4] and Sabah and Scriba [5] reported methods for aspartame based on capillary zone electrophoresis with UV-detection. Boyce [6] and Frazier et al. [7] later extended the method for the simultaneous determination of aspartame, saccharin and acesulfame K. More difficult again is the determination of cyclamate, but methods for this species alone, based on its detection by indirect UV measurements, have also been developed [8,9]. The concurrent determination of a range of sweeteners which includes cyclamate is best carried out using a more universal detector. Schnierle et al. [10] and Kappes et al. [11] demonstrated the possibility of using potentiometric detection in zone electrophoresis for cyclamate and other sweeteners and Herrmannová et al. [12] have described an isotachophoretic method covering a total of 8 sweeteners employing conductivity detection. The use of contactless conductivity detection (C^4D) in zone electrophoresis is an other attractive and simple alternative and Tanayanyiwa et al. [13] in 2004 demonstrated the detection of acesulfame K and cyclamate on a lab-on-chip device using this technique. More recently Bergamo et al. [14] described the determination of the 4 species, aspartame, cyclamate, saccharin and acesulfame K, by CE- C^4D . A difficulty encountered by Bergamo et al. was related to the fact that a relatively high pH value of 9.4 had to be used in order to render all species in the anionic charged form required for separation and detection. In CE a high electroosmotic flow is then present, which means that for the determination of anions usually a surface modification is carried out in order to reverse the electroosmotic flow, so that it is the same direction as the migration of the anions. This was, however, not found possible, as the most often used approach, dynamic coating of the capillary wall by addition of cetyltrimethylammonium bromide (CTAB) to the running buffer, was found to interfere with the separation of the sweeteners [14]. Separation of the anionic sweeteners was therefore carried out by sweeping them against their mobility with the electroosmotic flow, which is not ideal because of the resulting relatively long separation times.

In a separate development, it has very recently been shown that it is possible to superimpose a bulk flow when carrying out electrophoretic separations in narrow capillaries with inner diameters of 10 μm [15–17]. This was found to be useful for the optimization of separation time and efficiency, and in the determination of anions the compensation of the electroosmotic flow is possible without requiring chemical additives [16]. This operating parameter can be changed readily between measurements, or even instantly during a separation. Despite its utility, the employment of pressure assistance during electrophoretic separations has hitherto largely been considered impossible due to potential band broadening caused by the laminarity of the hydrodynamic flow. However, for the narrow capillaries this is not an issue. Note, that these pressure assisted CE methods are enabled by C^4D , as the detection technique, in contrast to UV-detection, can be readily implemented

on the narrow capillaries and allows measurements without degradation of the detection limits [15–17]. In addition, the use of narrow capillaries is preferable as the separation efficiency is generally better, *i.e.* also in the absence of pumping [15].

Herein a more detailed study of the benefit of the superimposition of a bulk flow in the determination of anions by CE- C^4D is presented. The artificial sweeteners are a worthwhile application of this technique due to the call for conductivity detection when determining cyclamate and the difficulties imposed by the electroosmotic flow when including aspartame.

2. Experimental

2.1. Solutions

Ultrapure water of 18 M Ω cm resistivity, obtained from a Milli-Q 185 system (Millipore, Saint-Quentin-en-Yvelines, France), was used to prepare all solutions. All reagents were of analytical grade. Cyclamic acid (cyclohexanesulfamic acid) sodium salt, saccharin sodium salt hydrate, 2-(cyclohexylamino)-ethanesulfonic acid (CHES) and tris(hydroxymethyl)aminomethane (Tris) were purchased from Sigma (Buchs, Switzerland); histidine (His), aspartame, acesulfame-K, and sodium hydroxide from Fluka (Buchs, Switzerland). Standards were prepared by dilution of aqueous stock solutions of 10 mM of the sweeteners, which were stored in the refrigerator at 4 °C. The solid samples were dissolved in deionized water and the soft drink samples were diluted with water as required. All sample solutions were degassed in an ultrasonic bath and filtered through 0.45 μm membrane filters (Macherey-Nagel, Oensingen, Switzerland) before injection. The background electrolyte for the separations consisted of a Tris/CHES buffer at pH 9.1 which was prepared fresh daily to minimize the uptake of carbon dioxide from air.

2.2. Instrumentation

Preliminary experiments and buffer optimization were carried out on an instrument built in-house similar to the one previously described [18] but using a dual polarity high voltage power supply with a range of ± 30 kV (Spellman CZE2000, Pulborough, UK). The system used for pressure assisted separations was also constructed in-house and employed a sequential-injection analysis (SIA) manifold for fluid manipulation and pressurization and is based on earlier designs reported by us [15–17,19,20]. A schematic drawing of the SIA-CE- C^4D system is given in Fig. 1. The syringe pump (Cavro XLP 6000) fitted with a 1 mL syringe and the 9-port channel selection valve (Cavro Smart Valve) were obtained from Tecan (Crailsheim, Germany) and used for flushing of the capillary, for aspiration and injection of the sample, and for creating the bulk flow through the capillary during separation. The different required backpressures were achieved with the help of a micro-graduated needle valve (P-470, Upchurch Scientific, Oak Harbor, WA, USA) and solenoid isolation valves from NResearch (HP225T021, Gümliigen, Switzerland). Split injection was accomplished by pumping the sample plug past the capillary inlet under partial pressurization. Note that a similar system for hydrodynamic injection, albeit using a pressurized gas for liquid propulsion, had been reported previously [21]. The two different effective injection volumes employed were achieved by changing the volume of the dispensed plug (90 μL and 2.5 μL) at a fixed pumping rate (13 pulses s^{-1}) and the two flow rates through the capillary during the separation were created by adjusting the pump rate (6 pulses s^{-1} and 156 pulses s^{-1}). The injection end of the capillary was electrically grounded while the separation voltage was applied at the detector end using a dual polarity high voltage power supply with a range of ± 30 kV

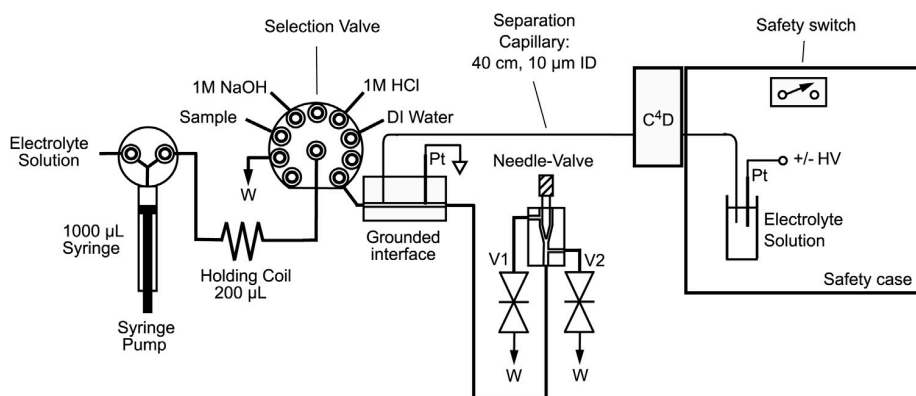


Fig. 1. Schematic drawing of the sequential injection analysis-capillary electrophoresis manifold with contactless conductivity detection (SIA-CE-C⁴D) employed for automated injection and superimposed hydrodynamic pumping. C⁴D: capacitively coupled contactless conductivity detector; HV: high voltage power supply. V1 and V2 are solenoid valves.

(Spellman CZE2000, Pulborough, UK). The high voltage end of the capillary was contained in a safety cage fitted with a microswitch to interrupt the voltage on opening to prevent accidental exposure of the operator. All connections for liquids were made with 0.02" ID and 1/16 in. OD Teflon tubing. Fused silica capillaries of 75 µm ID and 10 µm ID and 365 µm OD (Polymicro Technologies, Phoenix, AZ, USA) were used. These were conditioned by flushing with 1 M NaOH and water for 20 min each and then with the background electrolyte for 30 min before use. A C⁴D system built in-house [22,23] was employed and signals were recorded with an e-corder 401 data acquisition system (eDAQ, Denistone East, NSW, Australia). The entire system was operated from a notebook class computer which was hooked up to the syringe pump through a RS232–serial connection. Auxiliary output ports on the syringe pump were used to control the 9–port selection valve, the stop valves as well as the switching and polarity of the high voltage module, and provided a trigger for the start of the recording of the electropherograms with the data acquisition system. The necessary interface electronics to translate the logic signals to the appropriate power levels was constructed in-house. The software package Pumplink 32 (Tecan) was used to write the appropriate commands and sequencing for all operations. For robustness, the entire system, except for the computer, was assembled into a standard 19-in. rack with the fluidic parts mounted on the front panel to allow easy manipulation.

3. Results and discussion

3.1. Background electrolyte

The molecular structures of the four common sweeteners studied, namely aspartame, cyclamate, saccharin and acesulfame K, are shown in Fig. 2 along with their pK_a-values. For the determination of the latter three, cyclamate, saccharin and acesulfame K, a neutral or even slightly acidic background electrolyte would be suitable as the species are present in anionic form over a wide pH-range. However, for aspartame a pH-value of 9 or higher is required to obtain the anionic form. An electropherogram for the four analytes using conventional conditions employing a capillary of 75 µm ID is shown in Fig. 3 as a reference. The separation requires about 7 min but the last two peaks are just baseline resolved. Note that the analytes are swept to the detector against their electrophoretic mobility by the electroosmotic flow.

As discussed in the introduction, when superimposing a hydrodynamic flow it is necessary to use narrow capillaries of 25 µm or 10 µm ID. Recently it has also been recognized that in contrast to the use of wider capillaries when employing such narrow capillaries

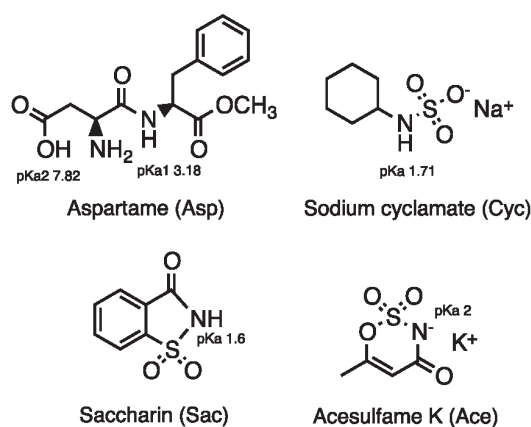


Fig. 2. Chemical structures of the artificial sweeteners employed shown with their pK_a-values.

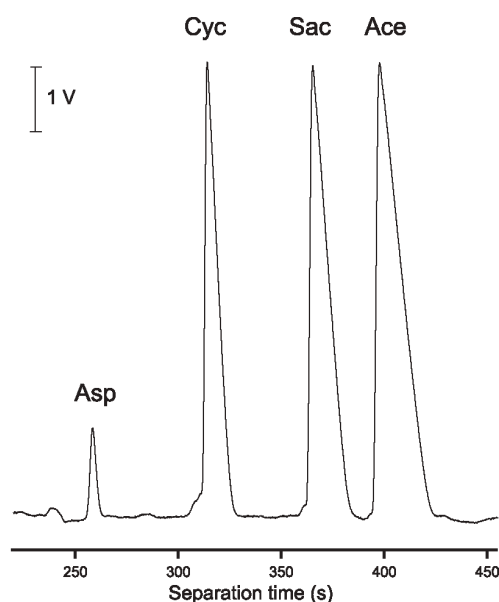


Fig. 3. Electropherogram for the 4 sweeteners obtained by a conventional separation without superimposed pumping. Aspartame: 270 µM; cyclamate: 390 µM; saccharin: 390 µM; acesulfame: K 400 µM. Background electrolyte: 100 mM Tris and 10 mM His at pH 9.4. Capillary: 75 µm ID, 68 cm and 60 cm total and effective lengths, respectively. Separation voltage: 30 kV. Injection: 30 s syphoning at 10 cm elevation.

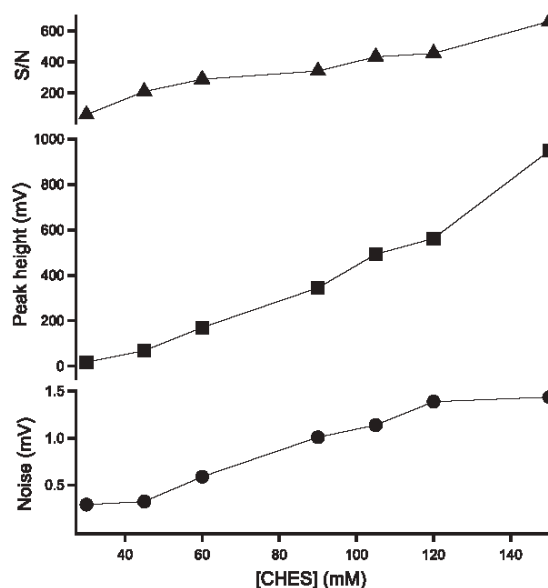


Fig. 4. Peak heights, baseline noise and signal-to-noise ratio (SN^{-1} = ratio of peak height to baseline noise) for 100 μ M acesulfame K in dependence on the buffer concentration in the range from 30 mM CHES (+80 mM Tris) to 150 mM CHES (+400 mM Tris). Capillary: 10 μ m ID, 40 cm and 32.5 cm total and effective lengths respectively. Separation voltage: 25 kV.

very high concentrations of buffers are required for best sensitivity [16,24]. The reason for this is at present not understood, and the effect is somewhat counter-intuitive as common wisdom calls for low conductivity buffers to minimize Joule heating effects. Nevertheless, an optimization of the buffer concentration for a Tris/CHES buffer at pH 9.1 was carried out by determining peak heights and baseline noise (maximum deviations from baseline for a 25 s interval) to determine the best sensitivity for injections of a solution of 100 μ M of acesulfame K. The results are shown in Fig. 4. The peak height was indeed found to increase with buffer concentration. While the baseline noise was also found to increase with buffer concentration this was more than compensated for by a more pronounced increase in peak height, leading to the best signal-to-noise ratio (SN^{-1}) in terms of peak height against baseline noise for the highest concentration. Consequently the concentration of 150 mM CHES and 400 mM Tris was adopted for further work. Note that even higher buffer concentrations were not possible due to the solubility limit.

Table 1

Calibration ranges, detection limits (LODs) and reproducibilities for the determination of artificial sweeteners with optimized hydrodynamic pumping for large and small injected amounts.

Analyte	Linear range (μ M)	Correlation coefficient, r^a	Limit of detection (μ M) ^b	Reproducibility of peak area (%RSD) ^c
Large plug				
Aspartame	20–1000	0.995	6.3	3.1
Cyclamate	15–1000	0.998	5.0	2.2
Saccharin	15–1000	0.995	4.0	2.9
Acesulfame K	10–1000	0.998	3.8	2.1
Small plug				
Aspartame	250–1000	0.998	75	1.8
Cyclamate	150–1000	0.998	50	1.6
Saccharin	150–1000	0.996	50	2.1
Acesulfame K	100–1000	0.995	30	1.2

Conditions: 90 μ L (large plug) and 2.5 μ L (small plug) dispensed through split injector. Capillary: 40 cm total and 32.5 cm effective lengths and 10 μ m ID. Separation voltage: 25 kV. Buffer: 150 mM CHES and 400 mM Tris.

^a 8 concentrations.

^b For peak heights equivalent to 3 times the baseline noise.

^c $n = 3$, 250 μ M.

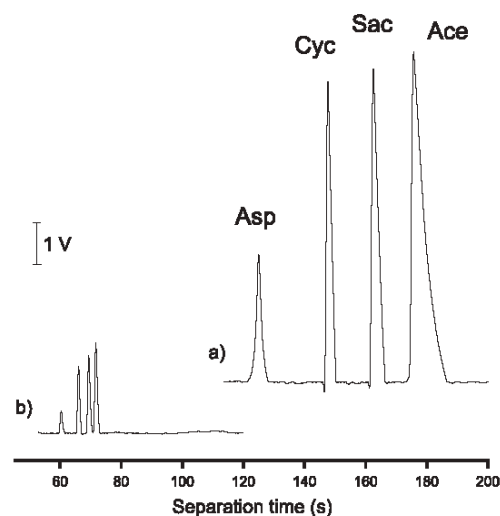


Fig. 5. Electropherograms for the separation of a standard solution of the 4 sweeteners at 1 mM with optimized hydrodynamic pumping for (a) large plug of injection and (b) small plug of injection. Background electrolyte: 150 mM CHES and 400 mM Tris at pH 9.1. Capillary: 10 μ m ID, 40 cm and 32.5 cm total and effective lengths respectively. Separation voltage: 25 kV.

3.2. Optimization of separations

Two different separations of the same standard mixture of the four sweeteners obtained with superimposed hydrodynamic pumping in a capillary of 10 μ m ID are shown in Fig. 5. It is, first of all, clear that significantly improved separation times are possible compared to the conventional separation shown above in Fig. 3. The separations were completed after about 3 min and 1½ min. The two electropherograms represent two different optimizations. Electropherogram (a) resulted for a relatively large injected amount in order to obtain good limits of detection. A sample plug of 90 μ L was pumped through the split injector. This led to tall peaks which are also relatively broad and required a relatively long residence time, *i.e.* a relatively low level of pumping (6 pulses s^{-1}). Note, that part of the difference in separation time arises from the fact that a shorter capillary could be used compared to the measurement shown in Fig. 3. This was possible because generally a better resolution is obtained with the narrower capillary [15]. Electropherogram (b) was obtained for a significantly reduced injected amount. The sample plug dispensed through the split injector was 2.5 μ L. This led to smaller peaks which could be separated more easily, hence

Table 2
Analysis of samples.

	Aspartame	Cyclamate	Saccharin	Acesulfame-K
Sugar substitute tablet	–	76.5 ± 0.9%	2.75 ± 0.05%	–
Confectionary 1	0.69 ± 0.02 mg g ⁻¹	–	0.090 ± 0.002 mg g ⁻¹	3.57 ± 0.04 mg g ⁻¹
Confectionary 1	–	–	1.44 ± 0.02 mg g ⁻¹	0.631 ± 0.006 mg g ⁻¹
Soft drink 1	–	240 ± 4 mg L ⁻¹	64.5 ± 0.9 mg L ⁻¹	151 ± 2 mg L ⁻¹
Soft drink 2	–	–	43.7 ± 0.6 mg L ⁻¹	48.9 ± 0.7 mg L ⁻¹
Soft drink 3	178 ± 4 mg L ⁻¹	283 ± 5 mg L ⁻¹	–	138 ± 2 mg L ⁻¹

The error limits are standard deviations ($n=3$).

a higher pumping rate (156 pulses s⁻¹) could be applied to speed up the analysis. Quantitative data for the two sets of conditions are given in Table 1. The limits of detection (LODs) are significantly different. For the large injected amount, with approximately 5 μ M for the four compounds, they are about 10 times lower than the values determined for the small injected sample plug (approx. 50 μ M). This clearly shows the compromise that needs to be made when fast separations are desired. A further consequence of the fast separation conditions is the shortening of the dynamic range. The repeatabilities of the measurements are similar, and the increased hydrodynamic flow employed for the smaller injected plug did not lead to a deterioration of precision.

3.3. Samples

To demonstrate the utility of the approach several samples were analyzed using either of the two sets of operating conditions. Electropherograms for a tabletop sweetener tablet and two confectionaries are shown in Fig. 6. The tablet consisted of cyclamate with a small proportion of saccharin. One of the sweets contained saccharine and acesulfame K, the other contained both of these sweeteners as well as aspartame. Note that other not identified peaks were also present, indicating that the operating conditions yielding the higher resolution was required. Three low calorie soft drinks were then analyzed using the faster separation conditions. The resulting electropherograms are given in Fig. 7, and reveal different compositions with regard to the sweetener mixture and

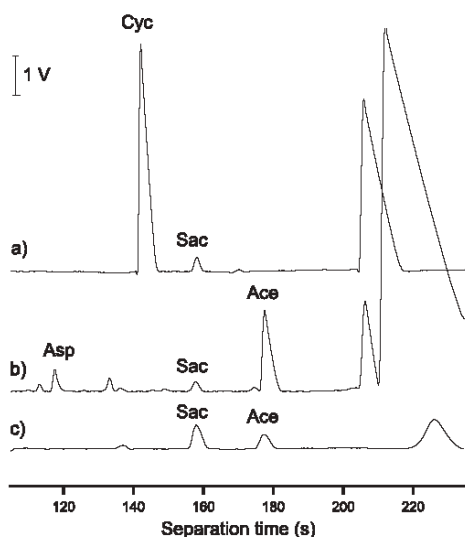


Fig. 6. Electropherograms with hydrodynamic pumping for solutions of a tabletop sweetener tablet (a) and two confectionary sweets (b) and (c) employing the conditions for high separation efficiency. Background electrolyte: 150 mM CHES and 400 mM Tris at pH 9.1. Capillary: 10 μ m ID, 40 cm and 32.5 cm total and effective lengths respectively. Separation voltage: 25 kV.

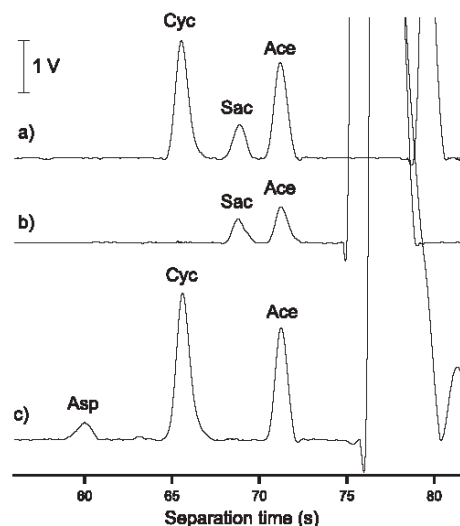


Fig. 7. Electropherograms with hydrodynamic pumping for three different soft drink samples after degassing and dilution employing the conditions for fast separations. Background electrolyte: 150 mM CHES and 400 mM Tris at pH 9.1. Capillary: 10 μ m ID, 40 cm and 32.5 cm total and effective lengths respectively. Separation voltage: 25 kV.

content. The quantitative results for these measurements are given in Table 2.

4. Conclusion

The use of superimposed hydrodynamic pumping was found to be of great benefit in the determination of the artificial sweeteners by CE-C⁴D. Four of the most commonly employed species could be determined concurrently, without requiring any special sample pretreatment. Readily optimized analysis times of less than 3 min were achieved. In practical applications, the optimization of operating conditions would normally have to take care of the required sensitivity first, by injecting an amount that leads to adequately sized peaks for the task. Secondly, the selectivity would have to be assured, *i.e.* the resolution of all peaks in dependence on the complexity of the sample. This is governed by the electrical field strength and the residence time of the sample in the field. The analysis time can then be optimized by adjustment of the rate of pumping until resolution is lost. Secondly the required sensitivity (by adjustment of the injected amount), and analysis time third. The ability to control the residence time with the superimposed pumping, rather than changing the length of the capillary, is of great help in these adjustments and a very useful feature is that it is readily adjustable and reversible. The conditions can be flexibly adjusted according to the demands of the samples at hand.

Acknowledgments

The authors are grateful to the Swiss National Science Foundation for financial support (Grant Nos. 200020-1263481/1 and 200020-137676).

References

- [1] M. Kroger, K. Meister, R. Kava, *Compr. Rev. Food Sci.* 5 (2006) 35.
- [2] A. Zygler, A. Wasik, J. Namieśnik, *TrAC Trends Anal. Chem.* 28 (2009) 1082.
- [3] J.J. Pesek, M.T. Matyska, *J. Chromatogr. A* 781 (1997) 423.
- [4] J.C. Walker, S.E. Zaugg, E.B. Walker, *J. Chromatogr. A* 781 (1997) 481.
- [5] S. Sabah, G.K.E. Scriba, *J. Pharmaceut. Biomed.* 16 (1998) 1089.
- [6] M.C. Boyce, *J. Chromatogr. A* 847 (1999) 369.
- [7] R.A. Frazier, E.L. Inns, N. Dossi, J.M. Ames, H.E. Nursten, *J. Chromatogr. A* 876 (2000) 213.
- [8] C.O. Thompson, V.C. Trenerry, B. Kemmery, *J. Chromatogr. A* 704 (1995) 203.
- [9] M. Horie, F. Ishikawa, M. Oishi, T. Shindo, A. Yasui, K. Ito, *J. Chromatogr. A* 1154 (2007) 423.
- [10] P. Schnierle, T. Kappes, P.C. Hauser, *Anal. Chem.* 70 (1998) 3585.
- [11] T. Kappes, B. Galliker, M.A. Schwarz, P.C. Hauser, *TrAC Trends Anal. Chem.* 20 (2001) 133.
- [12] M. Herrmannová, L. Křivánková, M. Bartoš, K. Vytřas, *J. Sep. Sci.* 29 (2006) 1132.
- [13] J. Tanyanyiwa, E.M. Abad-Villar, P.C. Hauser, *Electrophoresis* 25 (2004) 903.
- [14] A.B. Bergamo, J.A. Fracassi da Silva, D.P. de Jesus, *Food Chem.* 124 (2011) 1714.
- [15] T.D. Mai, P.C. Hauser, *Talanta* 84 (2011) 1228.
- [16] T.D. Mai, P.C. Hauser, *Electrophoresis* 32 (2011) 3000.
- [17] T.D. Mai, P.C. Hauser, *J. Chromatogr. A* 1267 (2012) 266.
- [18] P. Kubáň, H.T.A. Nguyen, M. Macka, P.R. Haddad, P.C. Hauser, *Electroanalysis* 19 (2007) 2059.
- [19] T.D. Mai, B. Bomastyk, H.A. Duong, H.V. Pham, P.C. Hauser, *Anal. Chim. Acta* 727 (2012) 1.
- [20] T.D. Mai, S. Schmid, B. Müller, P.C. Hauser, *Anal. Chim. Acta* 665 (2010) 1.
- [21] M. Vaheer, S. Ehala, M. Kaljurand, *Electrophoresis* 26 (2005) 990.
- [22] L. Zhang, S.S. Khaloo, P. Kubáň, P.C. Hauser, *Meas. Sci. Technol.* 17 (2006) 3317.
- [23] J. Tanyanyiwa, B. Galliker, M.A. Schwarz, P.C. Hauser, *Analyst* 127 (2002) 214.
- [24] P. Túma, E. Samcová, K. Štulík, *Electroanalysis* 23 (2011) 1870.

2.3 Referenced capacitively coupled conductivity detector for capillary electrophoresis

CE has been widely recognized as a universal detection technique as it measures electrolytic conductivity. Capillary zone electrophoresis (CZE) with the application of conductivity detection was confronted with possible complications when a high separation voltage is applied. However, this deficiency was circumvented with the inception of axial capacitively coupled contactless conductivity detection (C^4D) and was demonstrated over a wide range of applications. The standard arrangement of a C^4D cell is composed of two round electrodes placed axially around a capillary with a small gap in between. Electrodes are considered as capacitors and the gap in between as a resistor. Applied ac-voltage passes through the first electrode and the current is read through the second electrode, converted back to an ac-voltage with an operational amplifier, and afterwards amplified. For this setup, higher frequencies are employed due to low coupling capacitances. Also observed is an influence of direct capacitive coupling between electrodes called stray capacitance. An electric offset circuitry is usually adjusted manually, due to baseline changes caused by BGE conductivity. To avoid a temperature influence on conductivity detection as well as potential influence of the background signal on signal-to-noise ratio, a referenced approach was devised. New “sandwich” design of the referenced C^4D cell is illustrated in figure 9 below.

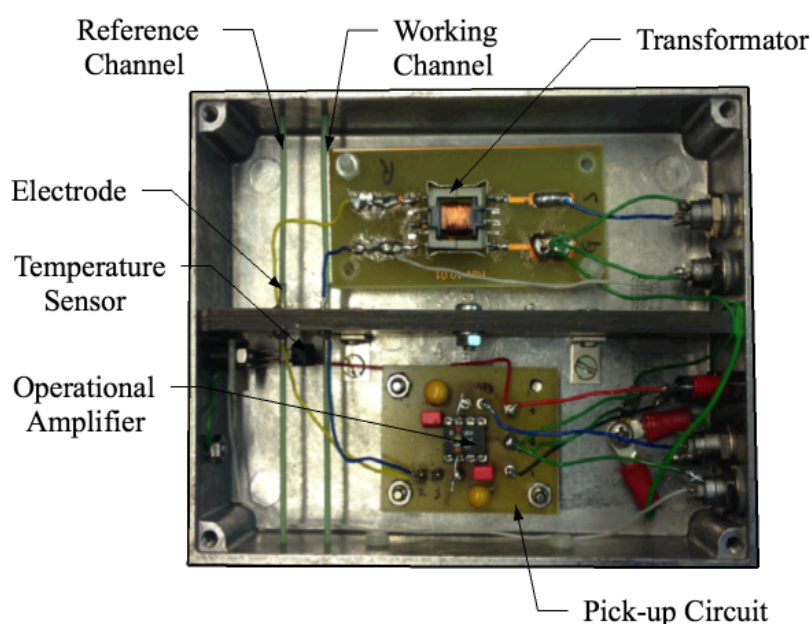


Figure 9. Picture of the referenced “sandwich” C⁴D cell

Placed in a grounded metallic box, the detector is split with a Faradaic shield into two parts: the excitation and pick-up component, respectively. A transformer is placed in the excitation section, producing AC signals to the working (blue) and referenced (yellow) channels. Round electrodes are attached on the “sandwich” made of two pairs of printed circuit boards (PCB). The thicker pair of PCBs provides the electric contact between two sections through electrodes. The thinner, grounded inner pair of 1 mm (2 x 0.5 mm) size, point with their copper sides toward each other, shielding the cell and preventing potential stray capacitance. When the AC current from the cell passes to the pick-up section, it is converted to voltage with operational amplifier (OPA). That signal is rectified after and the background signal is offset to zero. When the background signals are substantial, this zero adjustment has to be done manually when the baseline shifts. It is significantly easier to use the hand made transformer that increases the signal by a factor of 10 rather than the active amplifier as used before. Two windings of the transformer provide two opposite sign signals where one will lead to the electrode of the working channel and the other to the reference channel electrode, respectfully. In the pick-up section, when traced on the oscilloscope, large background signal from the conductivity of the buffer is observed when the working channel is employed. Vice versa, if only the reference channel is attached, the signal generated from the referenced capillary filled with the same buffer is inverted. When both channels are merged to the input of the operational amplifier, significantly decreased amplitude of the signal is attained and, in this manner, the meaningful part of the background signal is purged. To monitor the temperature drifts, we used a temperature sensor placed inside the cell. Evidently, the temperature sensitivity was reduced by utilization of the reference. To demonstrate functionality of the developed referenced C⁴D detector, three cations, namely sodium, potassium and lithium, were selected as exemplary analytes. The optimized background electrolyte (BGE) is comprised of 20 mM L-histidine adjusted to pH 4 with acetic acid and 2 mM 18-Crown-6. With these CE conditions, calibration curves were acquired up to 100 µM with a very good correlation coefficient (r higher than 0.997), with RSD% for peak areas of 1.3-3.4 % for three different internal diameter capillaries of 50 µm, 25 µm and 10 µm respectfully.

With a configuration of the developed cell in such a way, the performance of the detector is significantly improved. The influence of the temperature is notably reduced and adjustment of the electronic offset is now automated.

3rd project:

**Referenced Capacitively Coupled Conductivity Detector for Capillary
Electrophoresis**

Electroanalysis, (2013), 25, 2645-2650

Referenced Capacitively Coupled Conductivity Detector for Capillary Electrophoresis

Marko Stojkovic,^{†a} Boris Schlensky,^{†b} Peter C. Hauser^{*,†a}

^a Department of Chemistry, University of Basel, Spitalstrasse 51, 4056 Basel, Switzerland
tel: +41 61-267-1003; fax: +41 61-267-1013

^b EDAQ Pty. Ltd., 6 Doig Avenue, Denistone East, NSW 2112, Australia

*e-mail: Peter.Hauser@unibas.ch

Received: August 29, 2013

Accepted: October 18, 2013

Published online: ■ ■ ■, 2013

Abstract

A dual capacitively coupled contactless conductivity detector for capillary electrophoresis was developed. The two channels are arranged in a bridge configuration so that one of them acts as a reference whose signal is subtracted. This effectively compensates for the baseline conductivity of the separation buffer so that the electronic zero setting is not necessary. Changes in the buffer composition are automatically accounted for, as are temperature drifts. The system is demonstrated for the detection of inorganic model cations in capillary electrophoresis. Besides the use with two separate capillaries, one of which solely serves as reference, it was also found possible to use a single capillary which is looped back through the reference cell.

Keywords: Contactless conductivity detector, Capillary electrophoresis

DOI: 10.1002/elan.201300413

1 Introduction

The measurement of electrolytic conductivity can be considered a universal detection method for ions separated by chromatographic and electrophoretic techniques. For this reason it has long been the standard in ion-chromatography. For capillary zone electrophoresis the application of conductivity detection had been hindered by the small dimensions of the capillaries and the potential interference from the separation voltage, but these challenges were overcome by the introduction of the axial capacitively coupled contactless technique introduced by Zemann et al. [1] and da Silva and do Lago et al. [2] in 1998. The method is now commonly known as C⁴D for Capacitively Coupled Contactless Conductivity Detection. Many applications in diverse fields have been reported. Prominent is the detection of species which do not absorb UV-light and are thus not directly accessible on standard instruments fitted with a UV-detector. Recent reviews discussing applications of C⁴D are available [3–9].

A C⁴D cell consists of two tubular electrodes arranged along the axis of a capillary or tubing. Each electrode forms a capacitance with the electrolyte inside, having the capillary wall as dielectric, and the ion solution in the gap between the electrodes can be considered as an electrical resistance. To probe the conductance (which is the inverse of resistance) an AC-voltage is coupled into the solution via the first electrode and the resulting current read out

through the second electrode. Frequencies of several hundred kHz are required due to the small coupling capacitances. Following its introduction in 1998 several studies on the fundamental aspects of the cell, such as its frequency behaviour and effects of stray capacitance (i.e. direct capacitive coupling between the electrodes), have been reported [10–17] and the method has been characterized well. The cell current is converted to an AC-voltage with an operational amplifier and then rectified. An offset-circuitry is usually also required as small changes on a baseline caused by the background conductivity of the buffer contained in the capillary have to be monitored. A few variations of the basic arrangement have been reported. These include a cell with semicircular electrodes which are clamped onto the capillary and thus avoids having to thread the capillary through the tubular electrodes [18], the use of elevated excitation voltages for improved signal to noise ratios [19,20], a miniaturized cell which contains the electrodes and associated circuitry on a small printed circuit board [21], and a cell with a very high resolution analog-to-digital convertor [22].

A fundamental short-coming of C⁴D is the fact that it is a bulk method, i.e. a general solution property is measured, which causes the presence of a background signal. For a cell without effective shielding an appreciable contribution to the background signal may also arise from direct capacitive coupling between the electrodes (stray capacitance). The background signals tend to dominate the signal to noise ratio, and therefore adversely affect

the limits of detection. Small variations in this background signal will also cause drifts in the baseline. Conductivity detection of ion solutions is particularly susceptible to temperature changes due to temperature coefficients of around 2% [23]. Generally, in such situations a referenced approach is often adopted using an electronic bridge arrangement [24]. A well known example within the field of analytical chemistry is the thermal conductivity detector in gas chromatography [25]. For C^4D only two reports of referenced arrangements are known. Fercher et al. described an electrophoresis microchip with two C^4D cells, the first one placed close to the injection end of the separation channel, the second one close to its other end [26]. The signals were separately amplified, processed by a balancing circuitry and then subtracted. Shen et al. presented a similar arrangement employing two detector cells for a conventional capillary, but used a very special circuitry which included two resonating quartz crystals [27]. The arrangement for conventional capillaries reported herein employs a straightforward standard circuitry and a common cell.

2 Experimental

2.1 Instrumentation

The desktop function generator (GFG-8216A) used to obtain the sine wave was a product of Good Will Instrument (Taipei, Taiwan). The transformer was based on two E 13/7/4, N87 ferrite cores with a matching E 13/7/4 coil former, obtained from EPCOS (Munich, Germany) (product nos. B66305-G-X187 and B66306-C1010-T1). The primary winding consisted of 10 turns of enamelled copper wire of 0.2 diameter, and the secondary windings of 110 and 100 turns of enamelled copper wire of 0.1 mm diameter. The electrodes used in the construction of the cell were wire ferrules obtained from Vogt Verbindungstechnik (Lostorf, Switzerland, product no. 459706) and the guidance tube was a product of Upchurch (Oak Harbor, WA, USA, product no. F-185). The pick up amplifier was an OPA602 (Texas Instruments, Austin, TX, USA) and the rectifier was based on an integrated synchronous detector (AD630, Analog Devices, Norwood, MA, USA). More details on the circuitry are given in a previous publication [19]. The signals were recorded on a personal computer using an e-corder 401 data acquisition system (eDAQ, Deniston East, NSW, Australia). An oscilloscope (TDS1001B) from Tektronix (Beaverton, OR, USA) was employed for visualization of the signals. The temperature sensor was a LM35CZ (Texas Instruments). The electrophoresis experiments were carried out on an instrument constructed in-house employing a dual polarity high voltage supply (Spellman CZE2000, Pulborough, UK) with ± 30 kV maximum output voltage and polyimide coated fused silica capillaries of 365 μm OD and 10, 25 and 50 μm ID (from Polymicro, Phoenix, AZ, USA).

2.2 Chemicals and Procedures

All the chemicals were of analytical grade and were purchased from Fluka (Buchs, Switzerland), Merck (Darmstadt, Germany) or Sigma-Aldrich (Buchs, Switzerland). Stock solutions (5 mM) of sodium, potassium, lithium as chloride salts and nitrate, nitrite and sulfate as sodium salts were used as standards (100 μM) and were prepared daily. For all solutions deionized ultrapure water of 18 M Ω cm resistivity was used (prepared on equipment from Millipore, Saint-Quentin-en-Yvelines, France). The capillaries were preconditioned with 1 M NaOH for 15 min and water for 15 min, followed by 1 M HCl for 15 min, water for 15 min and the background electrolyte for 15 min. Injection was carried out by moving the capillary employed for the separation to the sample container followed by siphoning, while the reference capillary remained in the container with the background electrolyte.

3 Results and Discussion

3.1 Detector Design

A schematic drawing of the overall C^4D cell design is shown in Figure 1A. The detector is fitted into a grounded metallic box which is divided into excitation and pick-up sections by a Faradaic (grounded) shield. The excitation part contains the transformer which provides the appropriate AC signals to the working and reference channels as discussed below. The pick-up section holds an operational amplifier which converts the cell currents to a voltage. The arrangement of the two electrode pairs is illustrated in Figure 1B. The tubular electrodes are fitted into appropriate holes of a pair of printed circuit boards of 1.6 mm thickness and soldered in place to tracks which provide the electric connections to the excitation and pick-up circuitries. The electrodes contain polymeric guidance sleeves for alignment of the electrodes. The two boards holding the electrodes are sandwiched to an inner couple of printed circuit boards of 0.5 mm thickness which define the cell length as 1 mm. The inner boards have their copper layers on the inside, forming the grounded shield between excitation and pick up sections of the cell to minimize stray capacitance. The holes of 0.4 mm are just large enough to allow passage of the capillaries (with 365 μm OD).

The standard building blocks of the circuitry used in C^4D are shown in Figure 2A along with an illustration of the signal processing in Figure 2B. A sine wave is obtained with a function generator which is optionally boosted to elevated voltages with an amplifier in order to improve the signal-to-noise ratio [19,20,28]. The alternating current obtained from the cell is converted to a voltage with a pick-up amplifier. This signal is then rectified and low pass filtered, and the background signal is offset to zero, before a gain is applied and the signal is fed to an analog-to-digital converter (ADC) before further processing in the digital domain on a computer. The zero

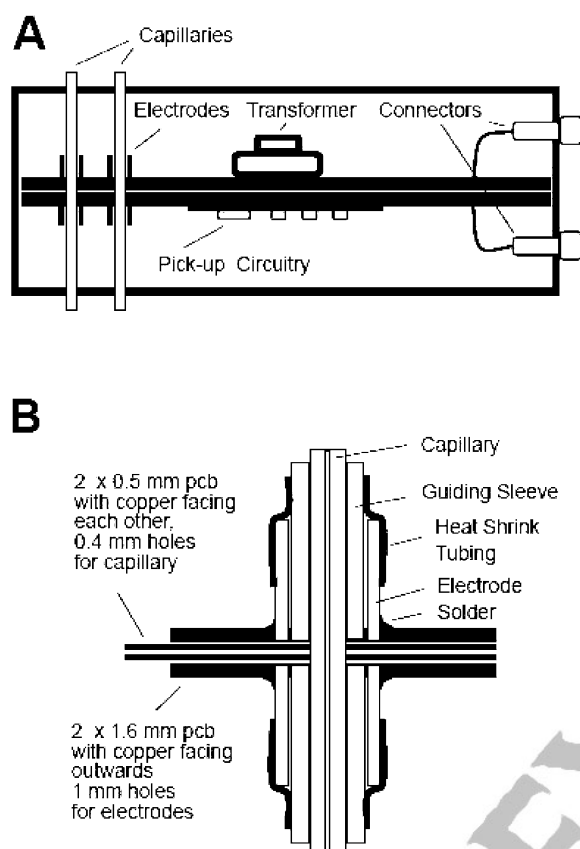


Fig. 1. A) Sketch of cell arrangement. B) Configuration of the electrode pairs.

setting is a complication that arises when signals have a large background and is due to the need for matching their effective dynamic range to the input range of the ADC. The process is illustrated in Figure 2B. Unless a special ADC with unusually high resolving power is employed [22], failure to carry out this match will result in digitization noise, or even in the loss of recognition of small peaks. Most reported designs of C⁴D circuitries therefore include such an offset stage. However, the zeroing of the baseline usually requires the intervention of the user (such as through the manual adjustment of a potentiometer) and may necessitate frequent re-adjustment if the baseline is drifting.

A schematic of the new circuitry is given in Figure 3. A sine wave of 250 kHz is produced with a standard external function generator, which has an output of 20 V_{p-p} (peak-to-peak voltage). This signal is then boosted to approximately 200 V_{p-p} by a small purpose made transformer contained in the cell itself. This is a much simpler approach than the use of an active booster amplifier as previously used in our group. The transformer has two secondary windings which create two signals of opposite sign, i.e. two sine waves with a phase shift of 180°. One of

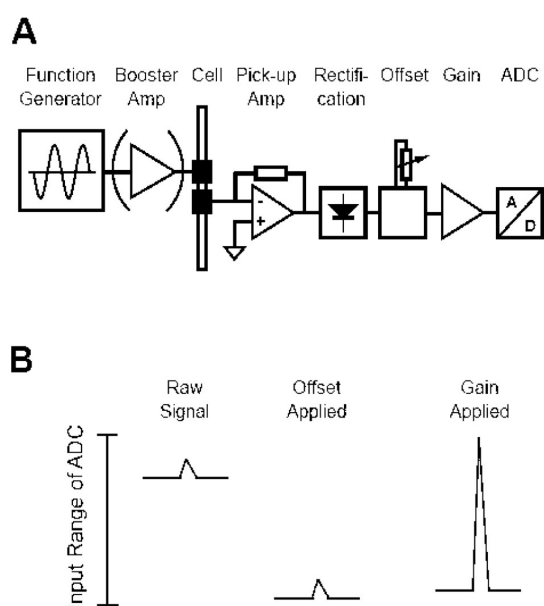


Fig. 2. A) Block diagram of standard circuitry. B) Illustration of the signal processing with offset and gain stages to match the input range of an analog-to-digital converter.

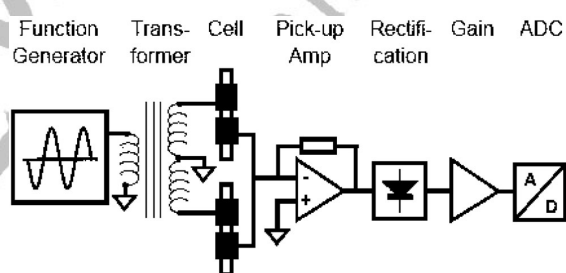


Fig. 3. Block diagram of the new circuitry.

these signals is fed to the excitation electrode for the working channel, while the other is brought to the reference excitation electrode. The two pick-up electrodes are connected to the input of an operational amplifier in the current-to-voltage converter configuration. The signal is then rectified and low pass filtered and brought to the data acquisition system. The offset circuitry is not needed as the use of the reference imparts an inherent subtraction of the background signal (if the reference capillary is filled with the separation buffer).

The fundamental principle of the referenced cell is illustrated by the oscilloscope traces of Figure 4. Trace A shows the signal generated through a capillary filled with buffer amplified by the pick-up amplifier (without connecting the reference arm). This corresponds to the usual cell arrangement with a single channel. A sine voltage of a relatively high amplitude is obtained, due to the buffer in the capillary. The peaks in the electropherogram corre-

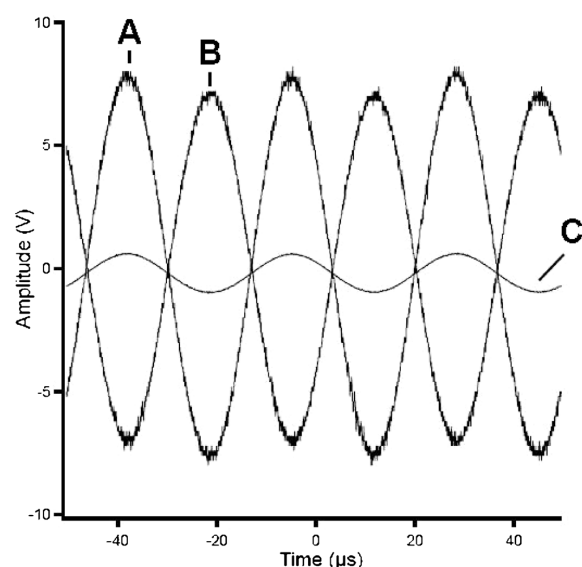


Fig. 4. Oscilloscope traces of the signal at the output of the pick-up amplifier for A) working channel connected to amplifier, B) reference channel connected, C) both working and reference channel connected (30 mM histidine/2-morpholinoethanesulfonic acid (MES) buffer in 50 μm ID capillary).

respond to small changes of this amplitude. Trace B shows the signal generated from the reference capillary filled with the same buffer. Note that the two signals are exactly 180° out of phase, i.e. inverted. Trace C shows the signal resulting when both channels are connected to the input of the amplifier, the usual mode of operation of the new design. A signal of much reduced amplitude is obtained due to the subtraction of the reference signal. The input of the operational amplifier is a so-called summing point which leads to an effective subtraction of the reference signal (with opposite sign) from the working signal. Thus a large part of the background signal is removed.

Note that the amplitude of the reference signal is slightly lower than that of the working channel. The reason for this is the fact that the secondary winding of the transformer for the reference signal deliberately has fewer windings so that its amplitude is about 10% lower than the signal. The reference voltage is thus always lower than the working voltage. This means that the compensation of the background signal is not complete, but on the other hand it prevents the net signal from crossing through zero should the balance not be perfect and thus assures a defined polarity of the net signal. Also clearly apparent is a cancellation of at least a substantial part of the electronic noise in the referenced approach.

3.2 Performance

The separation of the 3 model cations sodium, potassium and lithium is shown in Figure 5. Electropherogram A was acquired with only the working cell connected to the

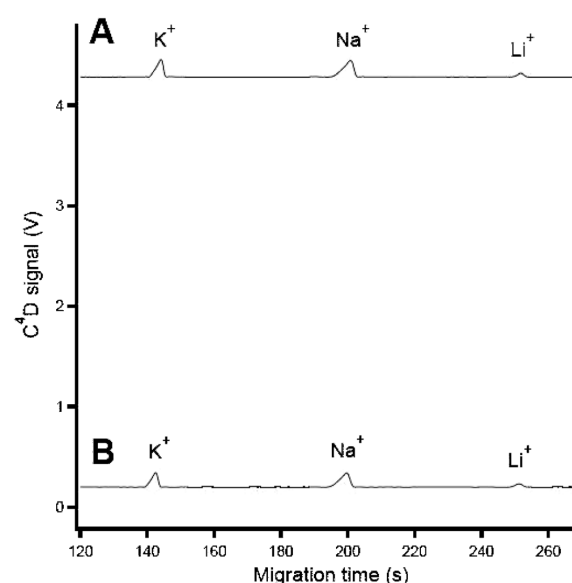


Fig. 5. Separation of 3 model cations at 100 μM . A) Conventional set-up without applying offset and gain. B) Referenced set-up (without applying gain). Capillary: 25 μm ID, 50 cm length. Injection: hydrodynamic, 45 s at 17 cm height. Buffer: 20 mM histidine adjusted to pH 4 with acetic acid, 2 mM 18-Crown-6. Separation voltage applied at injection end: +20 kV.

input of the pick-up amplifier. This corresponds to the usual situation. A large background signal due to the conductivity of the separation buffer is present. When the reference channel was also connected to the input electropherogram B was obtained. Clearly, the desired effect of removing a large fraction of the background signal is achieved, while the relevant signal is retained, i.e. the peaks are not affected by the reference. Note, that the reference capillary was of identical diameter and length as the separation capillary, filled with the same background electrolyte and placed into the same vials for application of the separation voltage.

The arrangement can compensate for any drifts which are common to both capillaries, but, of course, not effects which only occur in one of the capillaries. The ability of the referenced configuration to correct for temperature drifts was tested by warming the cell with a heat gun. The temperature inside the cell was monitored with an electronic temperature sensor and its signal recorded along with the output of the C^4D . The results are shown in Figure 6 for the 3 capillary diameters of 10, 25 and 50 μm . In part A the change in signals for the non-referenced cell configuration are shown along with the temperature profile on heating, while in part B the repeat measurements for the referenced configuration are given. Note, that the signals shown are not absolute, but deviations from the baseline. It is apparent that the temperature sensitivity is largely removed by use of the reference. The performance in the quantitative determination of

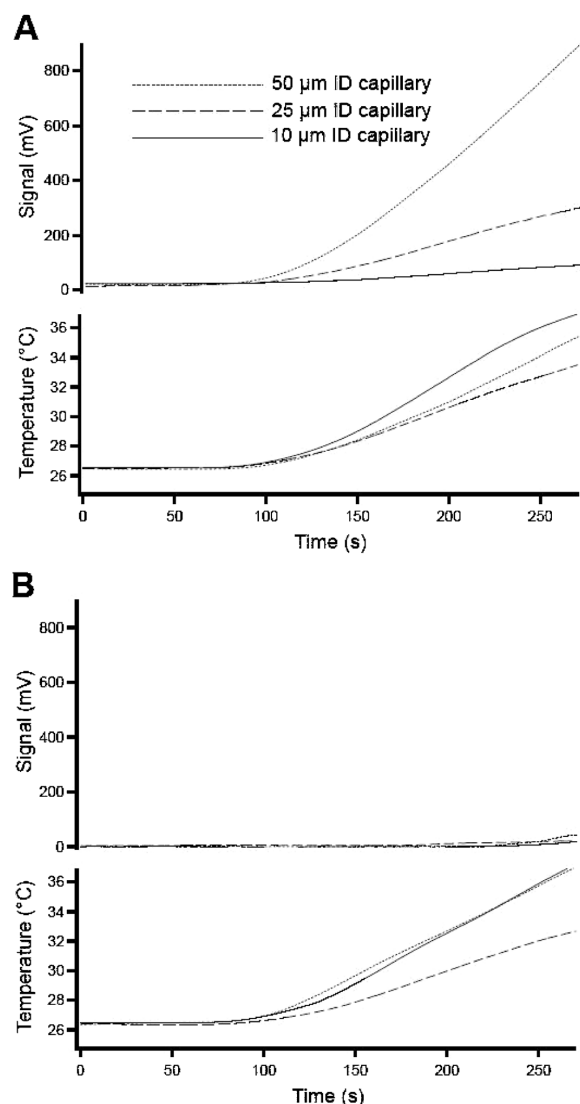


Fig. 6. Temperature stability of the cell. A) Conventional set-up. B) Referenced set-up. Buffer: 30 mM histidine/MES.

ions was investigated by acquiring calibration curves for the 3 model cations and the data is given for the 3 capillary diameters in Table 1. The numbers are comparable to typical values obtained with a standard single channel detector using the offset circuitry, so that these parameters must be determined by the electrophoretic procedures, not by the detector electronics. Note, that some of these performance parameters very much depend on how the separation procedure has been optimized (i.e. either for high separation efficiency, fast analysis time, wide dynamic range, or low limits of detection, see for example [29,30]) and a comparison between different quoted performance values for C⁴D is hampered by this fact.

Table 1. Statistical data for the quantification of K⁺, Na⁺ and Li⁺ in capillaries of 10, 25 and 50 μm inner diameter.

Analyte	Calibration range (μM) [a]	Correlation coefficient <i>r</i>	Reproducibility of peak area, %RSD [b]	Limit of detection (μM) [c]
50 μm ID				
Na ⁺	10–100	0.9999	1.3	1
K ⁺	10–100	0.9996	1.9	1.5
Li ⁺	10–100	0.9988	2.7	2.8
25 μm ID				
Na ⁺	5–100	0.9987	2.4	1
K ⁺	5–100	0.9971	2.9	1.5
Li ⁺	5–100	0.9973	3.1	2
10 μm ID				
Na ⁺	10–100	0.9995	2.6	1.5
K ⁺	10–100	0.9997	2.8	2.3
Li ⁺	10–100	0.9986	3.4	3

[a] 5 concentrations; [b] for 100 μM, *n*=3; [c] concentrations giving peak heights 3× the baseline noise.

The use of a second capillary is not a problem as the usual high voltage power supplies can easily provide the current for two capillaries, and the added consumption of background electrolyte is negligible, but the need to condition and flush two capillaries is a slight complication. It is however, also possible to work with a single capillary by looping the end of the separation capillary back through the reference part of the cell. This was readily possible on our instrument which was built-in house, but note that it may not be feasible on all types of commercial units due to space constraints. Electropherograms obtained for cations and anions using this approach are shown in Figure 7A and 7B. As the analytes travel through the detector twice, duplicate peaks are obtained, with reversed direction of deviation from the baseline and a wider separation for the second passage. The duplication of the peaks is unusual and is of no direct benefit, but one set of peaks can simply be ignored. Ideally the later set of peaks is made use of for quantification, by interchanging signal and reference cells, as this does not require an extension of the total capillary length, with a possible associated loss of field strength and resolution if it cannot be compensated for by an increase in separation voltage. However, the length of the capillary segment between the two electrode pairs may have to be optimized to avoid any overlap of peaks from the first and second passage.

4 Conclusions

A referenced C⁴D-configuration has been demonstrated. This approach considerably simplifies the operation of the detector, by not requiring an electronic offset which usually needs to be adjusted manually. A further significant advantage is the much reduced temperature sensitiv-

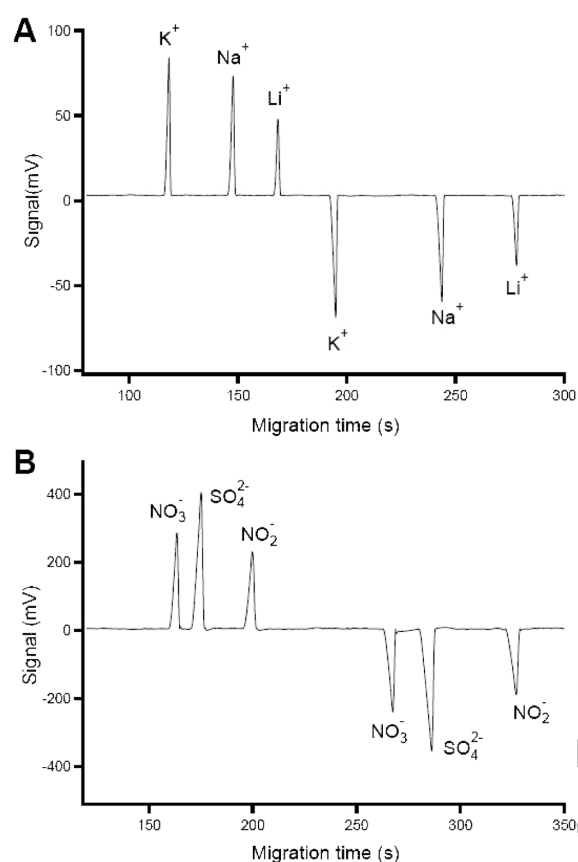


Fig. 7. Separation of A) 3 model cations and B) 3 model anions at 100 μM with the capillary looped back through the reference detector. Capillary: 50 μm ID, total length 60 cm, length to working cell 34.5 cm, length to reference cell 48 cm. Injection: hydrodynamic, 30 s at 10 cm height. Buffer: 12 mM histidine adjusted to pH 4 with acetic acid, 2 mM 18-crown-6 (cations), 30 mM histidine/MES (anions). Separation voltage applied at injection end: +20 kV (cations), -20 kV (anions).

ity. The need for a second capillary can be overcome by looping back a single capillary.

Acknowledgements

The authors are grateful for financial support by the Swiss National Science Foundation through Grant No. 200020-137676.

References

- [1] A. J. Zemann, E. Schnell, D. Volgger, G. K. Bonn, *Anal. Chem.* **1998**, *70*, 563.
- [2] J. A. F. da Silva, C. L. do Lago, *Anal. Chem.* **1998**, *70*, 4339.
- [3] F. Opekar, P. Tuma, K. Stulik, *Sensors* **2013**, *13*, 2786.
- [4] P. Kubáň, P. C. Hauser, *Electrophoresis* **2013**, *34*, 55.
- [5] P. Kubáň, P. C. Hauser, *Electrophoresis* **2011**, *32*, 30.
- [6] J. J. P. Mark, R. Scholz, F. M. Matsysik, *J. Chromatogr. A* **2012**, *1267*, 45.
- [7] W. K. T. Coltro, R. S. Lima, T. P. Segato, E. Carrilho, D. P. de Jesus, C. L. do Lago, J. A. F. da Silva, *Anal. Meth.* **2012**, *4*, 25.
- [8] A. A. Elbashir, H. Y. Aboul-Enein, *Biomed. Chromatogr.* **2012**, *26*, 990.
- [9] T. D. Mai, P. C. Hauser, *Chem. Record* **2012**, *12*, 106.
- [10] P. Tůma, E. Samcová, K. Štulík, *Electroanalysis* **2009**, *21*, 590.
- [11] J. G. A. Brito-Neto, J. A. F. da Silva, L. Blanes, C. L. do Lago, *Electroanalysis* **2005**, *17*, 1198.
- [12] J. G. A. Brito-Neto, J. A. F. da Silva, L. Blanes, C. L. do Lago, *Electroanalysis* **2005**, *17*, 1207.
- [13] M. Novotný, F. Opekar, K. Štulík, *Electroanalysis* **2005**, *17*, 1181.
- [14] S. E. Johnston, K. E. Fadgen, L. T. Tolley, J. W. Jorgenson, *J. Chromatogr. A* **2005**, *1094*, 148.
- [15] P. Kubáň, P. C. Hauser, *Electrophoresis* **2004**, *25*, 3387.
- [16] P. Kubáň, P. C. Hauser, *Electrophoresis* **2004**, *25*, 3398.
- [17] B. Gaš, J. Zuska, P. Coufal, T. van de Goor, *Electrophoresis* **2002**, *22*, 3520.
- [18] P. Tůma, F. Opekar, I. Jelínek, *Electroanalysis* **2001**, *13*, 989.
- [19] J. Tanyanyiwa, B. Galliker, M. A. Schwarz, P. C. Hauser, *Analyst* **2002**, *127*, 214.
- [20] J. Tanyanyiwa, P. C. Hauser, *Electrophoresis* **2002**, *23*, 3781.
- [21] J. A. F. da Silva, N. Guzman, C. L. do Lago, *J. Chromatogr. A* **2002**, *942*, 249.
- [22] K. J. M. Francisco, C. L. do Lago, *Electrophoresis* **2009**, *30*, 3458.
- [23] E. Pungor, *Oscillometry and Conductometry*, Pergamon Press, Oxford **1965**.
- [24] H. V. Malmstadt, C. G. Enke, E. C. Toren, *Electronics for Scientists*, Benjamin, New York **1963**.
- [25] R. P. W. Scott, *Chromatographic Detectors*, Marcel Dekker, New York **1996**.
- [26] G. Fercher, A. Haller, W. Smetana, M. J. Vellekoop, *Anal. Chem.* **2010**, *82*, 3270.
- [27] D. Shen, Y. Li, Z. Zhang, P. Zhang, Q. Kang, *Talanta* **2013**, *104*, 39.
- [28] J. Tanyanyiwa, P. C. Hauser, *Anal. Chem.* **2002**, *74*, 6378.
- [29] T. D. Mai, T. T. T. Pham, H. V. Pham, J. Sáiz, C. García Ruiz, P. C. Hauser, *Anal. Chem.* **2013**, *85*, 2333.
- [30] M. Stojkovic, T. D. Mai, P. Hauser, *Anal. Chim. Acta* **2013**, *787*, 254.

2.4 Real time monitoring in capillary electrophoresis (CE) using C^4D array detector

For monitoring purposes, it is important to set up the system that can perform injection, separation, detection and data acquisition in an independent way. An automated system based on CE- C^4D coupled with an SI manifold via an interface was used. To understand better dynamic processes of electrophoretic separation, another study was carried out by employing 16 C^4D detectors along the fused silica capillary. With a new arrangement, the whole system has been minimized appointing cells side by side on the capillary. External circuitries were not necessary due to the new cell design where all the electronic devices were placed into the detector cell using surface mount technology. Illustration of the detector is shown in figure 10.

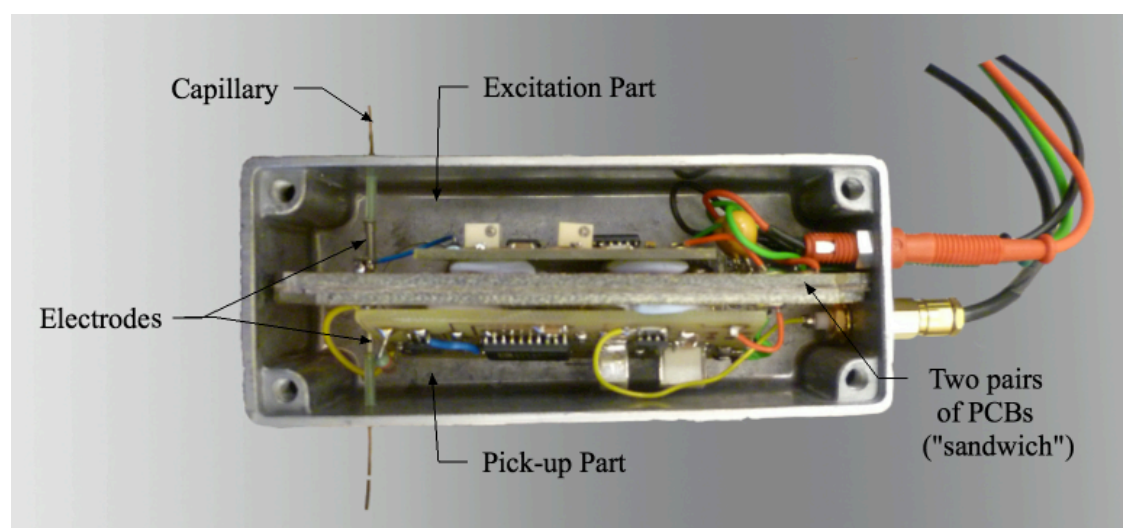


Figure 10. Illustration of the new revision of C^4D detector

The detector cell consists of excitation and pick-up components divided with two pairs of printed circuit boards in a so-called “sandwich”. On each side of the outer pair of boards is soldered an electrode on the copper surface and between separated with the gap made from the inner pair of printed circuit boards. Grounded copper layers of the inner PCBs are facing each other acting like a shield to separate the two parts of the cell. In both of the separated sections are smaller printed circuit boards with surface mounted electronic devices (SMD). On the excitation board is a sine wave generator and an operation amplifier which delivers an amplitude up to 20 V, peak-to-peak, whereas on the pick-up circuit is the current-to-voltage converter that brings the signal that is rectified and low-pass filtered and delivered straight to the

data-acquisition system. The reason for employment of an SIA manifold was that linear aligning of 16 detectors on the commercial CE instrument was impossible due to space limitation. Illustration of such a system is shown in figure 11.

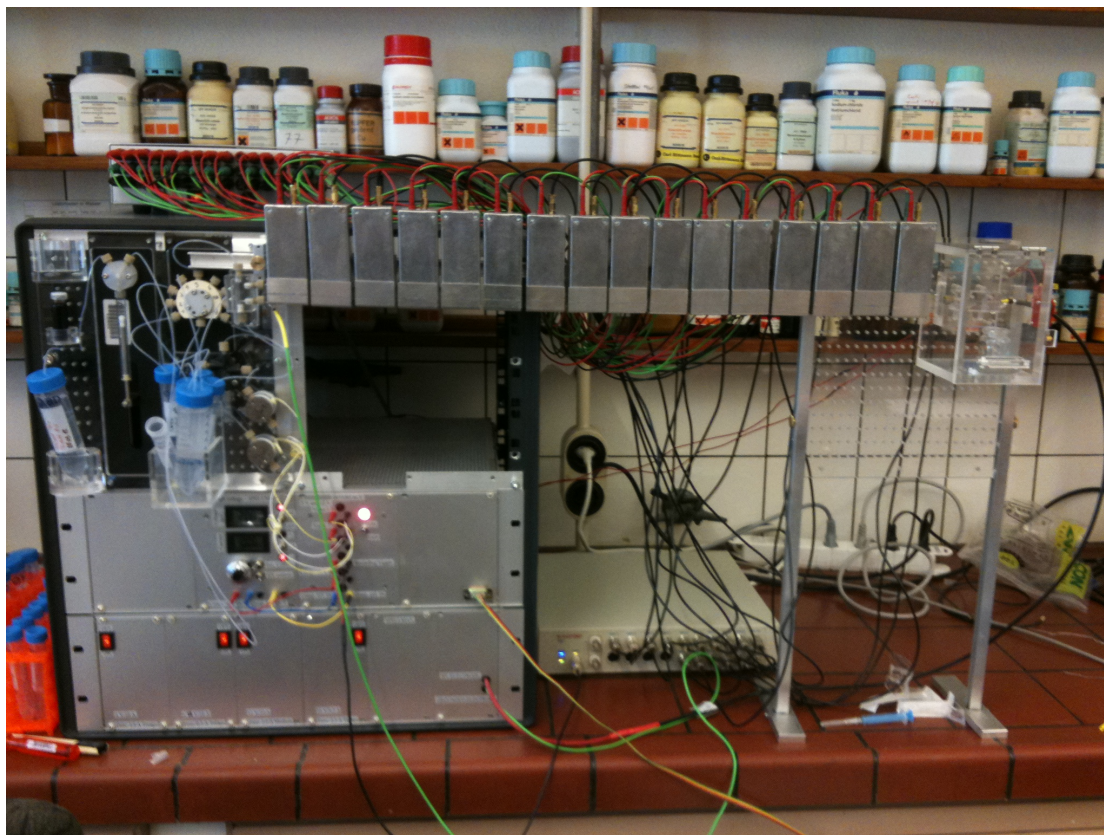


Figure 11. Picture of an array of 16 C⁴D detectors coupled with an SIA system

In a conventional SIA system setup, the micro-step syringe and multiport valve are connected with a holding coil and are utilized for liquid delivery to the grounded interface. Pressurization control was carried out with compressed nitrogen rather than a syringe pump, as it is more precise and more easily achieved with this approach. One capillary ending is placed in the interface whilst the other into the isolated buffer vial together with the high voltage electrode. First measurements with an array of 16 detectors were performed for electrophoretic separation of two inorganic cations, namely sodium and potassium. For all measurements, a capillary of 25 μm inner diameter was used. Hydrodynamic injection was performed and after applying the high voltage, monitoring of the separation process was very clearly observed since the first detector, showing traces and movement of the ions as well as the increase of the baseline resolution of the peaks while passing along the capillary through detectors.


Further application of the array arrangement elucidates the possible benefits in analyzing electrophoretic separations. For this purpose, two sample models were prepared. In the first, analytes were dissolved in water whereas in the other case analytes were dissolved in the background electrolyte. For both cases, the injection plug was 2 cm. For the first case, where the analytes were dissolved in water, separation was obtained faster and the peaks from the observed electropherograms were sharper. This is due to the stacking effect caused by the different conductivities between the sample and the background electrolyte. Also, a slight change in the peak shape described as dissymmetry (positive skewedness) was observed and can be accredited to electrodispersion. When the analytes were dissolved in buffer, separation was manifested with slower migration of the analytes and a wider, almost rectangular, peak shape. The exact behavior of the separation was confirmed with a dynamic computer simulation. Furthermore, parallel determination of inorganic cations and anions is investigated. The placement and amount of the injection plug was optimized. A hydrodynamic injection of a 1 cm sample plug was carried out. For positioning the plug exactly in the middle of the detector s array, and therefore choosing the middle of the efficient length of the capillary, precise timing and pressure control were applied. When the high voltage is employed, movement of the ions was obtained through 16 detectors where cations were migrating towards the negative electrode (cathode) and anions were migrating in the opposite direction towards the anode. Continuous progress of the separation and movement of the ions were determined from the electropherograms of 16 detectors. The complete demonstration of dynamics was again found to be in agreement with computer simulation.

This new arrangement can be considered as an impressive tool for real time monitoring of fundamental electrophoretic processes including separation dynamics and peak shapes, along with the background processes showing conductivity changes. In addition, miniaturization of the system is possible without special equipment and with modest mechanical and electronic skills.

4th project:

A contactless conductivity detector array for capillary electrophoresis

Electrophoresis, (2013), Manuscript in press

	ELPS	elps201300457	Dispatch: November 6, 2013	CE:
	Journal	MSP No.	No. of pages: 5	PE: XXXXX

Electrophoresis 2013, 0, 1–5

1

Marko Stojkovic¹
Israel Joel Koenka¹
Wolfgang Thormann²
Peter C. Hauser¹

Short Communication

Contactless conductivity detector array for capillary electrophoresis

¹Department of Chemistry,
University of Basel, Basel,
Switzerland
²Clinical Pharmacology
Laboratory, Institute for
Infectious Diseases, University
of Bern, Bern, Switzerland

A CE system featuring an array of 16 contactless conductivity detectors was constructed. The detectors were arranged along 70 cm length of a capillary with 100 cm total length and allow the monitoring of separation processes. As the detectors cannot be accommodated on a conventional commercial instrument, a purpose built set-up employing a sequential injection manifold had to be employed for automation of the fluid handling. Conductivity measurements can be considered universal for electrophoresis and thus any changes in ionic composition can be monitored. The progress of the separation of Na⁺ and K⁺ is demonstrated. The potential of the system to the study of processes in CZE is shown in two examples. The first demonstrates the differences in the developments of peaks originating from a sample plug with a purely aqueous background to that of a plug containing the analyte ions in the buffer. The second example visualizes the opposite migration of cations and anions from a sample plug that had been placed in the middle of the capillary.

Received September 16, 2013
Revised October 21, 2013
Accepted October 21, 2013

Keywords:

CE / Contactless conductivity detection / Sequential injection analysis
DOI 10.1002/elps.201300457

The elucidation of the dynamics of electrophoretic separations and processes is of high interest to explore and understand the basic phenomena occurring under the influence of the electric field applied to a liquid medium and to optimize configurations for electrophoretic analyses. Dynamic changes along the electrophoretic column can be investigated by computer simulation and experimental means [1]. Dynamic simulation provides plentiful data for any given electrophoretic system, namely the separation dynamics of sample components together with the ongoing changes of buffer components, pH, ionic strength, conductivity, and electric field strength along the separation column, and effects of fluid flow, including electroosmosis [2, 3]. Experimentally, dynamic processes can be explored with sensors that repeatedly scan the electrophoretic column [4], array or multiple detectors placed along part of or the entire separation space [5, 6], and whole column imaging [7].

Monitoring of the electric field strength or conductivity along the separation space can be considered universal for electrophoresis as it visualizes changes in ionic composition encountered in moving boundary electrophoresis, isotachopheresis, zone electrophoresis, and isoelectric focusing. The use of an array of 255 potential gradient sensors that were in contact with the liquid medium of a 10 cm capillary column of rectangular cross-section led to the visualization of the evolution of zone patterns in moving boundary electrophoresis

[5], isotachopheresis [5, 8, 9], and zone electrophoresis [5] and a similar device with 100 sensors was employed to study the dynamics of the electric field strength distribution in isoelectric focusing of simple buffer systems [6] and synthetic carrier ampholytes [10]. Different types of conductivity detectors for CE were developed over the years, the most appealing being those based on capacitively coupled contactless sensing, an approach that is not subject to corrosion and other deleterious surface phenomena that can occur at electrodes in contact with a liquid medium. Recent reviews are available [11–16]. A contactless conductivity detector cell (the method is often referred to as C⁴D for “capacitively coupled contactless conductivity detection”) is simple in construction, compact in size and inexpensive. The concurrent employment of more than one detector is therefore feasible. Indeed, Saito et al. [17] and Mai and Hauser [18] have made use of two cells placed on the same capillary. This allowed the independent optimization of the detector positions for the simultaneous determination of anions and cations in CZE. In a further development, Gaudry et al. [19] not only used two detectors but also two capillaries for concurrent separation. In another effort, Caslavská and Thormann employed two contactless conductivity detectors to follow bidirectional isotachopheretic zone patterns in double coated fused-silica capillaries that feature a strong EOF toward the cathode [20].

The detector design used in our research group has now been modified to allow placement of individual cells directly side by side on a capillary. This was enabled by appropriate sideways positioning of the cabling for external connections.

Correspondence: Professor Peter C. Hauser, Department of Chemistry, University of Basel, Spitalstrasse 51, 4056 Basel, Switzerland
E-mail: Peter.Hauser@unibas.ch
Fax: +41-61-267-10-13

Abbreviation: SIA, sequential injection analysis

Colour Online: See the article online to view Figs. 2 and 3 in colour.

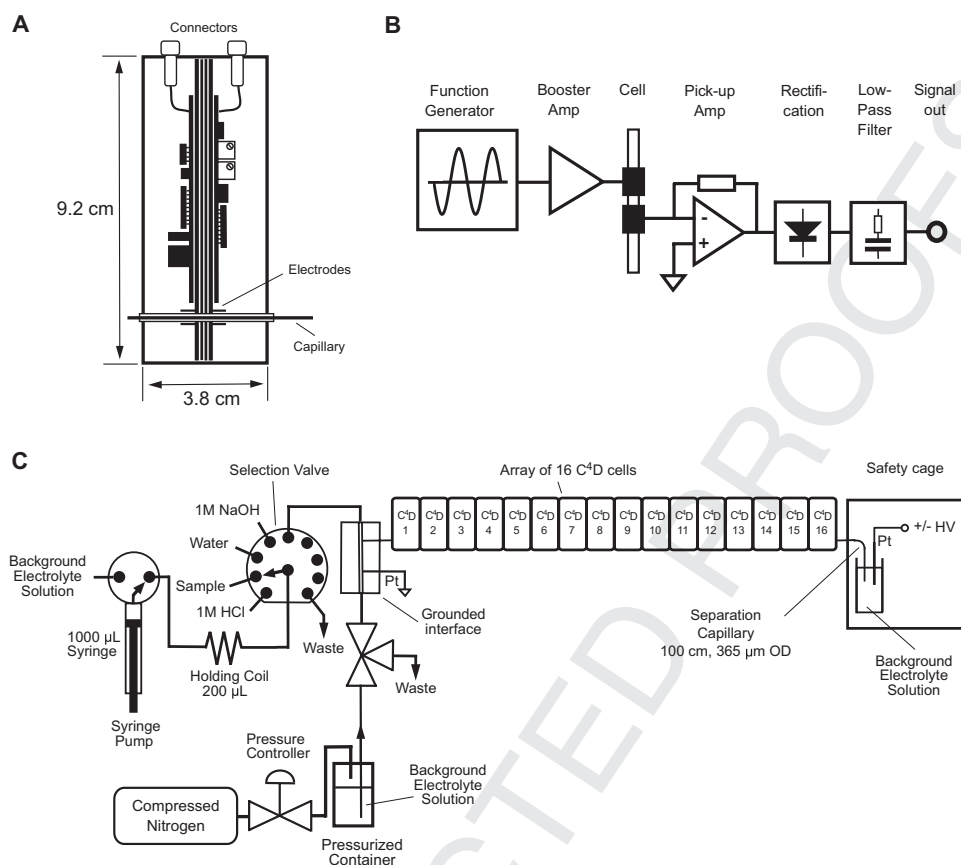


Figure 1. Schematic drawings of (A) geometry of each C⁴D-cell, (B) circuitry of the C⁴D-cells, (C) SIA-CE-C⁴D system with an array of 16 detectors.

Furthermore, the system was miniaturized overall by building the circuitry in the surface mount technology format. Therefore the entire electronic circuitry could be included in the same housing that contains the electrodes, rather than having part of it in an external housing as had previously been the case. In addition, due to the number of units required, the detector was designed for ease of fabrication. The printed circuit boards were etched in our laboratory, the components soldered by hand, and the mechanical work was limited to the cutting of the boards to size and the drilling of holes.

A schematic drawing of a cell is shown in Fig. 1A. The case is divided into two parts by a stack of four printed circuit boards, similar to the arrangement reported by Francisco and do Lago [21]. The two boards on the inside with a thickness of 0.5 mm each are completely covered by copper layers that are facing each other and are electrically grounded to form a Faradaic shield between the two cell halves. A hole of 0.4 mm diameter allows passage of the capillaries with external diameters of 365 µm. The two outer boards contain the electrodes consisting of metallic wire ferrules and some basic electrical connections. The spacing between the electrodes is defined by

the total thickness of the two inner boards and is thus 1 mm. The excitation and pick-up circuitries are built on separate smaller printed circuit boards that are mounted on either side of the sandwich of the four boards. A block diagram of the circuitry is given in Fig. 1B. The excitation part consists of an integrated circuit sine wave generator and an operational amplifier that brings the amplitude to 20 V peak-to-peak. On the pick-up side the cell current is converted to a voltage that is then rectified and low-pass filtered and passed directly to an external data-acquisition system. More general details on the circuitry can be found in earlier publications [22, 23].

Each cell has a width of about 40 mm. This allowed the placement of 16 individual detectors on a capillary of 100 cm total length. The detectors occupy a space of about 70 cm with sensing locations being about 4.4 cm apart. Some extra capillary length is required at the two ends to allow injections and to accommodate buffer reservoirs and high voltage electrodes. The assembly is illustrated in Fig. 1C. Due to space limitations and as the capillary has to be stretched linearly for placement of the detectors the use of a conventional commercial CE instrument was not possible. Instead,

a system based on a sequential injection analysis (SIA) manifold was employed [18, 24–28]. The conventional SIA setup with a holding coil consisting of a syringe pump (Cavro XLP 6000, Tecan, Crailsheim, Germany) and a 9-port channel selection valve (Cavro Smart Valve, Tecan), serves for aspiration and transport of solutions, including sample plugs, to the capillary interface. However, in departure to earlier systems that utilized the syringe pump to achieve pressurization for flushing with sodium hydroxide solution, water and buffer and for injection this was implemented with compressed nitrogen utilizing an electronic pressure controller (VSO-BT, Parker Hannifin, Etoy, Switzerland). While this requires an additional component, the control of pressurization is more easily achieved and more precise with this approach. The three-way valve needed for directing the flow was obtained from NResearch (Gümligen, Switzerland). The SIA-CE interface is made of Perspex and is connecting the liquid channel with the capillary and a grounded electrode, which are mounted through two T-junctions. Polyimide coated fused silica capillaries were obtained from Polymicro (Phoenix, AZ, USA). The capillary ending was placed into a vial, which was filled with the electrolyte solution together with the platinum wire serving as the high voltage electrode. A dual polarity high voltage power supply (± 30 kV, Spellman CZE2000, Pulborough, UK) was employed for application of the separation voltage. The assembly at the high voltage end was insulated in a safety box made from Perspex that was equipped with a micro switch to disrupt the high voltage on opening. All parts of the system were operated under computer control. The detector signals were captured with a 16-channel e-corder (EDAQ, Denistone East, NSW, Australia) and processed with the Chart software package (EDAQ).

The application of the detector array is illustrated in Fig. 2 for the simple example of the separation of Na^+ and K^+ . The stacked plots shows the signals recorded on all of the 16 detectors. In this case, the two ions happened to be already separated at the first detector located 4.5 cm from the injection end, but the further progress of zone electrophoresis is shown very clearly by comparing the traces obtained by the detectors at increasing distances on the separation channel. Note that the electropherograms have been normalized against the baseline signal. This is readily possible, as the circuitry does not have an offset facility. The reason for the normalization is a variation in the sensitivity of the detectors (with maximum deviations of approximately $\pm 60\%$ from the average), which is thought to be due to small differences in the geometry of the cell arrangement. The cells were produced by hand, so that the achievable mechanical precision was limited. The peaks are negative going, indicating a reduction in conductivity when the analyte ions are passing. This is mainly due to the difference in equivalent conductivity between the cations and the co-ion (H^+) from the acetic acid BGE employed for this separation. Negative peaks are a common feature of C^4D , and are often inverted in order to show them in the commonly expected sense, but they were left in the raw state in this case. The figure

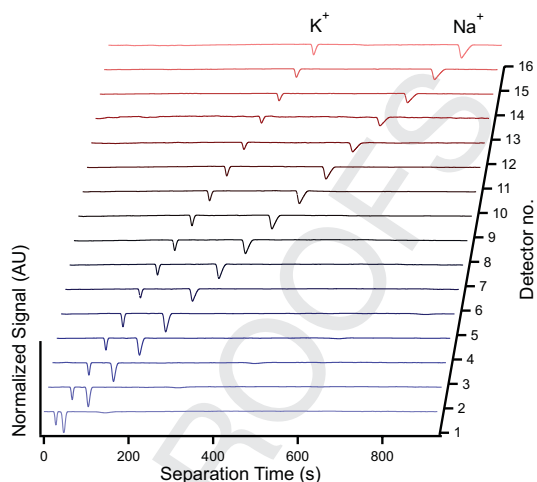


Figure 2. A $100 \mu\text{M}$ of Na^+ and K^+ separated in a BGE of 500 mM acetic acid in a capillary of $25 \mu\text{m}$ internal diameter and 100 cm length at 20 kV . The analytes were injected as NaCl and KNO_3 dissolved in pure water as a plug of 1 cm length (20 psi for 2873 ms).

very nicely demonstrates the capability of the detector array to directly monitor and study dynamic electrophoretic processes.

Examples of the potential benefits in examining electrophoretic separations are given in Fig. 3. The separation of the same cations is shown again in the panels of Fig. 3A and B. Hydrodynamic injection was employed in both cases, but for Fig. 3A the two model analytes were contained in pure water, while for Fig. 3B they were contained in the BGE. The length of the injected plug was 2 cm in both cases. For clarity, only the signals of the first four detectors are shown. Clearly, the peaks for the two ions injected in water are sharper and separation occurs faster. The reason for this is the transient stacking effect taking place at the cathodic buffer interface when the high voltage is turned on. As is the case with the shorter initial zone length (Fig. 2), separation of the two compounds is already complete at the location of the first detector. Also apparent in Fig. 3A is a change of peak shape from a nearly Gaussian shape to a nonsymmetrical appearance. This is particularly clear for the slower ion, Na^+ . The increasing skewedness of the peak, and its expanding width at baseline, can be ascribed to electrodispersion. The peaks of Fig. 3B did not experience the stacking effect as the sample plug did not have a lower conductivity compared to the BGE and are thus wider. Furthermore, as separation of the two cations progresses more slowly compared to the case of Fig. 3A, a transient-mixed zone is monitored at the location of the first detector. The interesting shape of the conductivity signal reveals three zones, the first representing K^+ , the second a transient-mixed zone containing both cations and the third one Na^+ . At the location of the second detector, the two cations are almost completely separated,

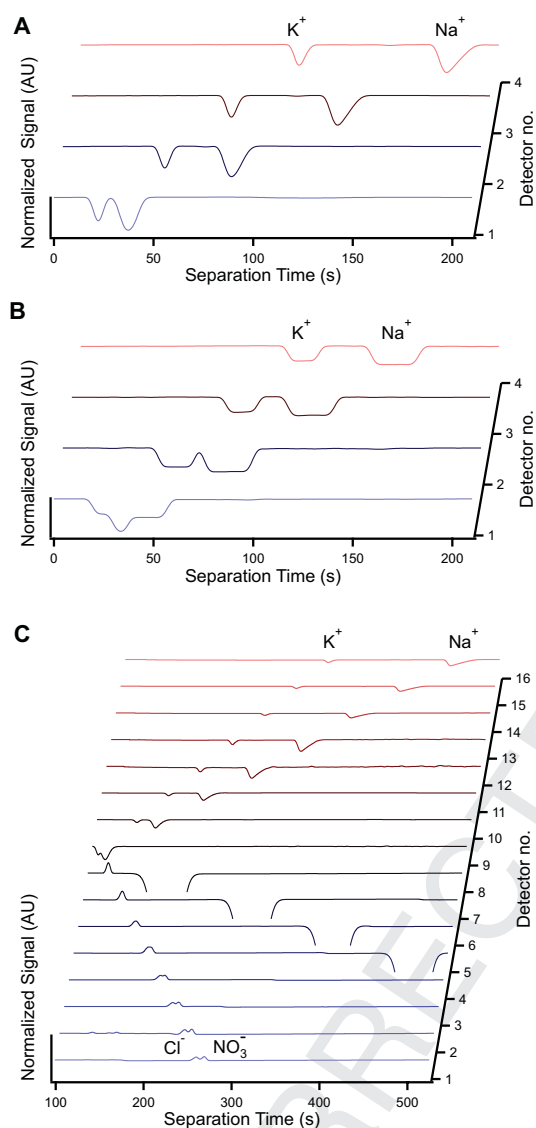


Figure 3. (A) A 100 μ M of Na^+ and K^+ injected as purely aqueous solution. Sample plug: 2 cm (20 psi for 5746 ms). Other conditions are as for Fig. 2. (B) A 100 μ M of Na^+ and K^+ injected dissolved in BGE. Sample plug: 2 cm. Other conditions are as for Fig. 2. (C) A sample plug of 1 cm length of 100 μ M of $NaCl$ and KNO_3 injected as a purely aqueous solution was placed by hydrodynamic pumping between detectors 8 and 9 before applying the separation voltage. Other conditions are as for Fig. 2.

whereas complete separation is monitored with detectors 3 and 4. Conductivities across the cationic sample zones are again lower compared to the conductivity of the BGE, and the mixed zone has a lower conductivity than the K^+ and Na^+ zones, presumably because of the displacement of the

highly conducting co-ion (H^+) from the BGE. The separation dynamics and conductivity distributions of the two configurations shown in Fig. 3A and B were found to be in complete agreement with those obtained by dynamic computer simulation using the SIMUL5 code of Hruška et al. [2] (data not shown).

In Fig. 3C the concurrent separation of cations and anions is monitored. A 1 cm long plug of a mixture of 100 μ M each of KNO_3 and $NaCl$ in pure water was injected hydrodynamically and then placed half-way down the separation capillary, i.e. exactly between detectors 8 and 9. This was possible by precise control and timing of the applied pressure for hydrodynamic pumping. The detector array also enables the operator to follow the movement of the sample plug through the capillary during this manipulation. When the desired position of the sample plug was reached the application of pressure was stopped and the electrophoretic separation started by turning on the high voltage. The electropherograms obtained with the 16 detectors show the subsequent progress of the separation. The cations migrate toward the cathodic capillary end and their movement and separations can be followed on the detector cells 9–16. The anions move in the opposite direction, i.e. toward the injection end of the capillary, and the progress of their separation can also be followed with chloride being slightly faster than nitrate. In contrast to the cationic part, conductivities across the anionic zones are higher compared to the conductivity of the background electrolyte. This and the entire dynamics were again found to be in agreement with computer simulations (data not shown). Note that a dilute acetic acid solution was employed as BGE. At the low pH value of 2.5, a strongly reduced EOF toward the cathode was expected, and thus the fast migrating inorganic anions were not expected to be swept with an appreciable cathodic EOF as would be the case with a buffer of neutral or alkaline pH. In fact, it was found that there was a small flow toward the anode under the conditions used, as evidenced by the large, partly covered, negative going conductivity peak visible for detectors 8 to 4 that represents the fluid element originally occupied by the sample prior to power application. The origin of this anodic flow is not clear and was not yet further investigated.

In conclusion, an SIA manifold for injection was used to construct a CE system with an array of contactless conductivity detectors along the separation capillary. This was possible, as the injection approach does not require the movement of the capillary. The new system allows the simultaneous monitoring of electrophoretic processes throughout a large part of the separation channel and is deemed to have a high potential as a tool to study the fundamental processes underlying the evolution of separations as well as the shapes of peaks and boundaries. C⁴D features a universal response to any changes in ionic composition of the liquid medium in the capillary. Therefore, it is possible to also monitor background processes exhibiting conductivity changes that are not accessible by optical detection. It should furthermore prove useful for the study of reaction kinetics.

The authors are grateful for financial support by the Swiss National Science Foundation through grants 200020-126384 and 200020-137676.

The authors have declared no conflict of interest.

References

- [1] Mosher, R. A., Saville, D. A., Thormann, W., *The Dynamics of Electrophoresis*, VCH Publishers, Weinheim 1992.
- [2] Hruška, V., Jaroš, M., Gaš, B., *Electrophoresis* 2006, **27**, 984–991.
- [3] Thormann, W., Breadmore, M. C., Caslavská, J., Mosher, R. A., *Electrophoresis* 2010, **31**, 726–754.
- [4] Hjertén, S., *Chromatogr. Rev.* 1967, **9**, 122–219.
- [5] Thormann, W., Arn, D., Schumacher, E., *Electrophoresis* 1984, **5**, 323–337.
- [6] Thormann, W., Mosher, R. A., Bier, M., *J. Chromatogr.* 1986, **351**, 17–29.
- [7] Wu, X.-Z., Huang, T., Liu, Z., Pawliszyn, J., *Trends Anal. Chem.* 2005, **24**, 369–382.
- [8] Thormann, W., Arn, D., Schumacher, E., *Sep. Sci. Technol.* 1984, **19**, 995–1011.
- [9] Thormann, W., Arn, D., Schumacher, E., *Electrophoresis* 1985, **6**, 10–18.
- [10] Thormann, W., Egen, N. B., Mosher, R. A., Bier, M., *J. Biochem. Biophys. Methods* 1985, **11**, 287–293.
- [11] Kubáň, P., Hauser, P. C., *Electrophoresis* 2013, **34**, 55–69.
- [12] Mai, T. D., Hauser, P. C., *Chem. Record* 2012, **12**, 106–113.
- [13] Coltro, W. K. T., Lima, R. S., Segato, T. P., Carrilho, E., de Jesus, D. P., do Lago, C. L., da Silva, J. A. F., *Anal. Methods* 2012, **4**, 25–33.
- [14] Kubáň, P., Hauser, P. C., *Electrophoresis* 2011, **32**, 30–42.
- [15] Kubáň, P., Hauser, P. C., *Electrophoresis* 2009, **30**, 176–188.
- [16] Trojanowicz, M., *Anal. Chim. Acta* 2009, **653**, 36–58.
- [17] Saito, R. M., Brito-Neto, J. G. A., Lopes, F. S., Blanes, L., da Costa, E. T., Vidal, D. T. R., Hotta, G. M., do Lago, C. L., *Anal. Methods* 2010, **2**, 164–170.
- [18] Mai, T. D., Hauser, P. C., *J. Chromatogr. A* 2012, **1267**, 266–272.
- [19] Gaudry, A. J., Guijt, R. M., Macka, M., Hutchinson, J. P., Johns, C., Hilder, E. F., Dicinovski, G. W., Nesterenko, P. N., Haddad, P. R., Breadmore, M. C., *Anal. Chim. Acta* 2013, **781**, 80–87.
- [20] Caslavská, J., Thormann, W., *Electrophoresis* 2006, **27**, 4618–4630.
- [21] Francisco, K. J. M., do Lago, C. L., *Electrophoresis* 2009, **30**, 3458–3464.
- [22] Tanyanyiwa, J., Galliker, B., Schwarz, M. A., Hauser, P. C., *Analyst* 2002, **127**, 214–218.
- [23] Zhang, L., Khaloo, S. S., Kubáň, P., Hauser, P. C., *Meas. Sci. Technol.* 2006, **17**, 3317–3322.
- [24] Mai, T. D., Schmid, S., Müller, B., Hauser, P. C., *Anal. Chim. Acta* 2010, **665**, 1–6.
- [25] Mai, T. D., Hauser, P. C., *Talanta* 2011, **84**, 1228–1233.
- [26] Mai, T. D., Hauser, P. C., *Electrophoresis* 2011, **32**, 3000–3007.
- [27] Mai, T. D., Hauser, P. C., *Electrophoresis* 2013, **34**, 1796–1803.
- [28] Stojkovic, M., Mai, T. D., Hauser, P., *Anal. Chim. Acta* 2013, **787**, 254–259.

2.5 Study on the effect of the electrolyte concentration on the sensitivity of the axial capacitively coupled contactless conductivity detector when used with very narrow capillaries

2.5.1 Introduction

When we started this project, we observed an effect that was not initially understood. Namely, using small internal diameter capillary of 10 μm and with high concentration of background electrolyte solution resulted in higher signal-to-noise ratio. Therefore, we tried to explore the reasons for the effect on the sensitivity in capillary electrophoresis with contactless conductivity detection. To understand this behavior, foremost, we need to explain functionality and the fundamentals of the C^4D detector cell.

Two research groups, Zemann and co-workers [1] and Fracassi da Silva and Do Lago [2] introduced contactless conductivity detection to capillary zone electrophoresis independently. The principal setup of C^4D is still in use, although many modifications on the detector were reported since then and commercial detectors are currently available from at least a few vendors. The measuring cell is divided in two compartments with two pairs of printed circuit boards, on the outer pair of which two electrodes were attached, as is illustrated in Fig. 1A. The grounded inner pair acts as a Faradaic shield totally isolating the two sections. In this setup, the electrodes behave as capacitors and the solution in the capillary as a resistor forming the typical C^4D arrangement. This allows applying of an ac-voltage into the solution. The resulting current depends on the total conductivity of the solution, and can be picked up by the second electrode. The gap between the electrodes determines the cell volume and the cell can be represented by a simplified equivalent circuit diagram of a serial arrangement of capacitor-resistor-capacitor as shown in Fig. 1B. Due to the small distance between the electrodes of only 1 mm, stray capacitance can occur between electrodes, but is unwanted as it leads to a background current and is often reduced by placing a grounded shield between the electrodes (see Fig. 1A). However, stray capacitance cannot be fully eliminated as the capillary has to pass through the shield. The fundamental aspects of the method were previously studied in detail [3-7].

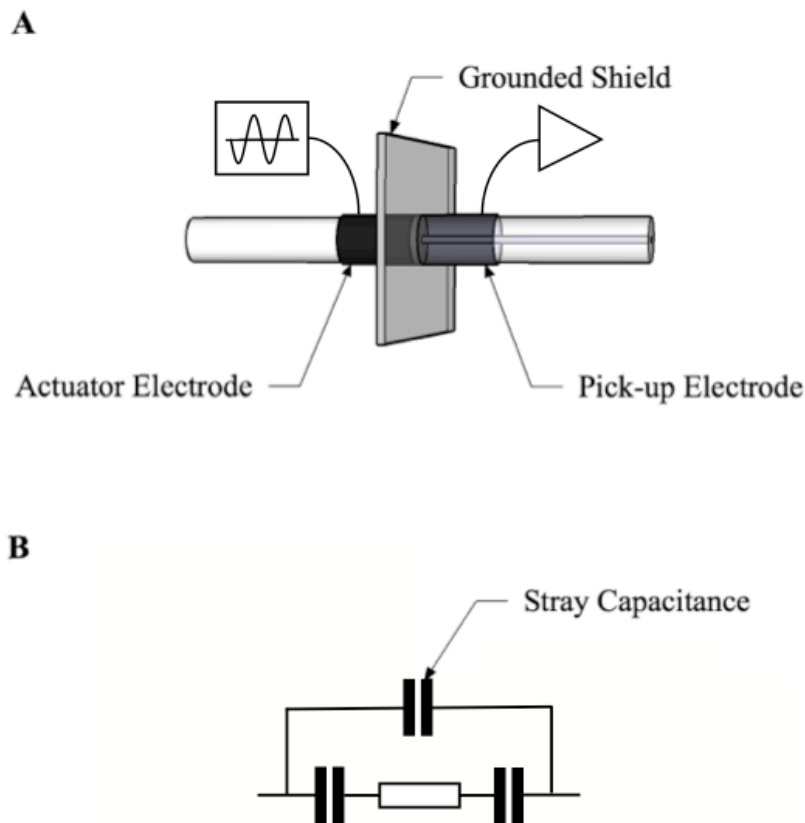


Figure 1. Overview of an axial C⁴D setup:

- A) Representation of an axial arrangement of the C⁴D cell and a Faradaic shield,
 B) Simplified equivalent circuit diagram with stray capacitance due to the direct coupling between the electrodes

Mainly, the detectors are employed with background electrolytes of low conductivity in order to avoid self-heating effect also known as Joule heating. This is more needed than in optical detection method in CZE. The reason is the fact that C⁴D is a bulk method, *i.e.* a background signal is always present, and the relatively high temperature coefficient of the conductivity of ion solutions. This is why relatively narrow capillaries of 50 μm or 25 μm inner diameter have generally been used more in CE-C⁴D. The employment of capillaries with such small internal diameters is basically of benefit as zone broadening is less pronounced in narrow tubings [8], but is not actually possible with optical detection due to the short pathlength and the necessary restricted aperture. In addition, it has been found that the limits of detection

with C⁴D do not worsen when going down to 10 μm internal diameter [9, 10]. Not entirely, but this can be described by the fact that both, signal and background noise scale with the diameter, so therefore the signal-to-noise ratio is favorably affected. During the separation, narrow capillaries of 25 μm and 10 μm internal diameter could be introduced with hydrodynamic pumping but with little penalty in peak dispersion. In such narrow capillaries, laminarity of the bulk flow can cause band broadening. Thus, hydrodynamic pumping can be considered as one of the parameters for electroosmotic compensation, for injection and positioning of sample plugs, as well as for optimization of separation and analysis time [9, 11, 12]. Recently, a fundamental study on the use of hydrodynamic pumping in small i.d. capillaries has been achieved [13].

One effect was previously noticed where it has been shown that relatively high buffer concentrations give the highest peaks when very narrow capillaries are employed, and hence, best detection limits [10, 11]. This result, however, was not expected nor predicted by the fundamentals of conductivity detection [3]. Deviation of the conductance value (ΔG) for a peak, determining sensitivity, is given by equation below but the concentration of the ions of the background electrolyte are not part of this equation.

$$\Delta G = c_A \frac{(\mu_A - \mu_S)(\mu_A + \mu_O)}{\mu_A} \cdot \frac{F}{K}$$

where

c_A = analyte ion concentration

μ_A = absolute mobility,

μ_S = absolute mobility of the electrolyte co-ion

μ_O = absolute mobility of the counter-ion

F = Faraday constant

K = the cell constant

This can be considered as a significant factor but the reason for such a behavior is still missing. Therefore, in order to explain in detail the unexpected effect of the buffer concentration on sensitivity and to gain an adequate understanding of the performance of C⁴D in CZE, specific investigations were carried out and are reported herein.

2.5.2. Experimental

All reagents used for the measurements were of analytical grade. Deionized ultrapure water, obtained from a Milli-Q system, of 17.7 M Ω cm resistivity and purity <5 ng g⁻¹ for total carbon was used for preparation of all solutions. Potassium chloride was purchased from Merck, L-Histidine (His) and Acetic acid from Fluka.

Stock solutions of potassium chloride have been prepared daily in concentrations of 10 mM and 444.44 mM and were used for the preparation of the standards. From the concentration of 444.44 mM KCl, standard solutions of 0.44 mM, 2.67 mM, 4.44 mM, 44.44 mM and 266.67 mM KCl were made respectively. In addition, from the concentration of 10 mM KCl, standard solution of 100 μ M KCl was prepared.

The electrolyte buffer solution consisted of 105 mM His and was adjusted at its pH value of 4 with the acetic acid. For that purpose, model 744 pH meter was used. Standard buffer solutions with the following concentrations of 2 mM, 8 mM, 12 mM, 25 mM, 35 mM, 55 mM and 70 mM were prepared from 105 mM His stock solution. Specific conductivities of all prepared standard solutions were measured using a model 660 conductometer.

For measurements done by CE-C⁴D, purpose made instrument has been used. A dual polarity high voltage supply with \pm 30 kV maximum output voltage and polyimide coated fused silica capillaries of 363 μ m outer diameter and 10 μ m and 50 μ m internal diameter were used for all the experiments. Detection was carried out with the C⁴D detectors built in-house together with excitation circuitry and detection electronics. An e-corder 401 data acquisition system was used for recording the detector signals and was connected to a computer. Purpose-made instrument was made of Perspex box, divided in two sections. First section is injection section and has a small buffer vial into which is inserted high-voltage platinum electrode. The first section has been separated from the second with a Perspex plate with a small hole for the capillary to pass through it. In the second section (so-called detection section) is a ground electrode that is merged to another buffer vial, also filled with the same volume of the buffer, and a detector cell through which the capillary is passing. In both sections, vials are on the same level in steady state to avoid hydrodynamic flow of the buffer inside the capillary. The polarity of the high voltage can be changed to negative or to positive, depending on the goal (if anions or cations are separated). In addition, a function generator and oscilloscope are used.

To avoid interference of changing the buffer concentration constantly after several measurements through one single capillary and rinsing the capillary after every measurement, in order to shorten the measurement time and establish proper equilibrium inside the capillary, we used individual capillaries for every buffer concentration for both, 10 μm and 50 μm i.d. capillaries. Notwithstanding to have uniform capillaries, they were all having total length of 50 cm with effective length of 43.5 cm. For 10 μm i.d., capillaries were flushed with 1 M NaOH and water for 20 min and then for 45 min with the background electrolyte solution to make sure that the proper equilibrium is established. For 50 μm i.d., capillaries were conditioned for 10 min with 1 M NaOH and water, and 20 min with the buffer solution.

Hydrodynamic injection by siphoning was employed for 50 μm i.d. capillaries for 30 seconds on 10 cm height, whereas for 25 μm i.d. capillary, time for injection was 45 seconds on 30 cm height. For capillaries of 10 μm i.d. problem occurred when longer time for hydrodynamic injection was applied due to very narrow internal diameter of the capillary and inappropriate injection plug of the sample needed for the injection. Therefore, for 10 μm i.d. capillaries, electrokinetic injection was carried out for 2 seconds. All the parameters for hydrodynamic injections were calculated with Poiseuille's equation.

2.5.3. Results and Discussion

While more quantitative conformation on this counter-intuitive buffer effect was previously investigated [13], only a tentative explanation for it was offered, namely that it was a consequence of stray capacitance in the detector [10]. The direct coupling between the electrodes through the gap in the shielding and laterally through the capillary wall can be considered as a shunt resistance and is more significant in relative terms when the cell resistance becomes larger, as is the case for narrow capillaries.

2.5.3.1. Investigation of the Influence of Stray Capacitance on the Effect of Buffer Concentration on the Peak Sensitivity

Considering that the stray capacitance can influence the effect of the buffer concentration on peak height then it should be possible to reduce or eliminate the impact by minimizing this unwanted by-pass. The C^4D detector cell used previously

in our research group was shielded, but was not designed for minimization of stray capacitance (by using the 10 μm capillaries). Therefore, we tried to reduce this effect with a new cell design. The detector cell is divided in two cell compartments that were to be totally shielded (to isolate two sections from each other and from outside), except for a hole just large enough to let the capillary pass. The design of the cell is depicted in Fig. 2.

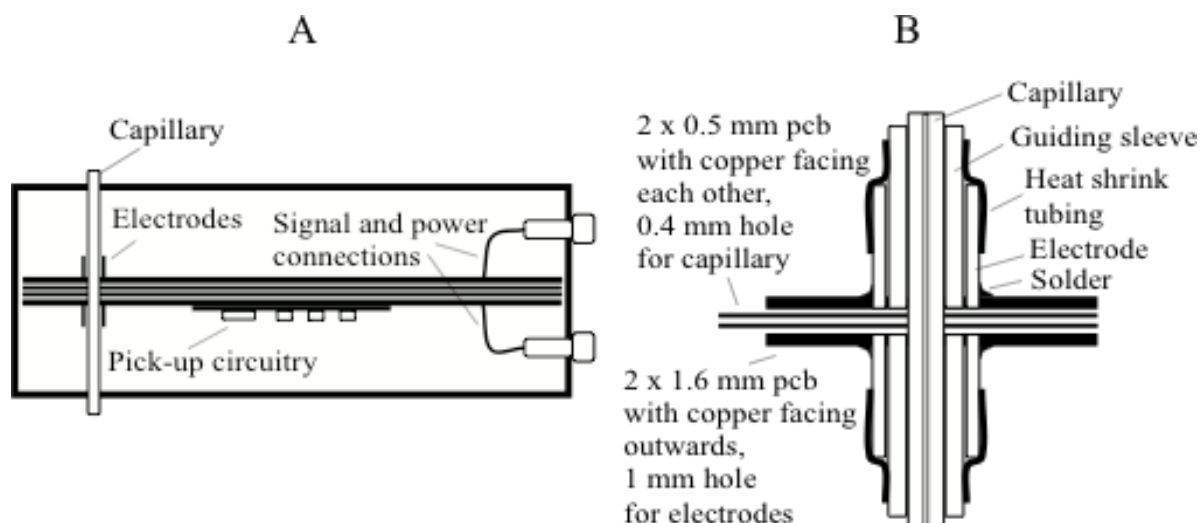


Figure 2. Design of a cell with minimum stray capacitance:

- A) Cross section of a detector cell;
- B) Zoomed cross section of electrodes and shield feedthrough (“sandwich”)

It is based on two printed circuit boards of 0.5 mm thickness which are coated with a 35 μm thick copper layer forming a grounded Faradaic shield between the two sections where the two copper sides face each other. A 0.4 mm diameter hole just admits capillaries with the standard outer diameter of 365 μm . The total thickness of 1.0 mm defines the length of the cell. The electrodes consist of wire ferrules of 0.6 mm internal diameter and have a wall thickness of only 0.15 mm. The fact that the diameter of the two electrodes is larger than that of the hole means that the ends face the shield which helps to minimize direct coupling. The electrodes and associated circuitry are mounted on a further pair of printed circuit boards (1 mm thickness) sandwiched two the inner pair. Guiding sleeves mounted inside the electrodes (but not passing through the shield) allow easy alignment of the capillary. This assembly is mounted in a die cast aluminum case, which ensures complete individual shielding of

the excitation and pick-up part. An external function generator provided excitation and the current signal was converted to a voltage using an operation amplifier in the current follower configuration. A specific operational amplifier that has a very flat frequency response (OPA655) was used in order to avoid a measurement bias by the electronic circuitry. C^4D -cells can be characterized by acquiring their Bode plots, a graph of cell current vs. frequency of the applied sine wave. Stray capacitance would be evident in these plots by a significant rise in the signal at the high frequency end [6]. Bode plots for a capillary of 10 μm i.d. filled with a typical background electrolyte and a dry 10 μm i.d. capillary are shown in Fig. 3. The response for the capillary filled with buffer corresponds to the expected, *i.e.* a rise of signal with frequency until a plateau is reached, which is just attained within the frequency limit of the measuring set-up employed. For the dry cell a small signal is measureable, which can only be due to stray capacitance. This indicates that stray capacitance is not completely absent for the new cell optimized for the narrow inner diameter capillary, but is relatively small.

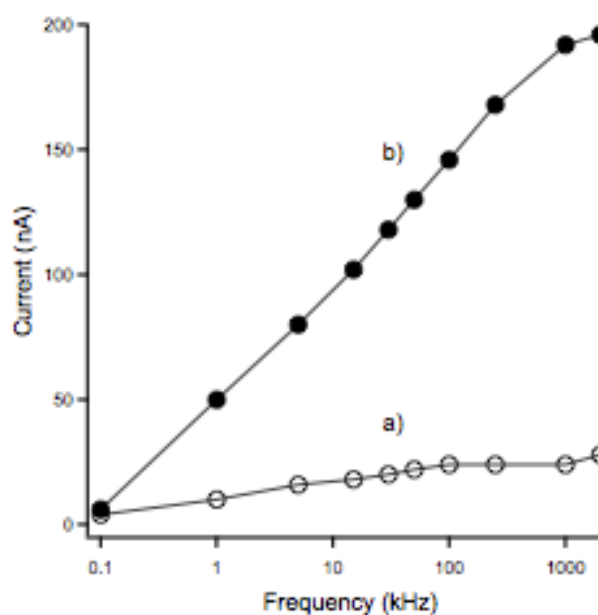


Figure 3. Bode plots for the cell currents for:

- a) dry 10 μm i.d. capillary,
- b) the same capillary filled with a 50 mM histidine buffer adjusted to pH 4.0 with acetic acid

Investigation was then further taken by testing if the effect of the background electrolyte concentration on sensitivity is present even with the minimum stray capacitance cell. An electrolyte solution consisting of L-histidine, which was adjusted with acetic acid to a pH of 4.0, was employed. The peak heights for the injection of $100 \mu\text{M K}^+$ into this buffer employed over a wide concentration range were determined. As can be seen from Fig. 4, for a capillary with the standard diameter of $50 \mu\text{m}$ some variation is evident, and for the $10 \mu\text{m}$ capillary a strong relationship of peak height with the electrolyte concentration is evident. Note, that the absolute peak heights are not relevant and that the highest buffer concentrations could not be tested with the larger diameter capillary due to excessive Joule heating. The behaviour for the $10 \mu\text{m}$ capillary matches that observed for other detectors used in our laboratory. They were not optimized for minimum stray capacitance in view of employment with $10 \mu\text{m}$ capillaries [11].

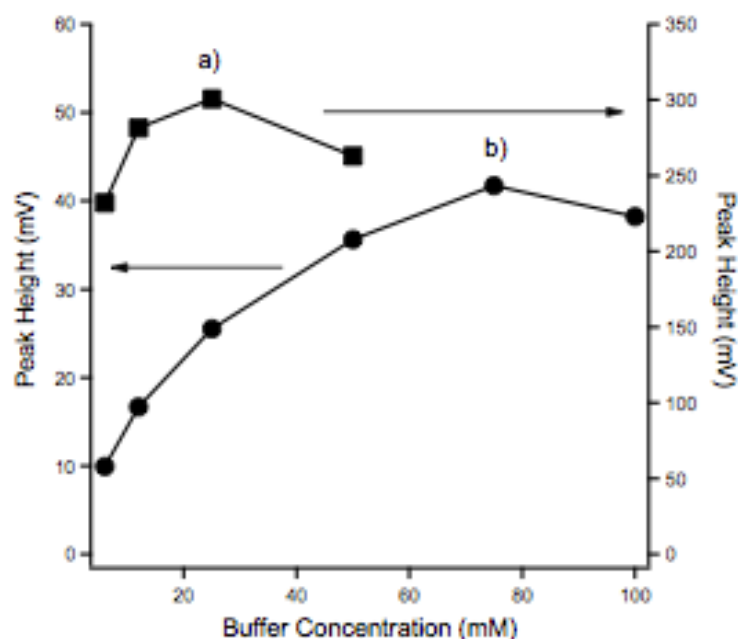


Figure 4. Dependence of the peak height of $100 \mu\text{M K}^+$ on the buffer concentration for:
a) $50 \mu\text{m}$ i.d. capillary,
b) $10 \mu\text{m}$ i.d. capillary.

Buffer: from 5 mM to 100 mM L-Histidine, adjusted with acetic acid to pH 4. Capillary length: 50 cm (42 cm effective); separation voltage: 20 kV; hydrodynamic injection of a sample plug length is identical for both capillary diameters.

The effect is thus systematic, but in consideration that the results for the new cell alignment were almost identical to those for the previous cell, renders the stray capacitance hypothesis doubtful.

2.5.3.2. Explanation From the Fundamental Aspect

It was thus considered that the effect may therefore be intrinsic to the principle of measurement. As discussed in the introduction, the cell can be approximated as a serial arrangement of capacitor - resistor - capacitor, with a possible bypass capacitance, as shown in Fig. 1. It is not possible to determine the value of the resistance directly, but applying an ac-voltage and recording the resulting current can test the impedance of the entire assembly.

The total ac-impedance (Z) of a serial arrangement of elements is given by its sum [14], *i.e.*:

$$Z = Z_1 + Z_2 + Z_3 + \dots \quad (\text{equation 1})$$

For the equivalent circuitry of the cell:

$$Z = Z_c + Z_r + Z_c = Z_r + 2 \cdot Z_c \quad (\text{equation 2})$$

Z_c represents the impedances of the capacitors formed by the electrodes, while Z_r is the impedance of the solution contained in the capillary. This corresponds simply to the solution resistance, R (which is the inverse of conductance):

$$Z_r = R \quad (\text{equation 3})$$

The impedance of the electrodes is given by their capacitance, C , and is frequency (f) dependent:

$$Z_c = \frac{1}{2\pi f C} \quad (\text{equation 4})$$

As has been shown previously, the cell resistance can be approximated [6, 7] by the conductivity of the solution (κ) and length of the gap between the electrodes (l_{gap}) as well as the internal diameter of the capillary (d):

$$R = \frac{l_{gap} \cdot 4}{\kappa d^2 \pi} \quad (\text{equation 5})$$

The electrode impedances can be calculated from the formula for a coaxial capacitor:

$$C = \frac{2\pi \varepsilon_0 \varepsilon_r l_{el}}{\ln \frac{D}{d}} \quad (\text{equation 6})$$

l_{el} is the length of the electrodes, D the internal diameter (i.d.) of the electrode ($D = 600 \mu\text{m}$), ε_0 the relative permittivity of vacuum ($\varepsilon_0 = 8.854 \cdot 10^{-12} \text{ F} \cdot \text{m}^{-1}$) and ε_r the relative permittivity of the insulation. The latter is composed of the silica wall of the capillary ($\varepsilon_r = 4$) and the guiding sleeve of the cell made from PEEK ($\varepsilon_r = 3.2$).

From the generalized Ohm's law, the cell current (i) is then given by the following formula (V is the applied voltage):

$$i = \frac{V}{R + 2 \cdot Z_c} = \frac{V}{R + \frac{1}{\pi f C}} \quad (\text{equation 7})$$

After substitution the current is given by:

$$i = \frac{V}{\frac{l_{gap} \cdot 4}{d^2 \pi \kappa} + \frac{\ln \frac{D}{d}}{2\pi^2 \varepsilon_0 \varepsilon_r l_{el} f}} \quad (\text{equation 8})$$

The cell current can now be calculated from the fundamental data. Modelled Bode plots for $50 \mu\text{m}$ and $10 \mu\text{m}$ i.d. capillaries, filled with electrolyte solution are given in Fig. 5A, where it can be seen that the modelling comes close to the practical results considering the approximations. As the Bode plots could be fairly well predicted by calculation for the narrow capillary of $10 \mu\text{m}$, this basic model can therefore be adopted with some faith. An examination of equation 8 shows that a linear dependence of the cell current on the conductivity is only obtained if the capacitive term, the second part of the denominator, is negligible. This corresponds to the plateau region of the Bode plots, and for this reason the cells should be operated in

this frequency range to obtain maximum sensitivity. The frequency of 300 kHz corresponds to the maximum possible with our electronic circuitry according to its bandwidth limit.

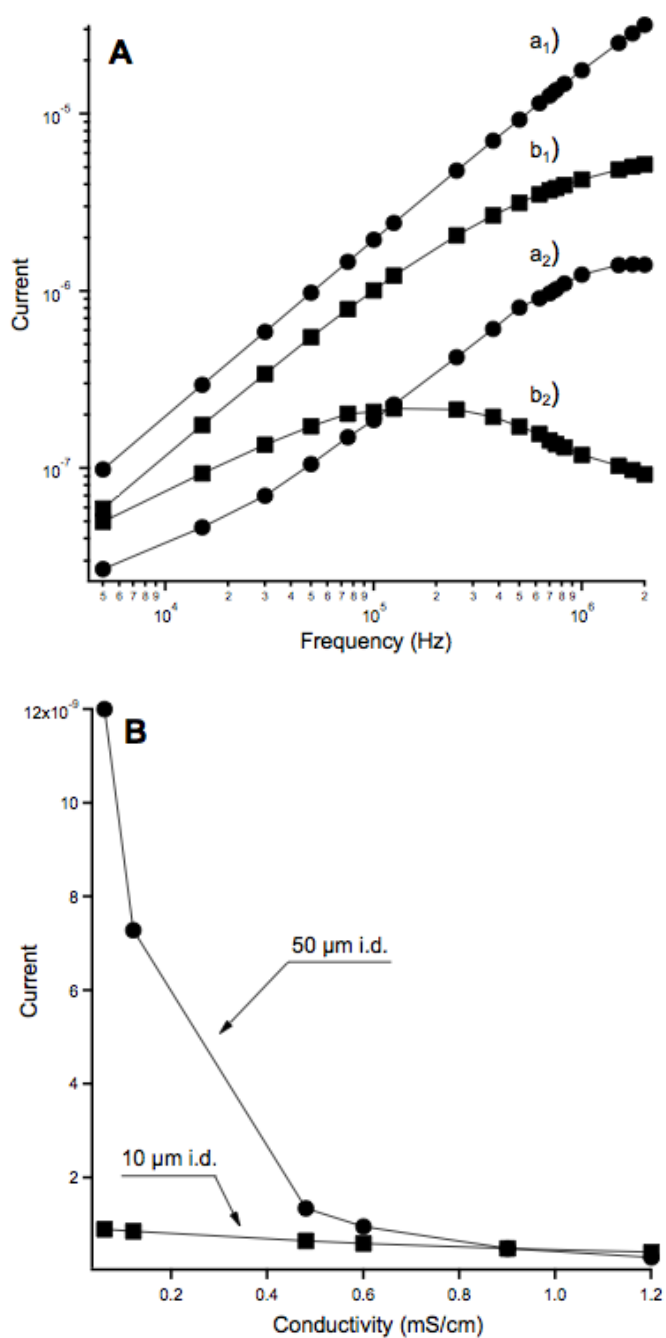


Figure 5. (A) Bode plots for capillaries filled with 444.44 mM KCl for 50 μm i.d. with modelled (a_1) and measured (a_2) values and for 10 μm i.d. capillary for modeled (b_1) and measured (b_2) values;

(B) Current changes vs. Resistance for fixed frequency of 300 kHz

On the other side, at the high frequency (*i.e.* >1 MHz), current response is linear and the sensitivity is independent of the buffer concentration. Regarding equation 8, in case of lower frequency capacitive term cannot be neglected. Actually, an increase in buffer concentration is expected to lead to a decrease of peak height, as shown in Fig. 5B. The calculated current responses are given in dependence of the buffer concentration for a fixed frequency of 300 kHz. This indicates the dependence of peak height on the background conductivity and hence buffer concentration. This is not in agreement with experimentally found results for the 10 μm i.d. capillary where an increase of peak height is observed. It is thus not likely that the behavior is inherent to the detector.

2.5.3.3. *Stacking Phenomena*

As the concentration effect is not generated by the cell, then the reason has to be related to factors influencing the peaks in the capillary. The effect has to be dependent on both the concentration and the capillary diameter. However, increasing the concentration of the buffer will also increase the current that passes through the capillary, which in turn will increase heat generated in the capillary causing a variety of problems. Low conductivity buffers are usually employed to minimize Joule heating, as the background signal is always prompted along with the high temperature produced from the conductivity of the solutions [8]. This is more pronounced for larger diameters, but does not explain the concentration effect. Band broadening caused by electrodispersion is reduced when higher concentration of the buffer and narrow diameter capillaries are employed.

However, a second process is the transient stacking. Sample stacking phenomena can occur if the composition of the sample plug is different from the composition in the background buffer. This phenomenon can be explained in the following way: the introduced sample is a low conductivity solution whereas the background electrolyte is a high conductivity solution. As both solutions are present in capillary when voltage is applied, the low conductivity region of the sample will be more influenced by a higher electric field than the background buffer region. Therefore, sample ions will move faster in the low conductivity region compared to the high conductivity region. Such a change in sample movement across the concentration boundary will

reduce the sample zone length and provide zone with higher concentration. This results in greater, sharper peaks and better sensitivity when the difference in conductivities between buffer and the sample is higher, as shown in Fig 6A.

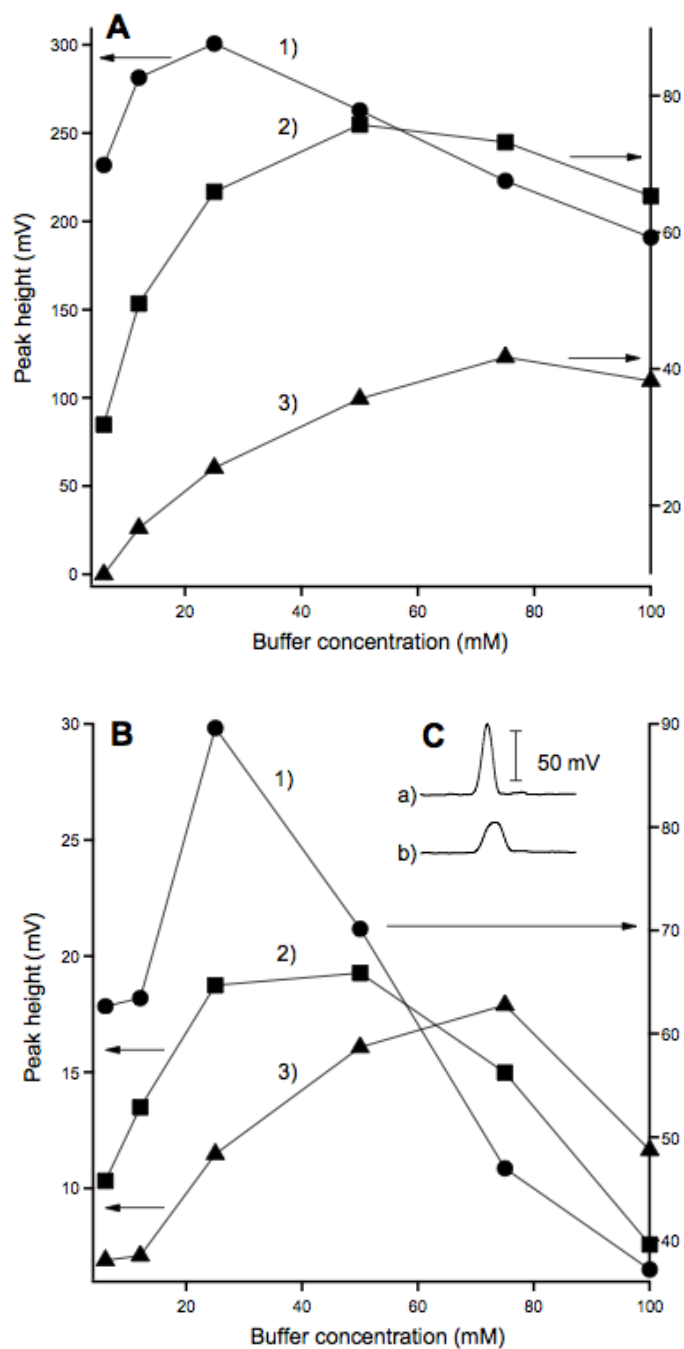


Figure 6. Peak heights of 100 μM K^+ vs. concentrations of L-Histidine buffer, adjusted at pH 4.0 with acetic acid in: 1) 50 μm , 2) 25 μm and 3) 10 μm i.d. capillaries of 50 cm length, for injections of (A) sample diluted in water, (B) sample diluted in buffer for evenly spaced concentrations and (C) Insert of the peaks with sample in a) water and in b) buffer;

For comparison, capillary diameters of 50 μm , 25 μm and 10 μm i.d. were employed and as observed, maximum peak heights were found for different buffer concentrations. For the narrow capillary diameter of 10 μm i.d., transient stacking effect is more pronounced for higher BGE concentrations. This nicely illustrates the effect of the buffer concentration on sensitivity. Following the pattern, when the conductivity of the sample is the same as the conductivity of the buffer, no stacking effect should be present. In Fig. 6B has been shown that although significantly reduced, some appearance of the sample stacking effect is still present but on a much smaller scale. We should expect minimum difference between conductivities of the sample and the buffer, and therefore peak heights should not vary much. Resulting curves for three diameters should form plateau regions. Electropherograms of injections when the sample is diluted in water and in buffer, as presented in Fig. 6C, show the peak shapes that confirm the presence of stacking phenomena. It has been supposed that the injection of the sample in the buffer will have more Gaussian shape. A further investigation has been carried out and documented in Fig 7. Injections were introduced into 10 μm i.d. capillary by varying the proportions of the sample in different concentrations of the same buffer used as a background electrolyte. Thus, the BGE concentration was constant.

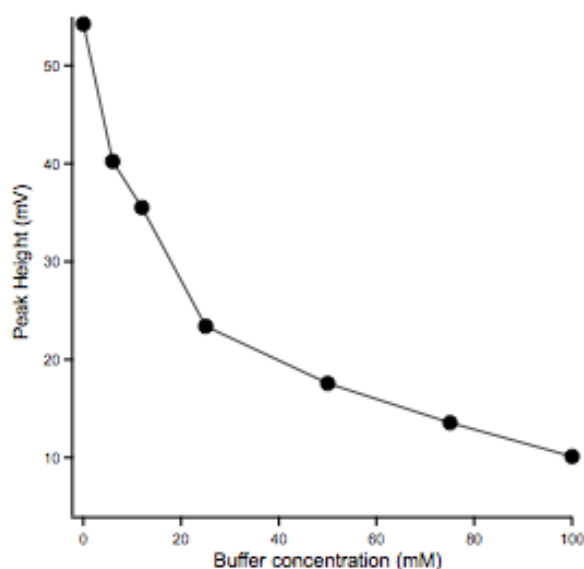


Figure 7. 10 μm capillary, injections into high concentration buffer of 100 mM L-Histidine adjusted on pH 4.0 with acetic acid, but sample in range of different concentrations of buffer: from water, over diluted buffers (6 mM, 12 mM, 25 mM, 50 mM and 75 mM), to buffer at full concentration of 100 mM L-Histidine.

This is just a confirmation that the effect of buffer concentration on sensitivity is not present for injections with sample in buffer. It can be considered as concentration dependent, but not dependent on the diameter.

Therefore, it clearly opens the possibility that the effect must be the result of a combination of at least two processes, *i.e.* sample stacking in all cases more pronounced for higher buffer concentration, or some behavior of electronics that results from cell design or from electrophoretic processes that have synergistic effect.

2.5.4. Conclusion

Better understanding of the influence of the buffer concentration on the sensitivity for the axial C⁴D detector has been examined. We concluded that the higher concentrations of the electrolyte solution are giving the best results in terms of sensitivity, when capillaries with narrower internal diameter are employed. Especially the tailored C⁴D detector has been made without serious difficulties, even with modest electric equipment. Then this detector was used to investigate the effect of the cell capacitance when extended electrodes are engaged in the cell and proper shielding with specific “sandwich” design is performed. Several theoretical aspects were reviewed but the effect is still not proven. It has been concluded that there is a possibility that the concentration effect is not coming only from one factor but instead, presence of multiple factors can have an influence on this effect, including cell design, electronics and/or electrophoretic processes. Thus, further investigation should be carried out as some of the findings can explain some of the problem’s aspects, potentially lead to its solution.

2.5.5. References

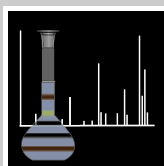
- [1] A. J. Zemann, E. Schnell, D. Volgger, G. K. Bonn, *Anal. Chem.* **1998**, *70*, 563-567.
- [2] J. A. F. da Silva, C. L. do Lago, *Anal. Chem.* **1998**, *70*, 4339-4343.
- [3] J. G. A. Brito-Neto, J. A. Fracassi da Silva, L. Blanes, C. L. do Lago, *Electroanalysis* **2005**, *17*, 1198-1206.
- [4] J. G. A. Brito-Neto, J. A. Fracassi da Silva, L. Blanes, C. L. do Lago, *Electroanalysis* **2005**, *17*, 1207-1214.
- [5] S. E. Johnston, K. E. Fadgen, L. T. Tolley, J. W. Jorgenson, *J. Chromatogr. A* **2005**, *1094*, 148-157.
- [6] P. Kubáň, P. C. Hauser, *Electrophoresis* **2004**, *25*, 3387-3397.
- [7] P. Kubáň, P. C. Hauser, *Electrophoresis* **2004**, *25*, 3398-3405.
- [8] S. Hjertén, *Electrophoresis* **1990**, *11*, 665-690.
- [9] T. D. Mai, P. C. Hauser, *Talanta* **2011**, *84*, 1228-1233.
- [10] P. Tůma, E. Samcová, K. Štulík, *Electroanalysis* **2011**, *23*, 1870-1874.
- [11] T. D. Mai, P. C. Hauser, *Electrophoresis* **2011**, *32*, 3000-3007.
- [12] T. D. Mai, P. C. Hauser, *J. Chromatogr. A* **2012**, *1267*, 266-272.
- [13] T. D. Mai, P. C. Hauser, *Electrophoresis* **2013**, *34*, 1796-1803.
- [14] P. Horowitz, W. Hill, *The Art of Electronics*, 2nd ed., Cambridge University Press, Cambridge, **1989**.

Appendix

For one of the previously described projects (Chapter 2.1), we were invited by the editor of CHIMIA to contribute this article for the special column of volume 67, 2013.

Highlights of Analytical Sciences in Switzerland

CHIMIA International Journal for Chemistry, (2013), 67



Highlights of Analytical Sciences in Switzerland

Division of Analytical Sciences

A Division of the Swiss Chemical Society

Determination of PCR Products by Capillary Electrophoresis with Contactless Conductivity Detection

Marko Stojkovic^a, Narasimha Rao Uda^a, Peter Brodmann^b, and Peter C. Hauser^{*a}

^{*}Correspondence: Prof. Dr. P.C. Hauser^a, Tel.: +41 61 267 10 03, Fax: +41 61 267 10 13, E-mail: peter.hauser@unibas.ch. ^aDepartment of Chemistry, University of Basel, Spitalstrasse 51, CH-4056 Basel. ^bBiosafety Laboratory, State Laboratory Basel City, Kannenfeldstrasse 2, CH-4012 Basel

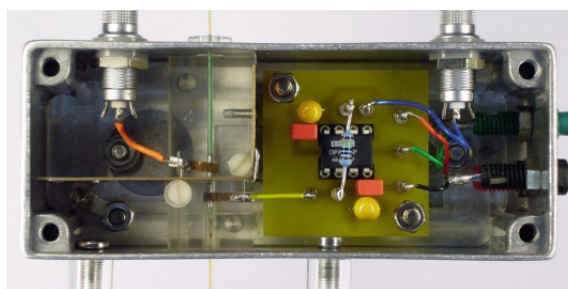
Keywords: Capillary electrophoresis · Contactless conductivity detection · PCR

The detection of polymerase chain reaction (PCR) products is widely used in DNA analysis for such diverse tasks as the determination of paternity, genetic fingerprinting in forensics, identification of pathogens, diagnosis of genetic diseases, recognition of banned genetically modified food items or the identity of meat samples. The standard method for this analysis is planar gel electrophoresis in which the DNA fragments are separated by their size. This method is well established, but it is hard to automate, time consuming, and requires staining for visualization on the plate. Data processing requires awkward optical scanning of the plate.

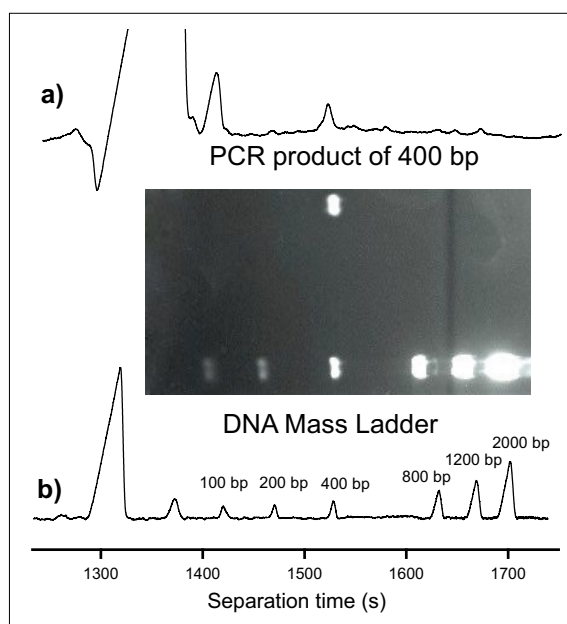
Capillary electrophoresis (CE) is an alternative which allows faster separations and the direct electronic acquisition of electropherograms with characteristic peaks whose areas are directly related to the amount of the species in question. The method is relatively simple as only the application of a high voltage is required and high pressure pumps as in column chromatography are not needed. Contactless conductivity detection is a fully electronic universal technique which is much easier to implement than optical detection on the narrow capillaries needed in electrophoresis which have inner diameters of typically 50 μm . The electrodes are placed on the outside of the capillary and thus cannot deteriorate by contact with solutions. The conductivity measurement of the solution inside the tubing is enabled by capacitive coupling of an AC-voltage into the capillary and the similar coupling of the resulting current out of the capillary on a pair of tubular electrodes. The term C⁴D, for capacitively coupled contactless conductivity detection, has become widely accepted for this technique. Due to the low power requirements it also possible to construct complete portable CE-C⁴D instruments which can be run from batteries.

As an example of the application, the identification of genetically modified soybean (Roundup Ready), which is banned from importation into Switzerland, was carried out. PCR primers were designed to yield a fragment of 400 base-pairs for the GM-soybeans.

The method allows the relatively fast analysis of PCR products yielding the results in a standard electropherogram on a simple and inexpensive instrument.



In-house constructed C⁴D-cell.



Electropherograms obtained by CE-C⁴D for the PCR-product of the Roundup Ready soybean (a) and a mixture of mass standards (ladder) (b), shown together with a picture of the stained plate for the separations carried out by conventional planar gel electrophoresis.

Received: April 16, 2013

References

- M. Stojkovic, N. R. Uda, P. Brodmann, M. Popovic, P. C. Hauser, *J. Sep. Sci.* **2012**, *35*, 3509.
T. D. Mai, T. T. T. Pham, H. V. Pham, J. Sáiz, C. García Ruiz, P. C. Hauser, *Anal. Chem.* **2013**, *85*, 2333.

Can you show us your analytical highlight?

Please contact: Dr. Veronika R. Meyer, EMPA St.Gallen, Lerchenfeldstrasse 5, 9014 St.Gallen
Phone: +41 58 765 77 87, Fax: +41 58 765 77 62, Mail to: veronika.meyer@empa.ch

3. References

- [1] E. M. Abad-Villar, P. Kubán, P. C. Hauser, *J. Sep. Sci.* **2006**, *29*, 1031-1037.
- [2] R. P. Baldwin, *Electrophoresis* **2000**, *21*, 4017-4028.
- [3] J. F. Banks, *Electrophoresis* **1997**, *18*, 2255-2266.
- [4] N. W. Barnett, C. E. Lenehan, S. W. Lewis, *Trac-Trends Anal. Chem.* **1999**, *18*, 346-353.
- [5] R. Burakham, J. Jakmunee, K. Grudpan, *Anal. Sci.* **2006**, *22*, 137-140.
- [6] R. Burakham, S. Lapanantnoppakhun, J. Jakmunee, K. Grudpan, *Talanta* **2005**, *68*, 416-421.
- [7] G. Chen, Y. Lin, J. Wang, *Talanta* **2006**, *68*, 497-503.
- [8] R. Chen, H. Cheng, W. Wu, X. Ai, W. Huang, Z. Wang, J. Cheng, *Electrophoresis* **2007**, *28*, 3347-3361.
- [9] X.-W. Chen, J.-H. Wang, *Anal. Chim. Acta* **2007**, *602*, 173-180.
- [10] L. A. Colon, R. Dadoo, R. N. Zare, *Anal. Chem.* **1993**, *65*, 476-481.
- [11] S. W. Compton, R. G. Brownlee, *BioTechniques* **1988**, *6*, 432-440.
- [12] P. Coufal, J. Zuska, T. van de Goor, V. Smith, B. Gaš, *Electrophoresis* **2003**, *24*, 671-677.
- [13] E. Dabek-Zlotorzynska, V. Celo, M. M. Yassine, *Electrophoresis* **2008**, *29*, 310-323.
- [14] B. L. De Backer, L. J. Nagels, *Anal. Chem.* **1996**, *68*, 4441-4445.
- [15] M. Deml, F. Foret, P. Boček, *J. Chromatogr. A* **1985**, *320*, 159-165.
- [16] C. Desiderio, D. V. Rossetti, F. Iavarone, I. Messana, M. Castagnola, *J. Pharm. Biomed. Anal.* **2010**, *53*, 1161-1169.
- [17] A. Economou, *Trac-Trends Anal. Chem.* **2005**, *24*, 416-425.
- [18] G. L. Ellman, K. D. Courtney, V. Andres, Jr., R. M. Feather-Stone, *Biochem. Pharmacol.* **1961**, *7*, 88-95.
- [19] L. Y. Fan, H. L. Chen, X. G. Chen, Z. D. Hu, *J. Sep. Sci.* **2003**, *26*, 1376-1382.
- [20] Q. Fang, F.-R. Wang, S.-L. Wang, S.-S. Liu, S.-K. Xu, Z.-L. Fang, *Anal. Chim. Acta* **1999**, *390*, 27-37.
- [21] X. Fang, W. Wang, L. Yang, K. Chandrasekaran, T. Kristian, B. M. Balgley, C. S. Lee, *Electrophoresis* **2008**, *29*, 2215-2223.
- [22] Z.-L. Fang, Z.-S. Liu, Q. Shen, *Anal. Chim. Acta* **1997**, *346*, 135-143.
- [23] Z. L. Fang, Q. Fang, *Fresenius' J. Anal. Chem.* **2001**, *370*, 978-983.

- [24] A. Fernández-la-Villa, D. F. Pozo-Ayuso, M. Castaño-Álvarez, *Electrophoresis* **2010**, *31*, 2641-2649.
- [25] J. A. Fracassi da Silva, C. L. do Lago, *Anal. Chem.* **1998**, *70*, 4339-4343.
- [26] B. Gaš, M. Demjaněnko, J. Vacík, *J. Chromatogr. A* **1980**, *192*, 253-257.
- [27] X. Y. Gong, P. C. Hauser, *Electrophoresis* **2006**, *27*, 468-473.
- [28] K. Grudpan, *Talanta* **2004**, *64*, 1084-1090.
- [29] R. M. Guijt, C. J. Evenhuis, M. Macka, P. R. Haddad, *Electrophoresis* **2004**, *25*, 4032-4057.
- [30] E. H. Hansen, M. Miró, *Trac-Trends Anal. Chem.* **2007**, *26*, 18-26.
- [31] E. H. Hansen, M. Miró, *Appl. Spectrosc. Rev.* **2008**, *43*, 335-357.
- [32] E. H. Hansen, J. Wang, *Anal. Lett.* **2005**, *37*, 345-359.
- [33] R. Haselberg, G. J. de Jong, G. W. Somsen, *J. Chromatogr. A* **2007**, *1159*, 81-109.
- [34] R. Haselberg, G. J. de Jong, G. W. Somsen, *Electrophoresis* **2011**, *32*, 66-82.
- [35] C. Henry, *Anal. Chem.* **1996**, *68*, 747A-751A.
- [36] J. Hernández-Borges, C. Neusüß, A. Cifuentes, M. Pelzing, *Electrophoresis* **2004**, *25*, 2257-2281.
- [37] E. F. Hilder, A. J. Zemmann, M. Macka, P. R. Haddad, *Electrophoresis* **2001**, *22*, 1273-1281.
- [38] S. Hjertén, *Chromatogr. Rev.* **1967**, *9*, 122-219.
- [39] L. A. Holland, A. M. Leigh, *Electrophoresis* **2002**, *23*, 3649-3658.
- [40] B. Horstkotte, O. Elsholz, V. C. Martín, *Int. J. Environ. Anal. Chem.* **2007**, *87*, 797-811.
- [41] B. Horstkotte, O. Elsholz, V. C. Martín, *Talanta* **2008**, *76*, 72-79.
- [42] M. Israëli, B. Lesbats, *J. Neurochem.* **1981**, *37*, 1475-1483.
- [43] J. W. Jorgenson, K. D. Lukacs, *J. Chromatogr. A* **1981**, *218*, 209-216.
- [44] J. W. Jorgenson, K. D. Lukacs, *Clin. Chem.* **1981**, *27*, 1551-1553.
- [45] J. W. Jorgenson, K. D. Lukacs, *Anal. Chem.* **1981**, *53*, 1298-1302.
- [46] D. Kaniánsky, V. Zelenská, M. Masár, F. Iványi, Š. Gazdíkova, *J. Chromatogr. A* **1999**, *844*, 349-359.
- [47] T. Kappes, B. Galliker, M. A. Schwarz, P. C. Hauser, *Trac-Trends Anal. Chem.* **2001**, *20*, 133-139.
- [48] T. Kappes, P. C. Hauser, *J. Chromatogr. A* **1999**, *834*, 89-101.
- [49] T. Kappes, P. C. Hauser, *Electroanalysis* **2000**, *12*, 165-170.

- [50] V. Kašička, *Electrophoresis* **2010**, *31*, 122-146.
- [51] J. H. Knox, *J. Chromatogr. A* **1994**, *680*, 3-13.
- [52] S. Kobayashi, T. Ueda, M. Kikumoto, *J. Chromatogr. A* **1989**, *480*, 179-184.
- [53] F. Kohlrausch, *Ann. Phys. Chem. (Leipzig)* **1897**, *62*, 209-239.
- [54] W. Kolch, C. Neusüß, M. Pelzing, H. Mischak, *Mass Spectrom. Rev.* **2005**, *24*, 959-977.
- [55] P. Kubáň, E. M. Abad-Villar, P. C. Hauser, *J. Chromatogr. A* **2006**, *1107*, 159-164.
- [56] P. Kuban, A. Engström, J. C. Olsson, G. Thorsén, R. Tryzell, B. Karlberg, *Anal. Chim. Acta* **1997**, *337*, 117-124.
- [57] P. Kuban, P. C. Hauser, *J. Chromatogr. A* **2007**, *1176*, 185-191.
- [58] P. Kubáň, P. C. Hauser, *Electroanalysis* **2004**, *16*, 2009-2021.
- [59] P. Kubáň, P. C. Hauser, *Electrophoresis* **2004**, *25*, 3398-3405.
- [60] P. Kubáň, P. C. Hauser, *Electrophoresis* **2004**, *25*, 3387-3397.
- [61] P. Kubáň, P. C. Hauser, *J. Chromatogr. A* **2006**, *1128*, 97-104.
- [62] P. Kubáň, P. C. Hauser, *Anal. Chim. Acta* **2008**, *607*, 15-29.
- [63] P. Kubáň, P. C. Hauser, *Electrophoresis* **2009**, *30*, 3305-3314.
- [64] P. Kubáň, P. C. Hauser, *Electrophoresis* **2009**, *30*, 176-188.
- [65] P. Kubáň, P. C. Hauser, *Electrophoresis* **2011**, *32*, 30-42.
- [66] P. Kubáň, B. Karlberg, *Anal. Chim. Acta* **2009**, *648*, 129-145.
- [67] P. Kubáň, P. Kubáň, P. C. Hauser, V. Kubáň, *Electrophoresis* **2004**, *25*, 35-42.
- [68] P. Kuban, P. Kuban, V. Kuban, *Anal. Bioanal. Chem.* **2004**, *378*, 378-382.
- [69] P. Kubáň, P. Kubáň, V. Kubáň, *Electrophoresis* **2002**, *23*, 3725-3734.
- [70] P. Kubáň, P. Kubáň, V. Kubáň, *Electrophoresis* **2003**, *24*, 1397-1403.
- [71] P. Kubáň, P. Kubáň, V. Kubáň, *Electrophoresis* **2003**, *24*, 1935-1943.
- [72] P. Kubáň, P. Kubáň, V. Kubáň, P. C. Hauser, P. Boček, *J. Chromatogr. A* **2008**, *1190*, 377-382.
- [73] P. Kubáň, M. A. Müri, P. C. Hauser, *Analyst* **2004**, *129*, 82-86.
- [74] S. Kulka, G. Quintas, B. Lendl, *Analyst* **2006**, *131*, 739-744.
- [75] F. Laugere, R. M. Guijt, J. Bastemeijer, G. van der Steen, A. Berthold, E. Baltussen, P. Sarro, G. W. K. van Dedem, M. Vellekoop, A. Bossche, *Anal. Chem.* **2002**, *75*, 306-312.
- [76] J. Lichtenberg, N. F. de Rooij, E. Verpoorte, *Electrophoresis* **2002**, *23*, 3769-3780.

- [77] S. Liu, P. K. Dasgupta, *Anal. Chim. Acta* **1993**, 283, 739-745.
- [78] M. D. Luque de Castro, J. Ruiz-Jiménez, J. A. Pérez-Serradilla, *Trac-Trends Anal. Chem.* **2008**, 27, 118-126.
- [79] T. D. Mai, B. Bomastyk, H. A. Duong, H. V. Pham, P. C. Hauser, *Anal. Chim. Acta* **2012**, 727, 1-7.
- [80] T. D. Mai, P. C. Hauser, *Electrophoresis* **2011**, 32, 3000-3007.
- [81] T. D. Mai, S. Schmid, B. Müller, P. C. Hauser, *Anal. Chim. Acta* **2010**, 665, 1-6.
- [82] Z. Malá, P. Gebauer, P. Boček, *Electrophoresis* **2013**, 34, 19-28.
- [83] A. F.-S. Marzanna Kurzawa, Aneta Jastrzębska, Edward Szłyk, *Pharm. Anal. Acta* **2012**, 3, 3:173.
- [84] M. Masár, D. Sydes, M. Luc, D. Kaniansky, H.-M. Kuss, *J. Chromatogr. A* **2009**, 1216, 6252-6255.
- [85] M. Masár, M. Žúborová, D. Kaniansky, B. Stanislawski, *J. Sep. Sci.* **2003**, 26, 647-652.
- [86] F.-M. Matysik, *Microchim. Acta* **2008**, 160, 1-14.
- [87] K. Mayrhofer, A. J. Zemann, E. Schnell, G. K. Bonn, *Anal. Chem.* **1999**, 71, 3828-3833.
- [88] R. B. R. Mesquita, A. O. S. S. Rangel, *Anal. Chim. Acta* **2009**, 648, 7-22.
- [89] F. E. P. Mikkers, F. M. Everaerts, T. P. E. M. Verheggen, *J. Chromatogr. A* **1979**, 169, 11-20.
- [90] H. Mischak, J. J. Coon, J. Novak, E. M. Weissinger, J. P. Schanstra, A. F. Dominiczak, *Mass Spectrom. Rev.* **2009**, 28, 703-724.
- [91] L. J. Nagels, I. Poels, *Trac-Trends Anal. Chem.* **2000**, 19, 410-417.
- [92] A. Nann, I. Silvestri, W. Simon, *Anal. Chem.* **1993**, 65, 1662-1667.
- [93] H. T. A. Nguyen, P. Kubáň, V. H. Pham, P. C. Hauser, *Electrophoresis* **2007**, 28, 3500-3506.
- [94] S. Nussbaumer, S. Fleury-Souverain, L. Bouchoud, S. Rudaz, P. Bonnabry, J.-L. Veuthey, *J. Pharm. Biomed. Anal.* **2010**, 53, 130-136.
- [95] M. A. L. Oliveira, C. L. d. Lago, M. F. M. Tavares, J. A. F. d. Silva, *Quím. Nova* **2003**, 26, 821-824.
- [96] F. Pal, E. Pungor, E. S. Kovats, *Anal. Chem.* **1988**, 60, 2254-2258.
- [97] M. Petsch, B. X. Mayer-Helm, R. Sauermann, C. Joukhadar, E. Kenndler, *Electrophoresis* **2004**, 25, 2292-2298.

- [98] S. Polesello, S. M. Valsecchi, *J. Chromatogr. A* **1999**, *834*, 103-116.
- [99] M. Pumera, J. Wang, F. Opekar, I. Jelínek, J. Feldman, H. Löwe, S. Hardt, *Anal. Chem.* **2002**, *74*, 1968-1971.
- [100] E. Pungor, F. Pal, K. Toth, *Anal. Chem.* **1983**, *55*, 1728-1731.
- [101] L. M. Ravelo-Perez, M. Asensio-Ramos, J. Hernandez-Borges, M. A. Rodriguez-Delgado, *Electrophoresis* **2009**, *30*, 1624-1646.
- [102] D. J. Rose, J. W. Jorgenson, *Anal. Chem.* **1988**, *60*, 642-648.
- [103] M. Rowena N. Monton, S. Terabe, *Anal. Sci.* **2005**, *21*, 5-13.
- [104] J. Ruzicka, *Analyst* **2000**, *125*, 1053-1060.
- [105] J. Růžička, *Anal. Chim. Acta* **1992**, *261*, 3-10.
- [106] J. Ruzicka, G. D. Marshall, *Anal. Chim. Acta* **1990**, *237*, 329-343.
- [107] E. Samcová, P. Tůma, *Electroanalysis* **2006**, *18*, 152-157.
- [108] L. Sanchez-Hernandez, C. Garcia-Ruiz, M. Luisa Marina, A. Luis Crego, *Electrophoresis* **2010**, *31*, 28-43.
- [109] P. Schmitt-Kopplin, M. Frommberger, *Electrophoresis* **2003**, *24*, 3837-3867.
- [110] P. Schnierle, T. Kappes, P. C. Hauser, *Anal. Chem.* **1998**, *70*, 3585-3589.
- [111] M. A. Schwarz, P. C. Hauser, *Lab Chip* **2001**, *1*, 1-6.
- [112] A. C. Servais, J. Crommen, M. Fillet, *Electrophoresis* **2006**, *27*, 2616-2629.
- [113] M. V. Smoluchowski, *Physik. Z.* **1905**, *6*, 529.
- [114] W. F. Smyth, P. Brooks, *Electrophoresis* **2004**, *25*, 1413-1446.
- [115] V. Šolínová, V. Kašička, *J. Sep. Sci.* **2006**, *29*, 1743-1762.
- [116] T. S. Stevens, H. J. Cortes, *Anal. Chem.* **1983**, *55*, 1365-1370.
- [117] L. Suntornsuk, *Anal. Bioanal. Chem.* **2010**, *398*, 29-52.
- [118] I. Surowiec, I. Kaml, E. Kenndler, *J. Chromatogr. A* **2004**, *1024*, 245-254.
- [119] F. Tagliaro, J. Pascali, A. Fanigliulo, F. Bortolotti, *Electrophoresis* **2010**, *31*, 251-259.
- [120] F. Tan, B. Yang, Y. Guan, *Anal. Sci.* **2005**, *21*, 955-958.
- [121] J. Tanyanyiwa, E. M. Abad-Villar, M. T. Fernandez-Abedul, A. Costa-Garcia, W. Hoffmann, A. E. Guber, D. Herrmann, A. Gerlach, N. Gottschlich, P. C. Hauser, *Analyst* **2003**, *128*, 1019-1022.
- [122] J. Tanyanyiwa, B. Galliker, M. A. Schwarz, P. C. Hauser, *Analyst* **2002**, *127*, 214-218.
- [123] J. Tanyanyiwa, P. C. Hauser, *Anal. Chem.* **2002**, *74*, 6378-6382.

- [124] J. Tanyanyiwa, S. Leuthardt, P. C. Hauser, *Electrophoresis* **2002**, *23*, 3659-3666.
- [125] J. Tanyanyiwa, K. Schweizer, P. C. Hauser, *Electrophoresis* **2003**, *24*, 2119-2124.
- [126] G. A. Theodoridis, C. K. Zacharis, A. N. Voulgaropoulos, *J. Biochem. Biophys. Methods* **2007**, *70*, 243-252.
- [127] W. Thongchai, B. Liawruangrath, S. Liawruangrath, *Talanta* **2010**, *81*, 565-571.
- [128] A. Tiselius, *Nova Acta Regiae Soc. Sci. Upsal.* **1930**, *7*, 107.
- [129] T. Tsuda, T. Mizuno, J. Akiyama, *Anal. Chem.* **1987**, *59*, 799-800.
- [130] P. Tůma, E. Samcová, K. Andělová, *J. Chromatogr. B* **2006**, *839*, 12-18.
- [131] P. Tůma, E. Samcová, F. Duška, *J. Sep. Sci.* **2008**, *31*, 2260-2264.
- [132] T. P. E. M. Verheggen, J. L. Beckers, F. M. Everaerts, *J. Chromatogr. A* **1988**, *452*, 615-622.
- [133] R. A. Wallingford, A. G. Ewing, *Anal. Chem.* **1987**, *59*, 678-681.
- [134] R. A. Wallingford, A. G. Ewing, *J. Chromatogr. A* **1988**, *441*, 299-309.
- [135] R. A. Wallingford, A. G. Ewing, *Anal. Chem.* **1989**, *61*, 98-100.
- [136] A. Wang, Y. Fang, *Electrophoresis* **2000**, *21*, 1281-1290.
- [137] J. Wang, E. H. Hansen, *Trac-Trends Anal. Chem.* **2003**, *22*, 225-231.
- [138] J. Wang, M. Pumera, *Anal. Chem.* **2002**, *75*, 341-345.
- [139] J. Wang, M. Pumera, G. Collins, F. Opekar, I. Jelinek, *Analyst* **2002**, *127*, 719-723.
- [140] J. Wang, M. Pumera, G. E. Collins, A. Mulchandani, *Anal. Chem.* **2002**, *74*, 6121-6125.
- [141] C.-H. Wu, L. Scampavia, J. Ruzicka, *Analyst* **2002**, *127*, 898-905.
- [142] C.-H. Wu, L. Scampavia, J. Ruzicka, *Analyst* **2003**, *128*, 1123-1130.
- [143] S. Wu, N. J. Dovichi, *Talanta* **1992**, *39*, 173-178.
- [144] A. Wuersig, P. Kuban, S. S. Khaloo, P. C. Hauser, *Analyst* **2006**, *131*, 944-949.
- [145] C. K. Zacharis, F. W. A. Tempels, G. A. Theodoridis, A. N. Voulgaropoulos, W. J. M. Underberg, G. W. Somsen, G. J. de Jong, *J. Chromatogr. A* **2006**, *1132*, 297-303.
- [146] A. J. Zemann, *Trac-Trends Anal. Chem.* **2001**, *20*, 346-354.
- [147] A. J. Zemann, *Electrophoresis* **2003**, *24*, 2125-2137.

- [148] A. J. Zemann, E. Schnell, D. Volgger, G. K. Bonn, *Anal. Chem.* **1998**, *70*, 563-567.
- [149] M. Zuborova, Z. Demianova, D. Kaniansky, M. Masar, B. Stanislawski, *J. Chromatogr. A* **2003**, *990*, 179-188.

4. Curriculum Vitae

Marko Stojkovic
Mülhauserstrasse 72
CH-4056 Basel
Tel: ++41 76 263 87 77
E-mail: marko.stojkovic@unibas.ch

Profile

MSc in Pharmaceutical Sciences and a perspective PhD candidate in Analytical chemistry. Possess a perennial successful leadership experience of managing 10 teaching assistants and up to 120 students in the practical classes for pharmacy students at the University of Basel. Has over one year of pharmaceutical industry experience as medical sales representative in Eastern Europe.

Distinctive social competence, practically oriented, entrepreneurial approach, strong perceptivity for complex situations, precise way of working

Education

2008 - (Est) - University of Basel, Department of Analytical Chemistry

- . PhD candidate in Analytical Chemistry
- . Dissertation: Further Development and Applications of Capillary Electrophoresis with Capacitively Coupled Contactless Conductivity Detection and Sequential Injection Analysis in Analytical Chemistry

1997 - 2006 - University of Belgrade, Faculty of Pharmacy, Serbia

- . MSc in Pharmaceutical Sciences (Distinction)
- . Master Thesis: Chemical analysis of different commercial wines

Additional Training

Education in:

- Bionalytical Sciences
- Applications of Analytical Chemistry: On-site Analysis, Electrophoresis of Pharmaceuticals, Toxicology
- Separation Techniques in the Pharmaceutical Industry
- Applied Electronics for Analytical Chemistry
- Analytical Aspects of Forensic Chemistry and Toxicology
- Deutsch als Fremdsprache: Sprechen und Schreiben (Sprachzentrum der Universität Basel, level B1)
- Deutsch als Fremdsprache: Mittelstufe I (Sprachzentrum der Universität Basel, level B1/B2)
- Anwendung der Neutronenaktivierungsanalyse in der Naturwissenschaft für Studierende aller naturwiissenschaftlichen Richtungen
- History of Chemistry
- Analytical and Bioanalytical Sciences

Computer skills

- Operating systems (Mac OS X, Windows NT/2000/XP/Vista/7)
- iLife, Photoshop CS, Final Cut Pro, Cinema 4D
- Labview (basic programming), Pumplink32, EndNote, ChemDraw, Intaglio, IgorPro, eDAQ, EAGLE, QUCS, WPrinCE, Origin, Sketchup
- Chemical Databases: SciFinder, Web of Science, Diverse Internet-Databases for chemists, pharmacists and biologists

Grants

2008 – 2012 Swiss National Science Foundation

Employment

UNIVERSITY OF BASEL, SWITZERLAND

AUGUST 2008 – PRESENT - RESEARCH AND DEVELOPMENT

Working on:

- . Developing the methods or the methods in use and reproducing published methods regarding the SOPs.
- . Documenting planning, developing, monitoring, rating for the instruments/devices and their performances optimized for scientific experiments.
- . Writing SOPs for the instruments in use or commercial devices in details to achieve uniformity of the operation of a specific function. Repeating applied unchanged processes and procedures and documenting them, supporting the segregation of causes and effects.
- . Performing safety regulations and keep recording all chemicals, solvents, intermediates within own area of responsibility.
- . Maintaining and evaluating all laboratory equipment, as well as validating raw data and interpreting results (quality and quantity).
- . Trained on regulations and standards: GMP, GLP, ICH, USP, EP, ISO 9001:2008.
- . Reporting about achieved results and discuss regarding improvement potential in own area of interest.
- . Responsible for the budget within the research group.
- . Development of the detector cells and further development and applications of capillary electrophoresis with capacitively coupled contactless conductivity detection and sequential injection analysis in analytical chemistry.

AUGUST 2011 – AUGUST 2012 - TEAM LEADER

- . Supervise group heads, teaching assistants and cooperate with the study coordinator from the pharmacy department.
- . Introduce new teaching assistants to the responsibilities and safety regulations and give them guided tour through the facilities.
- . Organize lectures, handle repairs and orders for equipment, make requests for financing thereof and handle orders documenting them, organize teaching assistants according to their experience, abilities and knowledge.
- . Update documentation and write manuals for the teaching assistants and make sure that they follow the SOPs for the equipment.

AUGUST 2010 – AUGUST 2011- GROUP HEAD ASSISTENT

- . Bestead team leader in training all first-time teaching assistants and prepare them ready for the following chapter/experiment in advance.
- . Bring problems concerning equipment/laboratory to the attention of the team leader.
- . Actively provide advice and assistance to students as they conduct work in the laboratory.
- . Grade laboratory reports for all students enrolled and enforce all safety regulations.
- . Proctor midterm exams and the final exam.
- . Provide feedback and assistance to the team leader as requested.

AUGUST 2008 – AUGUST 2010 - TEACHING ASSISTENT (GTF)

- . Provide and label chemicals for the students and introduce them in completing their exercises and experiments, as well as monitor the compliance of the students under department instructions concerning safety regulations and disposal of the chemicals.
- . Demonstrate and maintain the work of all equipment in the teaching laboratory

PHARMACEUTICAL COMPANY “IVANCIC AND SONS”, BELGRADE, SERBIA

JANUARY 2007 – JANUARY 2008 - MEDICAL REPRESENTATIVE, SALES DEPARTMENT

- . Medical advising patients on the use of company products, distribution and presentation of company products to hospitals, medical centers and pharmacies, daily and weekly reports on activities/results to the headquarters, discussions with doctors and pharmacist about the products, representing innovations and achievements of the company on professional conferences.

PHARMACY “SVETI SAVA”, BELGRADE, SERBIA

FEBRUARY 2008 – JULY 2008 - PHARMACIST

- . Processing prescriptions in a community pharmacy, counseling public on prescription and over-the-counter medications, preparing magisterial remedies for special cases (creams, lotions, powders, eye/nose/ear drops, syrups), organizing the drugs by diverse criteria such as therapeutic classes, alphabetical order or pharmaceutical form

Languages

- . Serbo-Croatian: Fluent (Mother tongue)
- . English: Fluent
- . German: Advanced (Level: B1/B2)
- . French: Basic (Level A1+)

Miscellaneous

- . Date of Birth: 21st of June 1978. (Serbia)
- . Civil Status: Married (2 daughters)
- . Swiss Working Permit: Visa category B (residence permit)
- . Personal interests: asian kitchen, reading, theatre, sports.
- . Publications: Two publications published, two publications in press and one in preparation.

5. List of publications and posters

5.1 Publications

1. **Marko Stojkovic**, Narasimha Rao Uda, Peter Brodmann, Milica Popovic, Peter C. Hauser
Determination of PCR products by CE with contactless conductivity detection
Journal of Separation Science, (2012), 35, 3509-3513
2. **Marko Stojkovic**, Thanh Duc Mai, Peter C. Hauser
Determination of artificial sweeteners by capillary electrophoresis with contactless conductivity detection optimized by hydrodynamic pumping
Analytica Chimica Acta, (2013), 787, 254-259
3. **Marko Stojkovic**, Boris Schlensky , Peter C. Hauser
Referenced Capacitively Coupled Conductivity Detector for Capillary Electrophoresis
Electroanalysis, (2013), 25, 2645-2650
4. **Marko Stojkovic**, Israel Joel Koenka, Wolfgang Thormann, Peter C. Hauser
A contactless conductivity detector array for capillary electrophoresis
Electrophoresis, (2013), *In press*
5. **Marko Stojkovic**, Narasimha Rao Uda, Peter Brodmann, Milica Popovic, Peter C. Hauser
Highlights of Analytical Sciences in Switzerland
Chimia-International Journal for Chemistry, (2013), 67

5.2 Posters

Marko Stojkovic, Worapan Pormsila, Benjamin Bomastyk, Thanh Duc Mai,
Thitirat Manhim, Peter C. Hauser

Contactless Conductivity Detection with conventional and micro-chip
electrophoresis

**25th International Symposium on Microscale Bioseparations. Prague, Czech
Republic, March 2010**